

research report

LRFD and LSD Resistance Factors for Cold-Formed Steel Compression Members

RESEARCH REPORT RP10-5

JULY 2010

Committee on Specifications
for the Design of Cold-Formed
Steel Structural Members



American Iron and Steel Institute

The material contained herein has been developed by researchers based on their research findings. The material has also been reviewed by the American Iron and Steel Institute Committee on Specifications for the Design of Cold-Formed Steel Structural Members. The Committee acknowledges and is grateful for the contributions of such researchers.

The material herein is for general information only. The information in it should not be used without first securing competent advice with respect to its suitability for any given application. The publication of the information is not intended as a representation or warranty on the part of the American Iron and Steel Institute, or of any other person named herein, that the information is suitable for any general or particular use or of freedom from infringement of any patent or patents. Anyone making use of the information assumes all liability arising from such use.

July 2, 2010

To: AISI Committee Members

Subject: Virginia Tech Research Report No. 10/04

Resistance Factor for Cold-Formed Steel Compression Members

Please find enclosed the final research report that summarizes our efforts to calculate the resistance factor for cold-formed steel compression members. A total of 675 column tests were considered in this study. Main Specification and Direct Strength Method calculations were performed on the collected data and the nominal axial strength each column was predicted. The resistance factor was calculated per cross-section type, ultimate limit state, and considering partially and fully effective columns according to both the LRFD and LSD methods. The observed trends demonstrate that DSM is a more accurate strength prediction approach than the Main Specification, and that defining DSM resistance factors by limit state (i.e. local, distortional, and global buckling) provide a viable option for increasing ϕ_c above 0.85. Recommended code revisions are summarized in Section 5.2 of this report. They are also provided here as a convenience to the reader:

1. Define LRFD resistance factors by limit state for DSM:

$$\phi_c P_n = \min(\phi_{ce} P_{ne}, \phi_{cl} P_{nl}, \phi_{cd} P_{nd}),$$

where $\phi_{ce}=0.80$, $\phi_{cl}=0.90$, and $\phi_{cd}=0.95$.

Defining resistance factors by limit state allows us to take advantage of DSM's strength prediction accuracy for columns with partially effective cross-sections. Higher resistance factor are supported by the calculations and data in this report - local-global buckling interaction goes to 0.90 and distortional buckling goes to 0.95. The increased resistance factors for locally slender columns come with a small price - a resistance factor of 0.80 for columns with fully effective cross-sections. This is a slightly unsavory result (supported by the data) that could be an acceptable compromise considering that most cold-formed steel columns designed with AISI-S100-07 are partially effective.

For comparison, the recommended Main Specification resistance factors (derived with the same data used to evaluate DSM) are also presented:

$$\phi_c P_n = \min(\phi_{ce} AF_n, \phi_{cl} A_e F_n, \phi_{cd} P_{nd})$$

where $\phi_{ce}=0.80$, $\phi_{cl}=0.80$, and $\phi_{cd}=0.95$.

Invent the Future

The lowered Main Specification resistance factor for the local buckling limit state reflects the observation made in this report that the Main Specification is less accurate than DSM.

2. Move the AISI Direct Strength Method into the Main Specification.

DSM was demonstrated throughout this research to be a more accurate predictor of column capacity than the Main Specification. Improved prediction accuracy facilitates higher resistance factors, see Recommendation #1.

3. Lower the LSD resistance factor to $\phi_c=0.70$ to provide a uniform probability of failure consistent with $\beta=3.0$.

Alternatively, the current LSD resistance factor of $\phi_c=0.80$ can be maintained by lowering β from 3.0 to 2.5 and decreasing the D/L ratio from 1/3 to 1/5 (see Section 4.2.9 of this report). DSM resistance factors by LSD limit state could also be considered.

4. The LSD load effects coefficient of variation, V_Q , could be decreased from 0.21 to 0.19 in AISI-S100-07, Chapter F, Section F1.1.

As demonstrated in Eq. (35) of this report, the coefficient of variation of the load effects is a function of dead to live load ratio. For D/L=1/5, $V_Q=0.21$. For D/L=1/3, $V_Q=0.19$. This reduction in COV is beneficial and will increase the calculated LSD resistance factor (and available column capacity) by approximately 5%.

We hope that our AISI COS friends and colleagues will carefully review our report and seriously consider its recommendations. Thank you to our AISI task group for their advice and guidance during this research program.

Sincerely,

Cris Moen

cmoen@vt.edu

Karthik Ganesan

gkarthik@vt.edu



**VIRGINIA POLYTECHNIC INSTITUTE
AND STATE UNIVERSITY**

The Charles E. Via, Jr. Department
of Civil and Environmental Engineering
Blacksburg, VA 24061

Structural Engineering and Materials

**LRFD and LSD Resistance Factors for
Cold-Formed Steel Compression Members**

**FINAL REPORT
CE/VPI-ST-10/04**

by
Karthik Gaanesan
Graduate Research Assistant

Dr. Christopher D. Moen
Assistant Professor

for the

American Iron and Steel Institute
1140 Connecticut Avenue, NW, Suite 705
Washington, D.C. 20036

JULY 2010

Resistance Factor for Cold-Formed Steel Compression Members

(ABSTRACT)

This research investigates if the LRFD strength reduction factor for cold-formed steel compression members can be increased above its current value of $\phi=0.85$, which was established by the LRFD Cold-Formed Steel Design Manual (1991) on the basis of 264 column tests. The resistance factor in the Canadian code for cold-formed steel compression members is also evaluated. A total of 675 concentrically loaded plain and lipped C-section columns, plain and lipped Z-section columns, hat and angle columns, including members with holes, are considered in the study. The predicted strengths are calculated with the AISI-S100-07 Main Specification and the AISI Direct Strength Method. The test-to-predicted strength statistics are employed with the first order second moment reliability approach in AISI-S100-07 Chapter F as well as a higher order method to calculate the resistance factor per cross-section type, ultimate limit state, and considering partially and fully effective columns. DSM is observed to predict the column capacity more accurately than the Main Specification, supporting a higher DSM resistance factor for columns failing in local buckling or distortional buckling limit states. The test-to-predicted ratios for plain and lipped angle columns exhibit a high coefficient of variation and become more and more conservative as global slenderness increases. It is concluded that fundamental research on the mechanics of angle compression members is needed to improve existing design methods.

Table of Contents

List of Figures.....	iv
List of Tables	vi
Chapter 1: Introduction.....	1
1.1 Load and Resistance Factor Design of Cold Formed Steel Compression Members	1
1.2 Code History.....	3
1.3 Objective and Scope of Research	6
1.4 Overview of Thesis	7
Chapter 2: AISI Specification.....	9
2.1 AISI Main Specification	9
2.1.1 Local-Global Buckling Interaction Limit State.....	9
2.1.2 Distortional Buckling Limit State.....	12
2.1.3 Capacity of Angle Columns	13
2.2 Direct Strength Method.....	15
Chapter 3: CFS Column Test Database	18
3.1 Overview of Database.....	18
3.2 Experimental Program Details	20

Chapter 4: Resistance Factor Equations and Calculations	27
4.1 Resistance Factor Derivation.....	27
4.2 Resistance Factor Results.....	36
4.2.1 All Columns.....	36
4.2.2 Columns with Holes.....	37
4.2.3 Columns without Holes.....	38
4.2.4 Partially and Fully Effective Sections.....	41
4.2.5 Resistance Factors by Limit State.....	43
4.2.6 Comparison of Prediction Accuracy with Cross-section Dimensions	44
4.2.7 Resistance Factors for Angle Columns	51
4.2.8 Resistance Factor using Modified Expressions for V_Q and V_R	55
4.2.9 Comparison of Resistance Factors for LSD	60
Chapter 5: Conclusions.....	63
5.1 Summary and Conclusions.....	63
5.2 Recommendations for Code Revisions	66
5.3 Future Work	68
References.....	70
Appendix 1.....	73
Appendix 2.....	96
Appendix 3.....	121

List of Figures

Figure 1. Probability distributions of the load effect, Q , and the resistance, R	2
Figure 2. History of AISI and AISC column curves.....	4
Figure 3. Distortional buckling mode of a Lipped C-section column with holes.....	6
Figure 4. Out-to-out dimensions of different types of columns used in this study.....	7
Figure 5. Effective width method	11
Figure 6. Elastic buckling curve generated using CUFSM	16
Figure 7. Boundary conditions definition.....	20
Figure 8. Web of the lipped C-section column for Pu specimens (Pu et al. 1999).....	25
Figure 9. The normal distribution curve.....	29
Figure 10. Main Specification test-to-predicted strength as a function of global slenderness.....	40
Figure 11. DSM test-to-predicted strength as a function of global slenderness	40
Figure 12. Main Specification test-to-predicted strength as a function of effective area-to-gross area	42
Figure 13. DSM test-to-predicted strength as a function of local-to-global buckling	43
Figure 14. Main Specification test-to-predicted strength as a function of flange width-to-thickness (B/t).....	46
Figure 15. DSM test-to-predicted strength as a function of flange width-to-thickness (B/t).....	46
Figure 16. Main Specification test-to-predicted strength as a function of lip width-to-thickness (D/t).....	47

Figure 17. DSM test-to-predicted strength as a function of lip width-to-thickness (D/t)	47
Figure 18. Main Specification test-to-predicted strength as a function of web height-to-thickness (H/t)	48
Figure 19. DSM test-to-predicted strength as a function of web height-to-thickness (H/t)	48
Figure 20. Main Specification test-to-predicted strength as a function of web height-to-flange width (H/B)	49
Figure 21. DSM test-to-predicted strength as a function of web height-to-flange width (H/B) ...	49
Figure 22. Main Specification test-to-predicted strength as a function of flange width-to-lip length (B/D)	50
Figure 23. DSM test-to-predicted strength as a function of flange width-to-lip length (B/D).....	50
Figure 24. Test-to-predicted strength of plain angle columns with and without PL/1000.....	53
Figure 25. Main Specification test-to-predicted strength ratio as a function of slenderness	54

List of Tables

Table 1. CFS column test database	19
Table 2. Resistance factors for columns with and without holes (Main Specification).....	37
Table 3. Resistance factors for columns with holes (Main Specification)	38
Table 4. Resistance factors for columns without holes (Main Specification)	39
Table 5. Resistance factors for columns without holes (DSM)	39
Table 6. Resistance factors for partially and fully effective columns	41
Table 7. Resistance factors by ultimate limit state	44
Table 8. Main Specification test-to-predicted strength ratios for angle columns.	52
Table 9. Resistance factors for angle columns (Main Specification)	53
Table 10. Resistance factors for angle columns with $\lambda c \leq 2$ (Main Specification).....	54
Table 11. Resistance Factors for angle columns (DSM).....	55
Table 12. Resistance factors for columns with and without holes (Main Specification).....	59
Table 13. Comparison of resistance factors for all columns for LSD (Main Specification).....	61
Table 14. Modified Main Specification limits.....	67
Table 15. Modified DSM prequalified limits.	67

Chapter 1: Introduction

1.1 Load and Resistance Factor Design of Cold Formed Steel Compression Members

A limit state, as defined by Hsiao (1990), is the condition at which the structural usefulness of a load-carrying element or member is impaired to such an extent that it becomes unsafe for the occupants of the structure. In simpler terms, the member is unable to resist the applied load and it fails. Cold-formed steel (CFS) compression members can fail due to yielding or column buckling. Elastic buckling analysis reveals at least three different buckling modes including local, distortional and Euler (flexural, torsional or flexural-torsional buckling). Thus for the design of CFS members, all the above limit states must be considered. The strength limit state of the load and resistance factor design (LRFD) method is expressed as

$$\phi_c R_n \geq \Sigma \gamma_i Q_i, \quad (1)$$

where the nominal resistance is R_n , ϕ_c is the resistance factor, γ_i is the load factor and Q_i is the load effect. The nominal resistance is the strength of the member for a given limit state. The resistance factor, ϕ_c , accounts for the uncertainties in the nominal resistance, R_n . The load effect, Q_i , is the force (e.g., bending moment, axial forces) acting on the member. A limit state is violated when the load effect, Q , is greater than the nominal resistance, R_n . The load effect, Q and the resistance, R are random parameters whose distributions are not typically known and only their means, Q_m and R_m and standard deviations σ_Q and σ_R are known. If the exact probability distributions of Q and R were known, the probability of failure, i.e., the probability of $(R - Q) < 0$ can be determined. Since the probability distributions of Q and R are not known, the relative reliability of a design is obtained using the reliability index, β . The reliability index is a relative measure of the safety of design and a higher value of β indicates a better design. Figure

Figure 1(a) presents the probability distributions of Q and R while Figure 1(b) presents the probability of failure. The area under $\ln(R/Q) \leq 0$ represents the probability of failure.

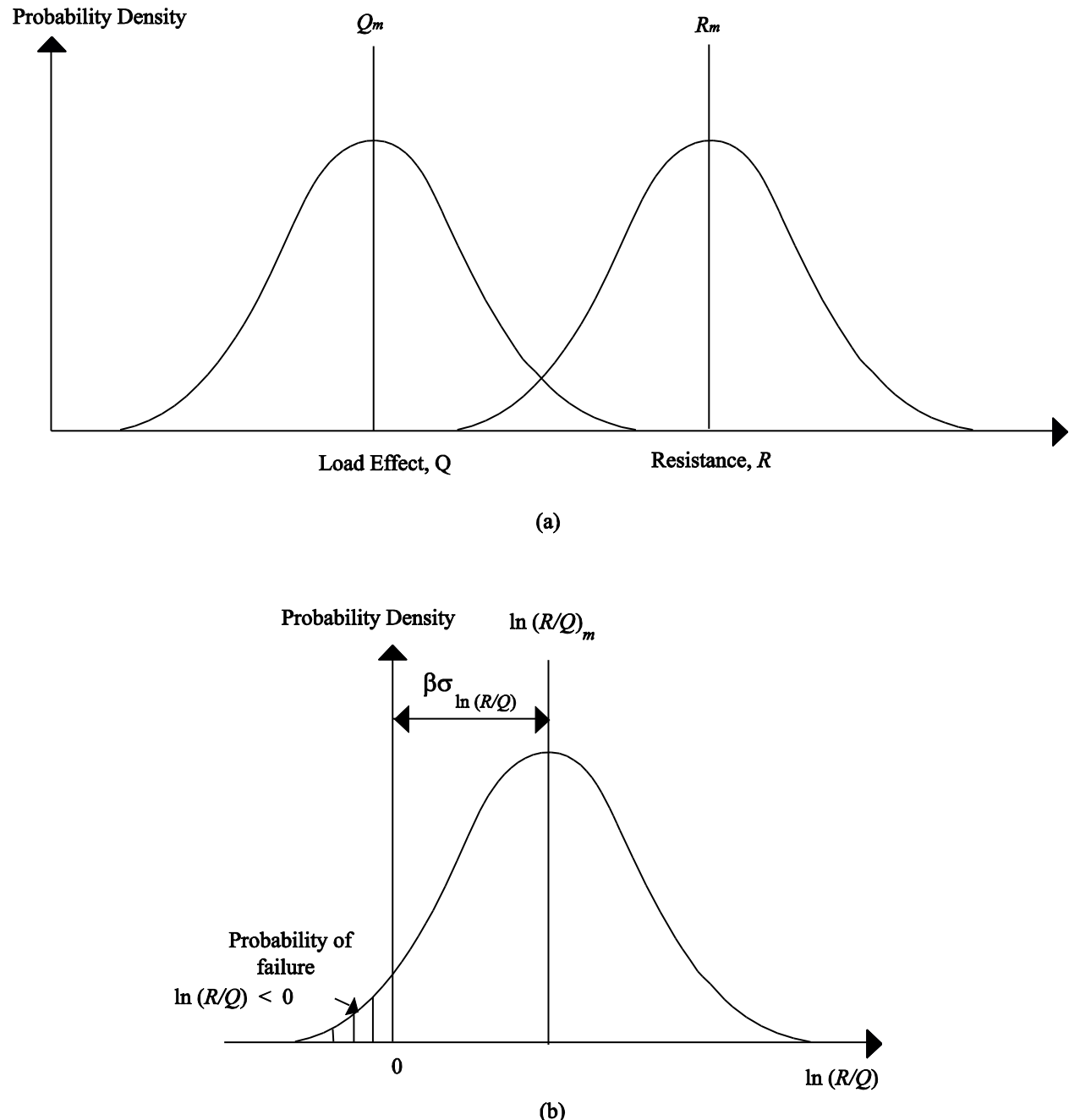


Figure 1. Probability distributions of the load effect, Q , and the resistance, R .

The reliability index, β , is the distance of the failure surface from the mean in standard deviations and this can be observed in Figure 1(b). The reliability index, β , is used as a measure of safety in structural reliability. The concept of the resistance factor, ϕ and the reliability index, β is discussed in greater detail in Chapter 4.

1.2 Code History

This section discusses the evolution of the American Iron and Steel Institute (AISI) North American Specification for the Design of Cold-Formed Steel Structural Members(AISI-S100 2007) since its inception. A review of the Main Specification's effective width method for predicting column capacity as well as the Direct Strength Method (DSM) is also presented.

In 1991, AISI implemented the LRFD approach for CFS members for the first time(AISI 1991). Hsiao (1990) developed the LRFD criteria for CFS similar to the way the American Institute of Steel Construction (AISC) developed LRFD criteria for hot-rolled steel(AISC 1986). Using AISC's LRFD criteria for hot-rolled steel as a basis, AISI adopted a value of 0.85 for the resistance factor, ϕ . For a given representative dead-to-live load ratio of 1/5, a value of 2.5 for the reliability index, β was adopted. The 1991 Specification determined the nominal axial strength (P_n) using

$$P_n = A_e F_n, \quad (2)$$

where A_e is the effective cross-sectional area at the nominal column buckling stress, F_n , calculated with the following expression:

$$\text{For } F_e > F_y/2, \quad F_n = \left(1 - F_y/4F_e\right), \\ F_e \leq F_y/2, \quad F_n = F_e. \quad (3)$$

The critical elastic global buckling stress, F_e is the minimum of the critical elastic flexural, torsional, or flexural-torsional buckling stress and F_y is the steel yield stress.

The next edition of the AISI Specification was published in 1996(AISI 1996). This edition modified the equations used to calculate the nominal global buckling capacity to match the 1993 edition of the AISC LRFD Specification (AISC 1993):

$$\text{For } \lambda_c \leq 1.5, \quad F_n = \left(0.658^{\lambda_c^2}\right) F_y, \\ \lambda_c > 1.5, \quad F_n = \left(0.877 F_y\right) / \lambda_c^2, \quad (4)$$

where slenderness, λ_c , is given by $\lambda_c = (F_y/F_e)^{0.5}$. Peköz and Sümmert(1992) studied 299 column and beam-column tests and showed that the revised column design equations were more accurate than Eq. (3). These equations also account for the initial crookedness and thus provide a better fit to test results. Figure 2 compares the curves produced using Eq. (3) and Eq. (4).

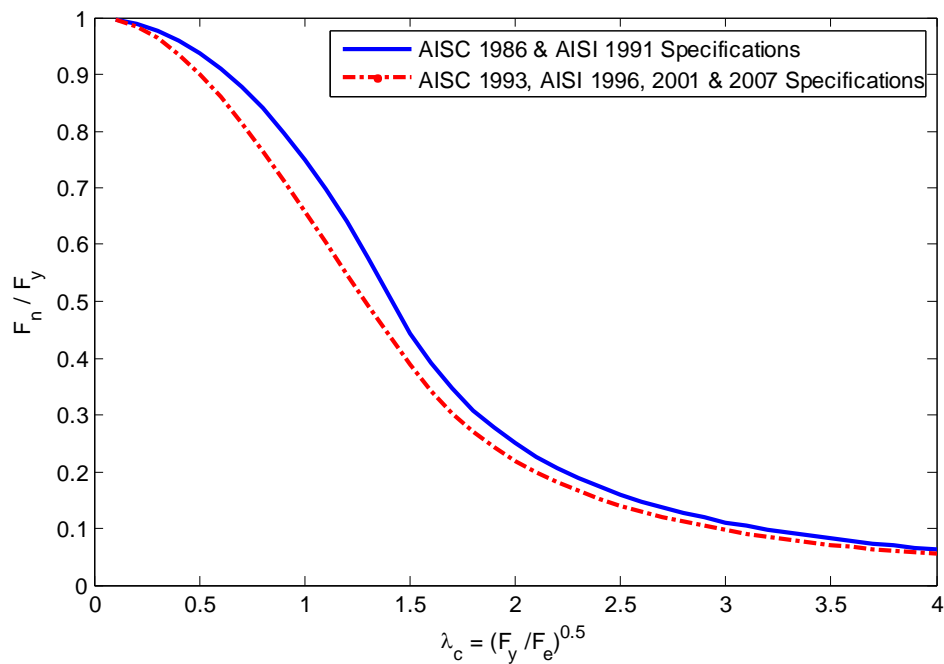


Figure 2.History of AISI and AISC column curves

It is to be noted that although the equations used to calculate the nominal global buckling capacity were modified, the resistance factor and the safety index were left untouched and they continue to be used even now. In 2001, all AISI standards were unified under the banner of the North American Specification (AISI 2001). While the LRFD method was used in the United States and Mexico, Canada adopted the Limit State Design (LSD) method. It is to be noted that while the design philosophy used for LRFD and LSD is the same, the two methods differ in the load factors, load combinations, assumed dead-to-live load ratios and the reliability indices.

A supplement to the 2001 Specification, published in 2004(AISI 2004), introduced a new strength prediction method called the Direct Strength Method (DSM)(Schafer 2002). DSM predicts column strength using the elastic buckling behavior of the whole cross-section. Unlike the Main Specification, DSM does not quantify the cross-section instabilities “element-by-element”. Instead, the long column strength (P_{ne}) is reduced based on the elastic local buckling load of the cross-section ($P_{n\ell}$). More information about the two design methods is presented in Chapter 2.

The most recent edition of the North American Specification was published in 2007 (AISI-S100 2007). The distortional buckling mode of failure, which was introduced in the 2004 Supplement (AISI 2004) containing DSM, was added to the Main Specification in the 2007 edition. This buckling mode occurs in open cross-sections and is characterized by the instability of a compressed flange (Figure 3). Distortional buckling occurs at half-wavelengths between the local and the flexural or the flexural-torsional buckling modes.

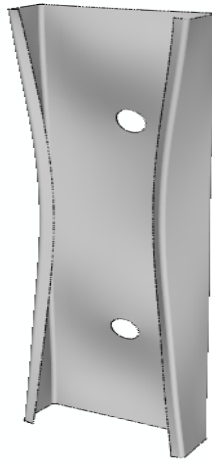


Figure 3. Distortional buckling mode of a Lipped C-section column with holes.

1.3 Objective and Scope of Research

The 1991 Specification(AISI 1991), which introduced the LRFD method for CFS for the first time, established the resistance factor on the basis of a total of 264 column tests. However, numerous column tests have been conducted since 1991 and with the availability of new data, a fresh look at the resistance factor is warranted. This research attempts to gather all available data and investigate the suitability of using $\phi = 0.85$ as an appropriate value for the resistance factor and consider a possible increase to $\phi = 0.90$ so as to make CFS more competitive with hot-rolled steel. While this forms the primary motivation, this study also evaluates the viability of providing resistance factors on the basis of limit states or on the basis of the cross-section slenderness. It also addresses the calibration of the Canadian resistance factor for cold-formed steel compression members, which uses a reliability index of $\beta = 3.0$. In this study, C-sections, Z-sections, hat sections as well as angle sections, both lipped and unlipped, inclusive of sections with holes are considered. This study draws its conclusions based on a total of 675 column tests including plain and lipped C-sections, plain and lipped Z-sections, hat and angle sections. Figure

4 pictorially presents the notations used for the out-to-out dimensions of each type of column used in this study.

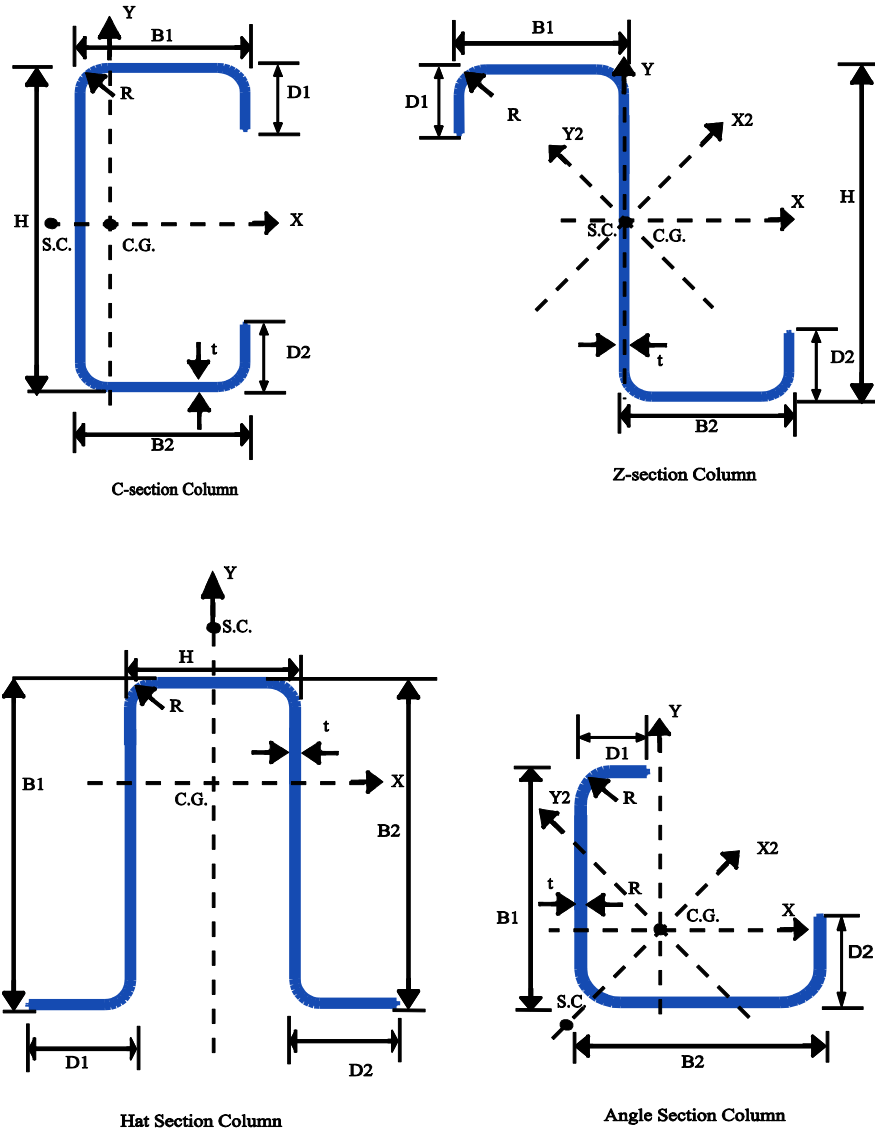


Figure 4. Out-to-out dimensions of different types of columns used in this study.

1.4 Overview of Thesis

This thesis begins with the presentation of the 2007 AISI Specification (AISI-S100 2007) for calculating the capacity of CFS compression members in Chapter 2, including both the Main Specification as well as the Direct Strength Method. The capacity prediction of CFS angle

columns using LRFD is also discussed at depth. Chapter 3explores the development of aCFS column test database that will be used later in the calculation of the resistance factor, ϕ . It discusses the source of each data set, the boundary conditions used in each experimental program and how each program is different from the other.

Chapter 4introduces the concept of a resistance factor and presents a derivation of the resistance factor for CFS compression members.Resistance factors are calculated for all the test data on the basis of limit states and also on the basis of the cross-section slenderness (partially and fully effective sections) for both the Main Specification and the Direct Strength Method. The resistance factors are calculated for both the LRFD and the LSD. This chapter also presents the test-to-predicted strength ratios and resistance factor results obtained for single anglecolumns. A modified method of calculating the resistance factor wherein the coefficient of variation is changed to include an additional term in Taylor Series expansion is also presented in this chapter.

Chapter 5 summarizes the results obtained in the resistance factor studies and also draws conclusions. Areas that require further study as well as recommendations for code changes are also addressed in this chapter. Appendix 1 summarizes the entire database with details about each compression member such as cross-section dimensions and yield stresses along with the test-to-predicted strength ratios for both the Main Specification and the Direct Strength Method. Appendix 2 presents a custom MATLAB (Mathworks 2009) code that this research uses to calculate the capacity of the columns according to the Main Specification and DSM. Appendix 3 presents the mathematical derivation of the resistance factor in a general form without the use of numerical values.

Chapter 2: AISI Specification

This chapter presents the procedure for calculating the capacity of CFS compression members using both the Main Specification as well as the Direct Strength Method in accordance with the 2007 AISI Specification (AISI-S100 2007).

2.1 AISI Main Specification

The Main Specification considers two limit states, local-global buckling interaction (including flexural, torsional or flexural-torsional buckling) and distortional buckling. The nominal column capacity, P_n , is considered to be the minimum of the two limit states.

2.1.1 Local-Global Buckling Interaction Limit State

The Main Specification (AISI-S100 2007) calculates the nominal axial capacity (P_n) of a column using Eq. (2), wherein, the nominal column buckling stress, F_n , is determined using Eq. (4). In order to use Eq. (4), slenderness, λ_c , as expressed by the equation, $\lambda_c = (F_y/F_e)^{0.5}$, must be determined. The critical elastic global buckling stress, F_e , is the minimum of the critical elastic flexural, torsional, or flexural-torsional buckling stress and F_y is the steel yield stress.

The elastic flexural buckling stress, F_e , for doubly-symmetric sections, closed cross-sections, and other cross-sections that are not subjected to either torsional or flexural-torsional buckling, can be calculated as follows:

$$F_e = \frac{\pi^2 E}{(KL/r)^2}, \quad (5)$$

where E is the modulus of elasticity of steel, K is the effective length factor, L is the lateral unbraced length of the member and r is the radius of gyration of the full unreduced cross-section about the axis of buckling.

If the section is also subject to torsional buckling, which is the failure of a column due to a twist without any bending, then the critical elastic global buckling stress, F_e , is taken as the minimum of F_e , as calculated by Eq. (5) and the torsional buckling stress, σ_t , calculated as follows:

$$\sigma_t = \frac{1}{Ar_o^2} \left[GJ + \frac{\pi^2 EC_w}{(K_t L_t)^2} \right], \quad (6)$$

where A is the full cross-sectional area, r_o is the polar radius of gyration of the cross-section about the shear center, G is the shear modulus, J is the Saint Venant torsion constant of the cross-section, E is the modulus of elasticity, C_w is the torsional warping constant of the cross-section, and $K_t L_t$ is the effective length for twisting. This mode of failure is possible for point symmetric shapes such as doubly symmetric I-shapes whose shear center and centroids coincide.

However, if the section is subject to flexural-torsional buckling, where the column fails due to simultaneous bending and twisting, then the critical elastic global buckling stress, F_e , is taken as the minimum of F_e , as calculated by Eq. (5) and the flexural-torsional buckling stress, which is calculated as follows:

$$F_e = \frac{1}{2\beta} \left[(\sigma_{ex} + \sigma_t) - \sqrt{(\sigma_{ex} + \sigma_t)^2 - 4\beta_o \sigma_{ex} \sigma_t} \right] \quad (7)$$

where σ_{ex} is the flexural Euler buckling stress about the x-axis, σ_t is the torsional buckling stress, and $\beta_o = 1 - (x_0/r_0)^2$, where x_o is the distance between the centroid and the shear center and r_o is the polar radius of gyration of the cross-section. Flexural-torsional buckling is a possible mode of failure of singly-symmetric sections in which the shear center and centroid do not coincide.

Now that the critical elastic global buckling stress, F_e , has been found, the slenderness, λ_c , and consequently the nominal column buckling stress, F_n , can be found. However, in order to calculate the nominal axial capacity of a column, P_n , using Eq. (2), the effective area, A_e of the column at F_n , must be determined. In order to calculate A_e , the Main Specification uses the “effective width method”. In this method, the non-uniform distribution of stress over the entire width, w , of a slender buckled element is assumed to be uniformly distributed over a fictitious effective width, b , of the element as shown in Figure 5. It was Von Karman(1932), who first suggested that the stress distribution at the central section of a stiffened plate be replaced by two widths of $(b/2)$ on each side of the plate, each subjected to an uniform stress, f_{max} , as shown in Figure 5.

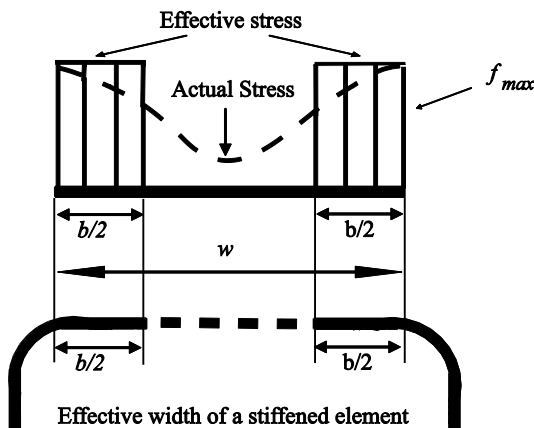


Figure 5. Effective width method

The effective width of a uniformly compressed stiffened element according to the 2007 AISI Specification (AISI-S100 2007) is expressed as

$$\begin{aligned} b &= w && \text{when } \lambda \leq 0.673, \\ b &= \rho w && \text{when } \lambda > 0.673, \end{aligned} \quad (8)$$

where w is the flat width of the element and ρ is the local reduction factor given by

$$\rho = (1 - 0.22/\lambda)/\lambda. \quad (9)$$

Here, λ is the slenderness factor given by

$$\lambda = \sqrt{f/F_{cr}}, \quad (10)$$

and f is the stress in the compression element. The column buckling stress, F_{cr} is given by

$$F_{cr} = k \frac{\pi^2 E}{12(1-\mu^2)} \left(\frac{t}{w} \right)^2, \quad (11)$$

where the plate buckling coefficient, $k = 4$ for a long simply supported plate, E is the modulus of elasticity of steel, t is the thickness of uniformly compressed stiffened element and μ is Poisson's ratio. For the case of a uniformly compressed infinitely long unstiffened element, the plate buckling coefficient is taken as $k = 0.43$. Once, the effective width, b , is determined, the effective area, A_e , can be found by summing the effective width, b over all the elements.

2.1.2 Distortional Buckling Limit State

Distortional buckling is characterized by instability of a compressed flange and involves rotation at the junction of the web and the flange in open cross-sections, e.g., C-sections and Z-sections. Distortional buckling occurs at half-wavelengths between the local and the flexural or the flexural-torsional buckling modes. The distortional buckling strength is calculated as follows:

For $\lambda_d \leq 0.561$; $P_n = P_y$,

$$\text{For } \lambda_d > 0.561; P_{nd} = \left[1 - 0.25 \left(\frac{P_{crd}}{P_y} \right)^{0.6} \right] \left(\frac{P_{crd}}{P_y} \right)^{0.6} P_y, \quad (12)$$

where $\lambda_d = \sqrt{P_y/P_{crd}}$, $P_y = A_g F_y$ and $P_{crd} = A_g F_d$, where A_g is the gross area of the cross-section and F_d is the elastic distortional buckling stress. The Main Specification (AISI-S100 2007) allows the use of a rational buckling analysis to calculate the elastic distortional buckling stress with freely available finite strip programs, for example, CUFSM (Schafer and Ádàny 2006), which is used in this research. The Specification (AISI-S100 2007) also provides simplified equations to calculate the elastic distortional buckling stress.

2.1.3 Capacity of Angle Columns

AISI provides additional design considerations for predicting the strength of angle columns which were added to the 1986 Specification (AISI 1986) on the basis of recommendations made by Peköz (1987). During his research, Peköz found the possibility of a reduction in the column strength due to the initial out-of-straightness (sweep) of angle sections and he recommended the use of an initial out-of-straightness of $L / 1000$. However, Popovic (1999) found that the inclusion of the additional moment due to the initial out-of-straightness made the predictions too conservative and recommended that the additional moment be applied only for angle sections whose effective area (A_e) at stress F_y is less than A_g , or in other words, a slender angle section.

The angle column capacity, P_n , is calculated including the compressive axial force and moment with an interaction equation:

$$\frac{\phi_c P_n}{\phi_c P_{no}} + \frac{\phi_c P_n L/1000}{\phi_b M_{ny}} \leq 1.0. \quad (13)$$

Here, P_{no} is the nominal axial capacity and M_{ny} is the flexural strength of the gross cross-section about the y-axis (see Figure 4).

The equal leg angle is a singly-symmetric section and hence nominal flexural strength, M_n , corresponding to global buckling is calculated according to equation C3.1.2.1-1 of the Main Specification (AISI-S100 2007):

$$M_n = S_c F_c \quad (14)$$

where, S_c is the elastic section modulus of the effective section calculated relative to the extreme compression fiber at F_c . The stress, F_c , is the critical global buckling stress and is determined as follows:

$$\begin{aligned} \text{For } 2.78F_y > F_e > 0.56F_y; \quad F_c = \frac{10}{9} F_y \left(1 - \frac{10F_y}{36F_e} \right) \\ \text{For } F_e \leq 0.56F_y; \quad F_c = F_e \end{aligned} \quad (15)$$

where F_e is the elastic critical global buckling stress calculated according to equation C3.1.2.1-10 of the Main Specification (AISI-S100 2007):

$$F_e = \frac{C_s A \sigma_{ex}}{C_{TF} S_f} \left[j + C_s \sqrt{j^2 + r_o^2 (\sigma_t / \sigma_{ex})} \right] \quad (16)$$

$$\sigma_{ex} = \frac{\pi^2 E}{(K_x L_x / r_x)^2} \quad (17)$$

$$\sigma_t = \frac{1}{A r_o^2} \left[GJ + \frac{\pi^2 E C_w}{(K_t L_t)^2} \right] \quad (18)$$

$$C_{TF} = 0.6 - 0.4(M_1 / M_2). \quad (19)$$

The effective length factors, K_x and K_y are for bending about the centroidal x -axis and y -axis respectively, K_t is the effective length factor for twisting, r_x and r_y are the radii of gyration of the cross-section about the centroidal principal axes, r_o is the polar radius of gyration of the cross-section about the shear center, $C_s = +1$ for moment causing compression on the shear center side of centroid and $C_s = -1$ for moment causing tension on the shear center side of centroid, M_1 and M_2 are the smaller and larger bending moments at the ends of the unbraced length in the plane of bending respectively, and L_x , L_y and L_t are the unbraced lengths for bending about x and y axes and twisting respectively.

2.2 Direct Strength Method

The AISI Direct Strength Method (DSM) uses cross-section elastic buckling behavior to predict column strength. Three elastic buckling modes are considered for CFS compression members – local, distortional and global, wherein the global mode includes flexural, torsional, or flexural-torsional buckling. The local buckling mode is determined for a member as a whole and not on an element-by-element basis as in the effective width method described in Eqs. (8) to (11). This research makes use of the finite strip analysis to perform the cross-section stability analysis, which is a specialized variant of the finite element method (Schafer and Ádàny 2006). Figure 6 presents an elastic buckling curve for a lipped C-section in pure compression obtained using CUFSM, a freely available program that employs the finite strip method to perform elastic buckling analysis of a CFS member.

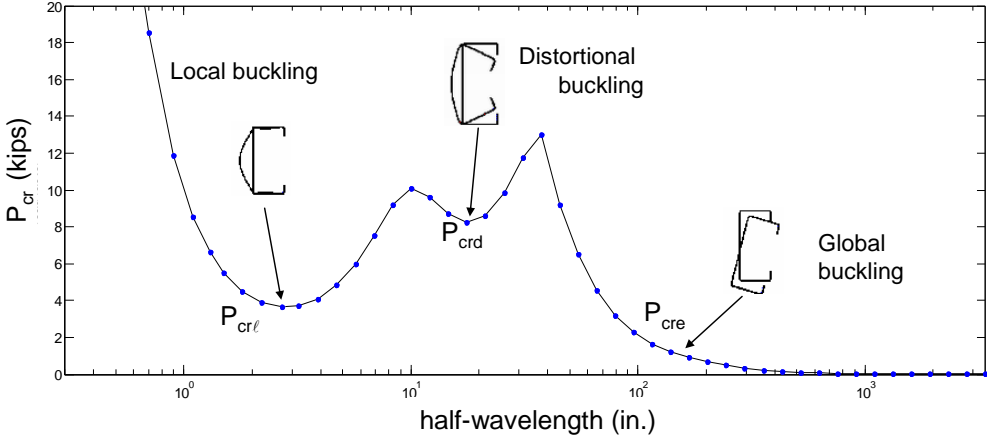


Figure 6. Elastic buckling curve generated using CUFSM

It can be observed from Figure 6 that for the considered lipped C-section in pure compression, the elastic buckling load for local buckling, P_{crl} , is lower than the elastic buckling load for distortional buckling, P_{crd} . Local buckling occurs at short half-wavelengths and buckling modes occurring at longer half-wavelengths are either distortional or global in nature.

According to Appendix 1 of the 2007 AISI Specification (AISI-S100 2007), the nominal axial strength (P_n) of a CFS column using DSM is:

$$P_n = \min(P_{n\ell}, P_{nd}, P_{ne}) \quad (20)$$

where $P_{n\ell}$, P_{nd} and P_{ne} are the nominal axial strengths for local, distortional and flexural, torsional or flexural-torsional buckling failures respectively. The nominal global capacity, P_{ne} is calculated with the same column curve described in Eq.(4), where $P_{ne} = F_n A_g$.

The nominal axial strength for local buckling, $P_{n\ell}$, is calculated as follows:

$$\text{For } \lambda_\ell \leq 0.776, \quad P_{n\ell} = P_{ne}, \quad (21)$$

$$\text{For } \lambda_\ell > 0.776 \quad P_{nl} = \left[1 - 0.15 \left(\frac{P_{crl}}{P_{ne}} \right)^{0.4} \right] \left(\frac{P_{crl}}{P_{ne}} \right)^{0.4} P_{ne}, \quad (22)$$

where $\lambda_\ell = \sqrt{P_{ne}/P_{crl}}$ where, P_{crl} is the elastic local buckling load determined using elastic buckling analysis. The distortional buckling capacity, P_{nd} , is calculated using Eq. (12) described earlier in Section 2.1.2.

Chapter 3 presents the CFS column test database which consists of 675 columns tests from 22 different experimental programs. The strength of each column present in the database is predicted using the AISI Main Specification and DSM equations presented in this chapter.

Chapter 3: CFS Column Test Database

3.1 Overview of Database

This chapter presents the CFS column test database which will be used to calculate the resistance factor, ϕ_c . When the resistance factor, ϕ_c , was first calculated for CFS members(AISI 1991), test results from 264 column tests were used.Given that since then, numerous column tests have been conducted, this study aimed at collecting as much data as possible. Thus the motivation behind this study was to expand the existing column data set with columntests of every kind – short, long and intermediate length columns that are either singly symmetric (C-sections, angle sections and hat sections)oranti-symmetric (Z-sections). An effort has also been made to collect data from experimental programs considering columns with holes. These holes are of different shapes – circular(Ortiz-Colberg 1981; Sivakumaran 1987), square(Pu et al. 1999; Sivakumaran 1987), oval (Sivakumaran 1987), rectangular (Miller and Peköz 1994) and slotted (Moen and Schafer 2008).

The CFS column test database contains a total of 675 columns testsfrom 22 different experimental programs. Plain and lipped C-sections, Z-sections, plain and lipped angle sections and hat sections, inclusive of members with holes, have been considered in this study. Doubly symmetric columns such as built-up I-sections (Weng and Pekoz 1990), (DeWolf et al. 1974) and box sections (DeWolf et al. 1974)have not been considered in this study. Eccentrically loaded columns(Loh and Peköz 1985) are also not considered in this study. Table 1provides a summary of the experimental programs included in the database. It also presents the maximum and minimum ratios of cross-sectional dimensions.

Table 1.CFS column test database

Reference	Section type	Holes	n	B/t		H/t		D/t		D/B		h_{hole}/H		λ_c	
				min	max	min	max	min	max	min	max	min	max	min	max
Thomasson 1978	Lipped C		13	69	159	207	472	14.0	32.4	0.2	0.2	---	---	0.9	1.2
Loughlan 1979	Lipped C		33	30	80	91	226	10.9	32.8	0.4	0.4	---	---	0.6	1.1
Dat 1980	Lipped C		43	19	23	33	41	8.3	10.1	0.4	0.4	---	---	0.4	1.9
Desmond et al. 1981	Lipped C		7	26	30	37	39	2.2	8.9	0.1	0.3	---	---	0.1	0.2
Desmond et al. 1981	Hat		11	51	51	42	42	7.5	29.9	0.2	0.6	---	---	0.2	0.4
Ortiz-Colberg 1981	Lipped C	✓	32	21	33	46	72	6.7	10.4	0.3	0.3	0.1	0.5	0.2	1.4
Ortiz-Colberg 1981	Lipped C		11	21	33	46	72	6.6	10.4	0.3	0.3	---	---	0.2	1.4
Mulligan 1983	Lipped C		37	33	100	64	355	7.4	21.3	0.2	0.2	---	---	0.1	1.1
Wilhoite et al. 1984	Plain Angles		7	23	23	---	---	---	---	---	---	---	---	1.9	2.0
Sivakumaran 1987	Lipped C	✓	42	26	32	58	118	7.9	9.8	0.3	0.3	0.2	0.6	0.2	0.2
Sivakumaran 1987	Lipped C		6	26	32	58	118	7.9	9.8	0.3	0.3	---	---	0.2	0.2
Polyzois, D. et al. 1993	Plain Z		13	30	51	77	137	---	---	---	---	---	---	0.2	0.5
Polyzois, D. et al. 1993	Lipped Z		72	35	56	76	137	2.4	36.2	0.1	0.7	---	---	0.1	0.4
Miller and Peköz 1994	Lipped C		43	17	40	43	175	5.2	9.0	0.2	0.3	---	---	0.2	2.8
Miller and Peköz 1994	Lipped C	✓	37	19	40	47	173	5.7	9.5	0.2	0.3	0.4	0.8	0.1	3.0
Moldovan 1994	Plain C		35	20	35	20	53	---	---	---	---	---	---	0.1	1.2
Moldovan 1994	Lipped C		29	19	46	32	65	6.3	13.7	0.2	0.4	---	---	0.1	1.0
Abdel-Rahman and Sivakumaran 1998	Lipped C	✓	8	22	33	80	108	6.9	10.3	0.3	0.3	0.3	0.4	0.1	0.2
Young and Rasmussen 1998a	Lipped C		12	25	34	66	66	8.0	8.6	0.2	0.3	---	---	0.2	1.7
Young and Rasmussen 1998b	Plain C		14	25	34	64	67	---	---	---	---	---	---	0.2	2.0
Popovic et al. 1999	Plain Angles		12	11	22	---	---	---	---	---	---	---	---	0.9	1.8
Pu et al. 1999	Lipped C	✓	30	43	65	82	122	13.3	20.0	0.3	0.3	0.2	0.4	0.1	0.1
Pu et al. 1999	Lipped C		6	43	65	82	122	13.3	20.0	0.3	0.3	---	---	0.1	0.1
Shanmugam and Dhanalakshmi 2001	Plain Angles		3	20	63	---	---	---	---	---	---	---	---	1.6	4.9
Young and Hancock 2003	Lipped C		42	21	68	41	68	4.7	7.4	0.1	0.2	---	---	0.7	0.9
Young 2004	Plain Angles		24	38	62	---	---	---	---	---	---	---	---	3.0	5.1
Chodraui et al. 2006	Plain Angles		4	25	25	---	---	---	---	---	---	---	---	1.7	2.0
Young and Chen 2008	Lipped Angles		25	44	84	---	---	9.1	17.4	0.2	0.2	---	---	0.4	4.2
Moen and Schafer 2008	Lipped C		12	36	43	92	139	7.8	11.1	0.2	0.3	---	---	0.3	0.7
Moen and Schafer 2008	Lipped C	✓	12	37	42	91	146	8.3	12.2	0.2	0.3	0.2	0.4	0.3	0.8

In all, there are a total number of 455 lipped C-sections, 72 lipped Z-section columns, 49 plain C-section columns, 13 plain Z-section columns, 50 plain angle columns, 25 lipped angle columns and 11 hat columns. Of the 455 lipped C-section columns, 161 contain holes. The Z-section, hat and anglecolumns do not containholes. Details about each experimental program including the boundary conditions, range of dimensions, and experimental set up are provided in Section 3.2.

3.2 Experimental Program Details

In this study, the predicted strengths were calculated for all the column test results summarized in Table 1 with the Main Specification and DSM. This section provides details about each experimental program. Full details of each study, including the dimensions and end restraints are provided in Appendix 1. Figure 7 presents a pictorial representation of the boundary conditions.

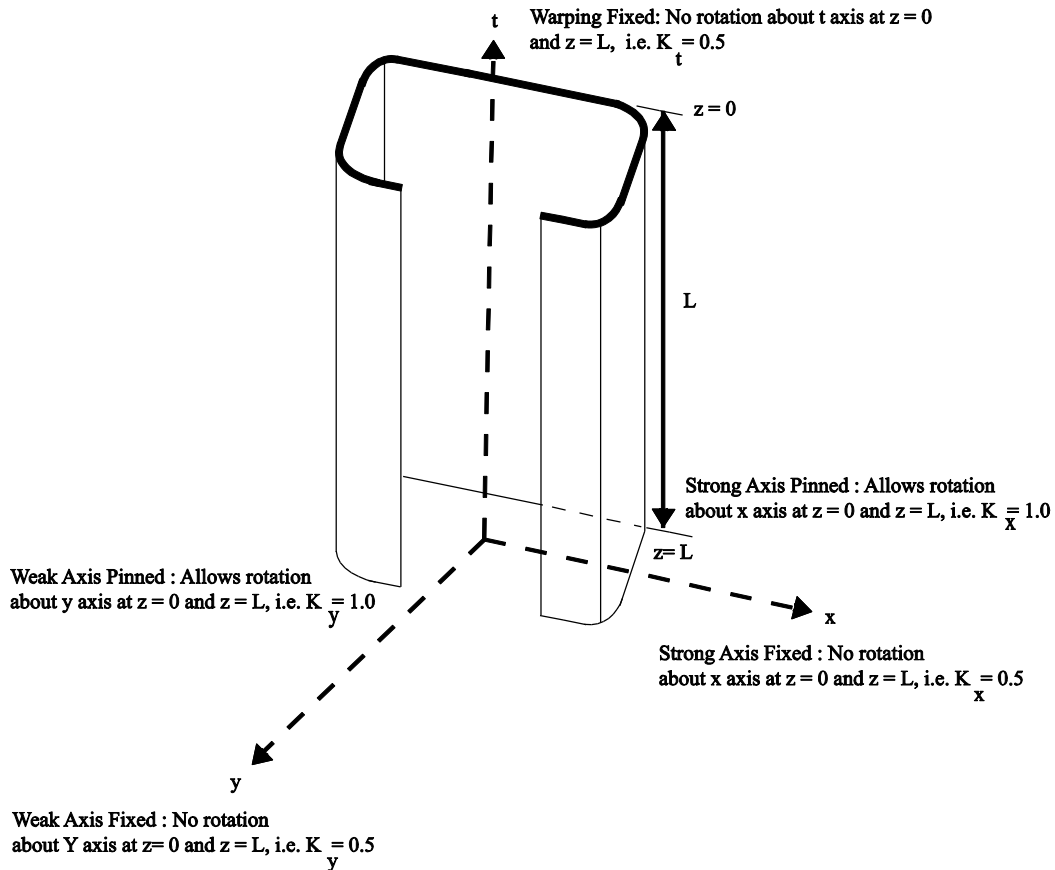


Figure 7. Boundary conditions definition.

The first set of column tests in the database were performed by Thomasson(1978) and consisted of a total of 13 lipped C-section columns. The web heights, lip and flange lengths of the columns were summarized by Peköz (1987) and Schafer (2000). The length of all the

members was kept constant at 105.9 inches. While there are minute differences in the web height, flange length and lip length of the members, there is a considerable difference in specimen thickness (0.025 in. to 0.055 in.) and this affects the local buckling behavior. Column tests were conducted assuming that the weak axis was pinned (warping free) and the other axes were fixed (warping fixed), i.e., effective length factors were $K_x = 0.5$, $K_y = 1.0$, and $K_t = 0.5$.

The next set of data was produced by Loughlan (1979) as summarized by Schafer (2000) consists of 33 lipped C-section columns differing in web height, lip and flange lengths. The thickness of all the examined sections ranged between 0.032 in. and 0.064 in. All the examined members were of intermediate lengths between 51 in. and 75 in. Strength predictions were made by assuming that the weak axis was pinned (warping free) and the other axes were fixed (warping fixed), i.e., effective length factors were $K_x = 0.5$, $K_y = 1.0$, and $K_t = 0.5$.

Research by Dat (1980) consisted of 43 lipped C-section columns without holes. The columns were made by roll-forming and by press-braking and were called rolled-formed channels (RFC) and press-baked channels (PBC) respectively. The thickness of all the examined sections was between 0.073 in. and 0.09 in. The lengths used in this study vary between 21 in. and 100 in. In the actual tests, the load was applied using the static method, wherein the load was slowly increased and stabilized at every load increment. Dat employed end fixtures that acted as knife edges allowing rotation only in the y direction. Thus for this experimental program, strength predictions were made by assuming that the y-axis was pinned, while the other axes are fixed, i.e. $K_x = 0.5$, $K_y = 1.0$, and $K_t = 0.5$.

Data from Desmond et al. (1981) consisted of 7 lipped C-section columns and 11 hat section columns without holes. Among the 11 hat section columns, 5 had lips that were inclined at an angle of 45 degrees. The sections were all stub columns with lengths less than 20 in. and were

fixed ended (warping fixed) with effective length factors $K_x = 0.5$, $K_y = 0.5$, and $K_t = 0.5$. This experimental program studied the effect of edge stiffeners on the local buckling behavior of the flange.

In the same year, Ortiz-Colberg (1981) presented his Master's thesis on column tests of 32 lipped C-section columns with holes and 11 lipped C-section columns without holes. The thickness of all the examined sections was between 0.049 in. and 0.076 in. The holes were all circular in shape and the data consisted of stub columns as well as intermediate and long columns. The stub columns were fixed-ended (warping fixed) with effective length factors $K_x = 0.5$, $K_y = 0.5$, and $K_t = 0.5$ while the intermediate and long columns were weak axis pinned, i.e. $K_x = 0.5$, $K_y = 1.0$, and $K_t = 0.5$.

The next experimental program conducted by Mulligan (1983) presented 37 lipped C-section columns without holes. There were 24 stub columns and 13 long columns. The thickness of all the examined sections was approximately 0.045 in. The stub columns were fixed-ended (warping fixed) with effective length factors $K_x = 0.5$, $K_y = 0.5$, and $K_t = 0.5$ while the long columns were weak axis pinned, i.e. $K_x = 0.5$, $K_y = 1.0$, and $K_t = 0.5$.

Soon after Mulligan, Wilhoite et al. (1984), analyzed 7 angle section columns. The columns were all equal legged and made of high strength press-braked steel. The thickness of all the examined sections was approximately 0.117 in. The long columns were weak axis pinned with effective length factors $K_x = 0.5$, $K_y = 1.0$, and $K_t = 0.5$.

Sivakumaran (1987) presented a total of 48 lipped C-section columns, of which 42 sections had holes and 6 sections did not contain holes. The holes were circular, square or oval in shape. The hole sizes ranged from 20% to 60% of the web flat width. The columns lengths

ranged between 8.0 in. and 10.3 in. The tests were conducted under flat pinned end conditions i.e. $K_x = 0.5$, $K_y = 1.0$, and $K_t = 0.5$.

The first and the only set of tests on Z-sections considered in this study was performed by Polyzois et al. (1993). This program consisted of 85 Z-section columns, of which 13 were plain Z-section columns and 72 were lipped Z-section columns. The columns were 18, 24 or 48 in. long and had an average thickness of approximately 0.058 in. The columns in this program were tested with fixed-fixed end conditions i.e. $K_x = 0.5$, $K_y = 0.5$, and $K_t = 0.5$.

Miller et al.(1994)performed an experimental program that consisted of a total of 80 lipped C-section columns of which 37 had holes. Among the 80 lipped C-sections, 44 were stub columns. Holes were present in 20 of the 44 stub columns. The stub columns ranged between 11 in. and 21 in. long while the long columns were between 47 in.and 100 in. long. The holes were rectangular in shape and varied in number, with some sections containing as many as 4 holes. The length, depth and the spacing of the holes are presented in Appendix 1. The stub columns were assumed to be fixed i.e. $K_x = 0.5$, $K_y = 0.5$, and $K_t = 0.5$ and for the long columns, rotation at the ends was free about one axis and fixed about the other for each test i.e. $K_x = 0.5$, $K_y = 1.0$, and $K_t = 0.5$ and also $K_x = 1.0$, $K_y = 0.5$, and $K_t = 0.5$.

Moldovan(1994)tested 64 C-section columns,of which 35 were plain C-section columns and 29 were lipped C-section columns. Of the 64 columns, 27 were stub columns with lengths ranging between 9 in. and 15 in. The long column lengths ranged between 42 in. and 78 in. The thickness of the lipped C-section columns varied between 0.070 in. and 0.120 in. while for plain C-section columns it varied between 0.070 in. and 0.160 in. The stub columns were assumed to be fixed i.e. $K_x = 0.5$, $K_y = 0.5$, and $K_t = 0.5$, while the long columns were assumed to have their weak axis pinned i.e. $K_x = 0.5$, $K_y = 1.0$, and $K_t = 0.5$.

Abdel-Rahman et al. (1998) conducted tests on 8 lipped C-section columns with holes. All 8 columns were stub columns with lengths ranging between 9 in. and 18 in. The holes were circular, square, rectangular or oval in shape. The thickness varied between 0.050 in. and 0.070 in. The columns are all fixed-ended with effective length factors, $K_x = 0.5$, $K_y = 0.5$, and $K_t = 0.5$.

In 1998, Young and Rasmussen published two papers, one containing 12 lipped C-section columns(1998a) and the other containing 14 plain C-section columns(1998b), both without any holes in the specimens. The columns ranged from stub columns to long columns i.e. between 11.0 in. and 118.0 in. long. The thickness of all the columns was approximately 0.058 in. and all columns were fixed-ended columns with effective length factors, $K_x = 0.5$, $K_y = 0.5$, and $K_t = 0.5$.

Popovic (1999) conducted tests on 12 plain angle section columns. The length of the angles varied between 21 in. and 101 in. while the thickness ranged from 0.090 in. to 0.180 in. The angles were equal-legged and their legs ($B1$ and $B2$) were 1.95 in. long. All angles in this program were fixed-ended with effective length factors, $K_x = 0.5$, $K_y = 0.5$, and $K_t = 0.5$.

The database also contains 36 lipped C-section column tests conducted by Pu et al.(1999). Of the 36 lipped C-section columns in this experimental program, 30 contained holes in them. Although 63 lipped C-section columns are presented, only 36 are considered in the present study. Columns with edge holes have been neglected while columns with a hole in the center of the web have been considered. Columns with holes that are a quarter of the web width away from the edge on the same side were considered as just one hole that extends from one side to the other as shown in Figure 8 when calculating the capacity (see Appendix 1). The columns were all stub columns approximately 14 inches in length and the holes were all square in shape. All the 36 lipped C-sections were assumed to be fixed-ended with effective length factors, $K_x = 0.5$, $K_y = 0.5$, and $K_t = 0.5$.

Shanmugam (2001) tested 3 plain angle section stub columns with equal legs with lengths ranging from 5 in to 12 in. All the columns were assumed to be fixed ended with effective length factors, $K_x = 0.5$, $K_y = 0.5$, and $K_t = 0.5$.

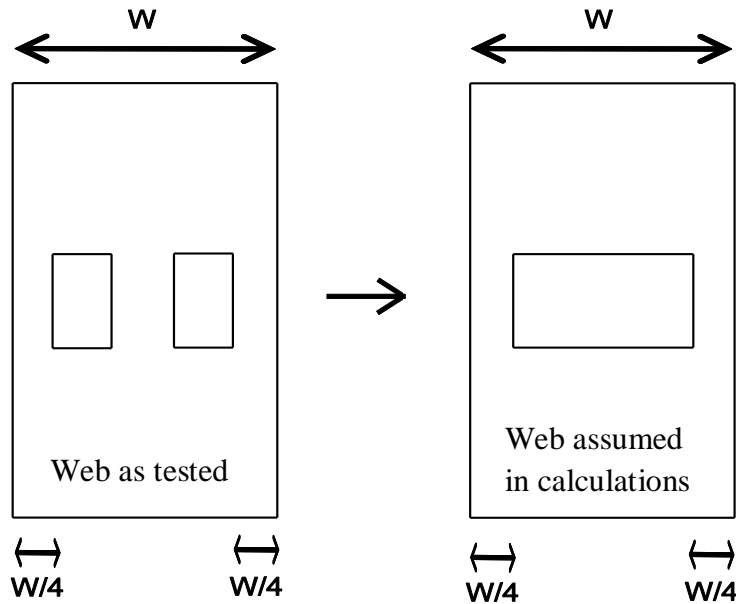


Figure 8. Web of the lipped C-section column for Pu specimens(Pu et al. 1999)

Young and Hancock (2003) conducted an experimental program on 42 lipped C-section columns. All the columns were of approximately the same length of 58 in. The columns had a nominal thickness that ranged between 0.060 in. and 0.090 in. The columns contained edge stiffeners that were inclined at different angles between 30 degrees and 150 degrees. Both inward and outward edge stiffeners were considered and the columns were compressed between fixed ends i.e. $K_x = 0.5$, $K_y = 0.5$, and $K_t = 0.5$.

Young(2004) also performed experiments on 24 plain angle columns. The length of the columns ranged between 9 in. and 136 in. The angles were all equal-legged and their thickness ranged from 0.045 in. to 0.073 in. The angle columns had fixed-fixed end conditions i.e. $K_x = 0.5$, $K_y = 0.5$, and $K_t = 0.5$.

Chodraui (2006) tested 4 plain angle columns. The column lengths varied between 24 in. and 66 in. Again, all the 4 angles were equal-legged and had a thickness of 0.090 inches. Strength predictions of all columns in this experimental program were made by assuming that the weak axis was pinned, i.e. $K_x = 0.5$, $K_y = 1.0$, and $K_t = 0.5$.

Young and Chen (2008) performed tests on 25 lipped angle columns of unequal flange width. The lengths of the angle columns ranged between 9 in. and 117 in. The angle columns had a nominal thickness that ranged between 0.038 in. and 0.073 in. All the angle columns in this program were fixed-ended with effective length factors, $K_x = 0.5$, $K_y = 0.5$, and $K_t = 0.5$.

Moen and Schafer (2008) tested a total of 24 lipped C-section columns, of which 12 had slotted holes in them. The length of the columns ranged between 24 in. and 48 in. The thickness of the columns was about 0.04 inches and they were all fixed-ended with effective length factors, $K_x = 0.5$, $K_y = 0.5$, and $K_t = 0.5$.

The strength of each column discussed in this chapter is predicted using the AISI Main Specification and DSM. In Chapter 4, the concept of a resistance factor is introduced and eventually it will be observed that resistance factor value depends on the predicted capacities. Further, Chapter 4 presents the calculated resistance factors for all the columns on the basis of cross-section type, limit state and partially and fully effective cross-sections.

Chapter 4: Resistance Factor Equations and Calculations

This chapter presents a detailed derivation of the resistance factor for both the LRFD and LSD methods in Section 4.1. The calculated resistance factors for columns in the CFS column test database according to both the Main Specification and the Direct Strength Method are presented in Section 4.2.

4.1 Resistance Factor Derivation

The resistance factor accounts for uncertainties in dimensions, material properties and strength prediction accuracy. Both the load effect, Q , and the resistance, R , are random parameters and their probability distributions are generally unknown. Only the means, Q_m and R_m and the standard deviations σ_Q and σ_R are known. Using these known values, the relative measure of safety of a design can be obtained using the reliability index, β . The following steps illustrate how the resistance factor, defined in Chapter F of the Specification (AISI-S100 2007), is derived starting with the definition of the reliability index.

Given that the exact probability distributions of the load effect, Q , and the resistance, R , are unknown, it is assumed that they follow a lognormal probability distribution and are independent. Thus the following transformations are defined:

$$\begin{aligned} X &= \ln R \\ Y &= \ln Q. \end{aligned} \tag{23}$$

Eq. (23) is of the form $Y = g(X_1, X_2, \dots, X_n)$, where X_1, X_2 and so on are random variables. The function, $g(X_1, X_2, \dots, X_n)$ is expanded using a Taylor Series expansion about the mean values:

$$Y = g(\mu_{X_1}, \mu_{X_2}, \dots, \mu_{X_n}) + \sum_{i=1}^n (X_i - \mu_{X_i}) \frac{\partial g}{\partial x_i} + \frac{1}{2} \sum_{i=1}^n \sum_{j=1}^n (X_i - \mu_{X_i})(X_j - \mu_{X_j}) \frac{\partial^2 g}{\partial x_i \partial x_j}. \quad (24)$$

The Taylor series expansion in Eq. (24) is truncated at linear terms to obtain a first order approximation for the mean and the variance. Thus the means based on a first order approximation are obtained as

$$\begin{aligned} X_m &= \ln R_m \\ Y_m &= \ln Q_m. \end{aligned} \quad (25)$$

Again, the variance of X based on first order approximation is obtained by differentiating the mean, X_m , with respect to the mean of the resistance, R_m :

$$\begin{aligned} \sigma_x^2 &= \left[\frac{d}{dR} (\ln R_m) \right]^2 \sigma_R^2 \\ \Rightarrow \sigma_x^2 &= \left[\frac{1}{R_m} \right]^2 \sigma_R^2 = V_R^2, \end{aligned} \quad (26)$$

where, V_R is the coefficient of variation of resistance. Similarly, it can be shown that variance of Y is also equal to the square of the coefficient of variation of the load effect, i.e $\sigma_Y^2 = V_Q^2$. Failure, Z_m , in terms of the mean of the resistance and the load effect is defined as

$$Z_m = \ln R_m - \ln Q_m = \ln(R_m/Q_m) \quad (27)$$

Since, the load effect, Q , and the resistance, R , are lognormal distributions, $\ln Q$ and $\ln R$ will become normally distributed. Thus failure, Z , is also normally distributed. The probability of failure, p_f , is expressed as

$$p_f = P(Z \leq 0) = 1 - \Phi\left(\frac{Z_m}{\sigma_Z}\right), \quad (28)$$

where, the standard deviation of z , $\sigma_z = \sqrt{V_R^2 + V_Q^2}$. The term, $\Phi(z)$, represents the area under the normal curve until the value of z . If the value of z is negative, then using the symmetric property of the normal curve, $\Phi(-z)$ can be denoted by $1-\Phi(z)$, as shown in Figure 9.

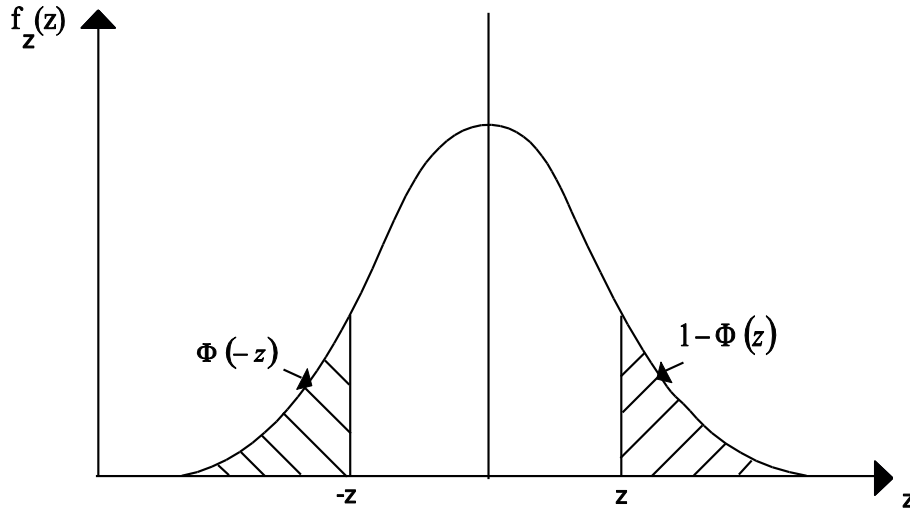


Figure 9. The normal distribution curve

Substituting Eq. (27) in Eq. (28),

$$p_f = 1 - \Phi \left(\frac{\ln(R_m/Q_m)}{\sqrt{V_R^2 + V_Q^2}} \right) = 1 - \Phi(\beta) \quad (29)$$

Thus, the reliability index, β , as established by Ravindra and Galambos (1978), according to first order approximation, is expressed as

$$\beta = \frac{\ln(R_m/Q_m)}{\sqrt{V_R^2 + V_Q^2}} \quad (30)$$

The resistance of the components of a structure determines its load carrying capacity. The resistance is influenced by material properties such as the material strength, modulus of elasticity as well as dimensions of the components. This dependence of resistance on the material properties and the dimensions of components induce an element of uncertainty. Three different

parameters, M , F and P are used to model the resistance including this uncertainty. Specifically, M accounts for the variation in the strength of the material, F accounts for the fabrication errors that result in variations in dimensions and P is used to account for the uncertainty arising from the chosen approximate method of strength prediction. In this research, the chosen methods of strength prediction are the Main Specification and DSM, which are used to predict the strengths of all the columns in the test database discussed in Chapter 3 and the test-to-predicted strength ratio provides a measure of the Professional factor, P . The product of the three parameters (M , F and P) and the nominal resistance (R_n), which is the strength of an element computed for nominal section properties and the specified material properties for a particular limit state, represents the actual resistance R . Thus the mean resistance, R_m can be expressed as

$$R_m = R_n (M_m F_m P_m). \quad (31)$$

The mean value of the load effect can be expressed as a function of the mean values of dead and live load intensities, D_m and L_m as follows:

$$Q_m = C(D_m + L_m), \quad (32)$$

where, C is the deterministic influence coefficient. Thus the coefficient of variation of resistance, V_R can be expressed in terms of the coefficients of variation of material properties, geometric properties and the test to predicted strength ratio, V_M , V_F and V_P respectively and V_R is expressed as

$$V_R = \sqrt{V_M^2 + V_F^2 + V_P^2}. \quad (33)$$

The coefficient of variation of the load effect, V_Q can be expressed in terms of the coefficients of variation of the dead and the live loads (V_D and V_L), and the mean values of the dead and live load intensities, D_m and L_m as

$$V_Q = \frac{\sqrt{D_m^2 V_D^2 + L_m^2 V_L^2}}{D_m + L_m}. \quad (34)$$

Hsiao(1990) developed the LRFD criteria for CFS members and suggested use of the values $M_m = 1.10, V_m = 0.10, F_m = 1.00, V_F = 0.05, D_m = 1.05D_n, V_D = 0.10, L_m = L_n, V_L = 0.25$. It can be seen that the coefficient of variation of the live load (V_L) is higher than the coefficient of variation of the dead load (V_D) indicating that the uncertainty with respect to the live load is higher.

Using the values recommended by Hsiao, the expressions for the mean resistance, R_m , in Eq. (31), the coefficient of variation of resistance, V_R , in Eq. (33) and the coefficient of variation of the load effect, V_Q , in Eq. (34), can be expressed as

$$R_n = \frac{R_m}{1.10P_m},$$

$$V_R = \sqrt{0.0125 + V_p^2},$$

$$V_Q = \frac{\sqrt{\left(1.05 \frac{D_n}{L_n}\right)^2 0.10^2 + 0.25^2}}{\left(1.05 \frac{D_n}{L_n}\right) + 1.0}. \quad (35)$$

The resistance factor, ϕ_c , the nominal resistance, R_n , the nominal values of the dead and live loads, D_n and L_n , and the load factors, α_D and α_L are related by the following equation:

$$\phi_c R_n = C(\alpha_D D_n + \alpha_L L_n), \quad (36)$$

where the deterministic influence coefficient, C , transforms the dead and live load intensities into load effects. Using the expression for the nominal resistance, R_n , in Eq. (35), Eq. (36) can be expressed as

$$\begin{aligned} \phi_c \frac{R_m}{1.10P_m} &= CL_n \left(\alpha_D \frac{D_n}{L_n} + \alpha_L \right) \\ \Rightarrow CL_n &= \frac{\phi_c \frac{R_m}{1.10P_m}}{\left(\alpha_D \frac{D_n}{L_n} + \alpha_L \right)} \end{aligned} \quad (37)$$

Using the values recommended by Hsiao, the mean value of the load effect, in Eq. (32), can be expressed as

$$\begin{aligned} Q_m &= CL_n \left(1.05 \frac{D_n}{L_n} + 1 \right) \\ \Rightarrow CL_n &= \frac{Q_m}{\left(1.05 \frac{D_n}{L_n} + 1 \right)}. \end{aligned} \quad (38)$$

Equating Eqs. (37)and (38), the following expression is obtained:

$$\frac{Q_m}{\left(1.05 \frac{D_n}{L_n} + 1 \right)} = \frac{\phi_c \frac{R_m}{1.10P_m}}{\left(\alpha_D \frac{D_n}{L_n} + \alpha_L \right)} \quad (39)$$

From Eq. (39), the ratio of the means of the resistance (R_m) to the load effect (Q_m) can be expressed as

$$\frac{R_m}{Q_m} = \frac{1.10P_m \left(\alpha_D \frac{D_n}{L_n} + \alpha_L \right)}{\phi_c \left(1.05 \frac{D_n}{L_n} + 1 \right)} \quad (40)$$

The ratio of the mean resistance to the mean load effect (R_m/Q_m) from Eq. (40), the coefficient of variation of resistance, V_R , and the coefficient of variation of the load effect, V_Q , from Eq. (35) are substituted in Eq. (30) and the following expression is obtained:

$$\beta = \sqrt{\frac{\ln \left(\frac{1.10P_m \left(\alpha_D \frac{D_n}{L_n} + \alpha_L \right)}{\phi_c \left(1.05 \frac{D_n}{L_n} + 1 \right)} \right)}{0.0125 + V_p^2 + \frac{\left(1.05 \frac{D_n}{L_n} \right)^2 0.10^2 + 0.25^2}{\left(1.05 \frac{D_n}{L_n} + 1.0 \right)^2}}} \quad (41)$$

Thus, rearranging the terms in Eq. (41), the expression for the resistance factor, ϕ_c , of a cold-formed steel column is as follows:

$$\phi_c = \frac{1.10P_m \left(\alpha_D \frac{D_n}{L_n} + \alpha_L \right)}{\left(1.05 \frac{D_n}{L_n} + 1 \right) \exp \left(\beta \sqrt{0.0125 + V_p^2 + \frac{\left(1.05 \frac{D_n}{L_n} \right)^2 0.10^2 + 0.25^2}{\left(1.05 \frac{D_n}{L_n} + 1.0 \right)^2}} \right)} \quad (42)$$

Equation(42) is an approximate equation for the resistance factor, ϕ , and is a function of the nominal dead-to-live load ratio (D_n/L_n), the load factors, α_D and α_L , the reliability index, β , the

mean of the test-to-predicted results, P_m , and the coefficient of variation of the test-to-predicted results, V_P . It was discussed earlier that P is a professional factor associated with the accuracy of the method used to predict the strengths. In this study, the strengths are predicted using the AISI Main Specification and DSM and the accuracy of the methods in predicting the strength is represented by the mean and the coefficient of variation of the test-to-predicted strength ratio.

The AISI LRFD strength prediction approach uses the following values for nominal dead-to-live load ratio (D_n/L_n), the load factors, α_D and α_L , and the reliability index, β : $D_n/L_n = 1/5$, $\alpha_D = 1.2$, $\alpha_L = 1.6$, $\beta = 2.5$. Substituting these values in Eq. (42), the resistance factor, ϕ_c , for LRFD is obtained as

$$\phi_c = \frac{1.10P_m \left(1.2 \frac{1}{5} + 1.6 \right)}{\left(1.05 \frac{1}{5} + 1 \right) \exp \left(\beta \sqrt{0.0125 + V_P^2 + \frac{\left(1.05 \frac{1}{5} \right)^2 0.10^2 + 0.25^2}{\left(1.05 \frac{1}{5} + 1.0 \right)^2}} \right)}$$

$$\Rightarrow \phi_c = 1.673 P_m e^{-2.5 \sqrt{V_P^2 + 0.055}}. \quad (43)$$

Similarly, substituting the values $D_n/L_n = 1/3$, $\alpha_D = 1.25$, $\alpha_L = 1.5$, $\beta = 3.0$, in Eq. (42), the resistance factor, ϕ_c , for LSD strength prediction method is obtained as

$$\phi_c = \frac{1.10P_m \left(1.25 \frac{1}{3} + 1.5 \right)}{\left(1.05 \frac{1}{3} + 1 \right) \exp \left[\beta \sqrt{0.0125 + V_p^2 + \frac{\left(1.05 \frac{1}{3} \right)^2 0.10^2 + 0.25^2}{\left(1.05 \frac{1}{3} + 1.0 \right)^2}} \right]} \quad (44)$$

$$\Rightarrow \phi_c = 1.562P_m e^{-3.0 \sqrt{V_p^2 + 0.047}}.$$

The results of the column tests summarized in Table 1 are used to calculate P_m and V_p . The predicted compressive strength (P_n) of the 675 columns according to both the Main Specification and the DSM were computed using a custom MATLAB code. The code consists of a series of functions that obtain the input data and then calculate the nominal capacity of each cross-section. The actual code corresponding to each function is provided in Appendix 2. The code begins with a basic starting file that obtains the input data which consists of the out-to-out cross-section dimensions, boundary conditions and material properties. This input data is then sent to two other functions, *cztemplate()* and *specgeom()*, which create the actual test specimen using the provided out-to-out dimensions and then convert the out-to-out dimensions into *xy* coordinates for use in CUFSM. These coordinates are then sent to the function *cutwp_prop2()*, which calculates the sections properties. Once the section properties are calculated, the *strip()* function is used to produce the elastic buckling curve. The *ftb()* function is then used to evaluate the roots of the classical cubic buckling equation. Then the *mainspec_compression()* and *Buckling()* functions are used to calculate the compressive strength of the CFS member according to the AISI Main Specification and DSM respectively. Once the strengths are evaluated, the test-to-predicted strength ratio (P_{test}/P_n) for each column can be found. The mean of the test-to-predicted strength ratio for all the 675 columns gives P_m and the coefficient of variation of the test-to-

predicted strength ratio of all the 675 columns gives V_P . These values are then substituted in the Eq. (43) and Eq. (44) to calculate the resistance factor corresponding to LRFD and LSD respectively. The test-to-predicted strength ratio for each column test has been furnished in Appendix 1. Section 4.2 presents the resistance factor calculated for columns classified on the basis of cross-section type, limit state and partially and fully effective cross-sections.

4.2 Resistance Factor Results

This section presents the calculated resistance factors for all the columns in the CFS column test database according to both the Main Specification and the Direct Strength Method.

4.2.1 All Columns

Table 2 presents the test-to-predicted statistics and resistance factors for columns with and without holes for the Main Specification. It should be noted that the only columns that contain holes are the lipped C-section columns. The resistance factors have been calculated for each type of column for both the LRFD (ϕ LRFD) and also the LSD (ϕ LSD). The third and the sixth rows of Table 2 present the resistance factor values computed for data with dimensional properties within prescribed Main Specification limits such as the lip angle ($140^\circ \geq \theta \geq 40^\circ$), the ratio of the diameter (d_h) of the hole to the flat width (w) ($0.5 \geq d_h/w \geq 0$), the flat width-to-thickness ratio ($w/t \leq 70$), the center-to-center hole spacing, the depth of the hole and the length of the hole. Thus, for all data whose dimensional properties are within the prescribed Main Specification limits, a total of 448 column tests, we find that the resistance factor according to the Main Specification for LRFD is 0.85. It can be observed from Table 2 that the coefficient of variation (COV) increases with the number of column tests. When the number of column tests is large, it means that the column test data comes from multiple researchers thereby producing a considerable spread of test results and increasing the COV. The plain Z-section columns as well as the lipped

Z-section columns come from a single source and thus have a smaller COV. The resistance factor for LSD ($\phi = 0.68$) is found to be approximately 19% lower than the resistance factor for LRFD ($\phi = 0.85$). This can be attributed to the higher dead-to-live load ratio of 1/3 for LSD compared to 1/5 for LRFD. The LSD also uses a higher reliability index of $\beta = 3.0$ compared to $\beta = 2.5$ for LRFD and this produces a lower resistance factor. A value of 3.0 for the reliability index corresponds to the probability of failure of approximately 1 in 1000 columns while $\beta = 2.5$ corresponds to the probability of failure of approximately 6 in 1000 columns. Thus a higher value of reliability index indicates a safer design and thus it can be observed that the use of a higher safety factor lowers the resistance factor value.

Table 2. Resistance factors for columns with and without holes (Main Specification)

Type of Section	Test-to-predicted Statistics		Resistance Factor		# of tests
	Mean (P_m)	COV (V_p)	ϕ LRFD	ϕ LSD	
Plain C	1.10	0.12	0.95	0.77	49
Lipped C	1.08	0.17	0.87	0.70	455
Lipped C (within Spec dimensional limits)	1.08	0.17	0.87	0.71	303
Plain Z	1.12	0.06	1.02	0.84	13
Lipped Z	0.88	0.11	0.76	0.62	72
Hat Sections	1.34	0.06	1.21	1.00	11
All Data (within Spec dimensional limits)	1.06	0.17	0.85	0.68	448
All Data	1.06	0.17	0.85	0.69	600

4.2.2 Columns with Holes

Table 3 presents the resistance factors for only columns with holes. It is to be noted that for all columns that include holes, only the Main Specification is used to calculate the resistance factor. This is because DSM currently provides no explicit provisions to predict the capacity of columns with holes. The resistance factor has been computed separately for columns with holes whose dimensional properties are within the prescribed Main Specification limits and also for

those that are outside the prescribed limits. It can be observed that a high value of the test-to-predicted strength mean and a low value of the COV produce a high value for the resistance factor. A high value of the mean indicates that the Main Specification predictions for columns with holes are overly conservative for the specimens considered.

Table 3. Resistance factors for columns with holes (Main Specification)

Type of Section	Test-to-predicted Statistics		Resistance Factor		# of tests
	Mean (P_m)	COV (V_p)	ϕ LRFD	ϕ LSD	
Lipped C (within Spec dimensional limits)	1.17	0.12	1.01	0.83	51
Lipped C (outside Spec dimensional limits)	1.15	0.14	0.97	0.79	110
Lipped C (All hole data)	1.16	0.13	0.98	0.80	161

4.2.3 Columns without Holes

Table 4 and Table 5 present the resistance factors for columns without holes corresponding to the Main Specification and DSM respectively. Since both the Main Specification and DSM can now be employed to calculate the compressive strength, we can compare the two methods. A total of 397 columns have dimensional properties that fall within the Main Specification limits (see Appendix 1) while 390 fall within the DSM prequalified limits (see Appendix 1). A comparison between the Main Specification and DSM shows that DSM has a higher resistance factor value of 0.87 versus 0.83 for the Main Specification. In fact, except for plain C-section and hat section columns, DSM consistently produces higher resistance factor values. It should be noted that the difference between the two methods is due to the difference in the prediction of the local buckling influence on the column capacity i.e. the difference between Eq. (2) and Eq.(22). The equations used in predicting the distortional and global buckling capacity is the same in both methods. It can also be observed that DSM has a smaller COV and thus it can be said that on an average, the DSM predicts the strength more accurately.

Table 4. Resistance factors for columns without holes (Main Specification)

Type of Section	Test-to-predicted Statistics		Resistance Factor		# of tests
	Mean (P_m)	COV (V_p)	ϕ LRFD	ϕ LSD	
Plain C	1.10	0.12	0.95	0.77	49
Lipped C	1.04	0.17	0.83	0.67	294
Plain Z	1.12	0.06	1.02	0.84	13
Lipped Z	0.88	0.11	0.76	0.62	72
Hat Sections	1.34	0.06	1.21	1.00	11
All Data (within Spec dimensional limits)	1.04	0.17	0.83	0.67	397
All sections without Holes	1.03	0.18	0.82	0.66	439

Table 5. Resistance factors for columns without holes (DSM)

Type of Section	Test-to-predicted Statistics		Resistance Factor		# of tests
	Mean (P_m)	COV (V_p)	ϕ LRFD	ϕ LSD	
Plain C	1.03	0.13	0.88	0.72	49
Lipped C (within prequalified limits)	1.07	0.14	0.90	0.73	245
Lipped C (outside prequalified limits)	1.01	0.17	0.81	0.66	49
Plain Z	1.12	0.06	1.02	0.84	13
Lipped Z	0.94	0.11	0.81	0.66	72
Hat Sections	1.24	0.04	1.13	0.94	11
All data (within prequalified limits)	1.05	0.14	0.87	0.71	390
All sections without Holes	1.04	0.15	0.87	0.70	439

Figure 10and Figure 11present the plots for the test-to-predicted strength ratios versus global slenderness for the Main Specification and the DSM respectively. On comparing Figure 10 with Figure 11, it can be seen that the scatter with DSM is less than the Main Specification, indicating that the COV is lesser for DSM. It can also be observed that all hat sections and plain Z-sections have a test-to-predicted strength ratio greater than 1 showing that the strength predictions are conservative for both methods.

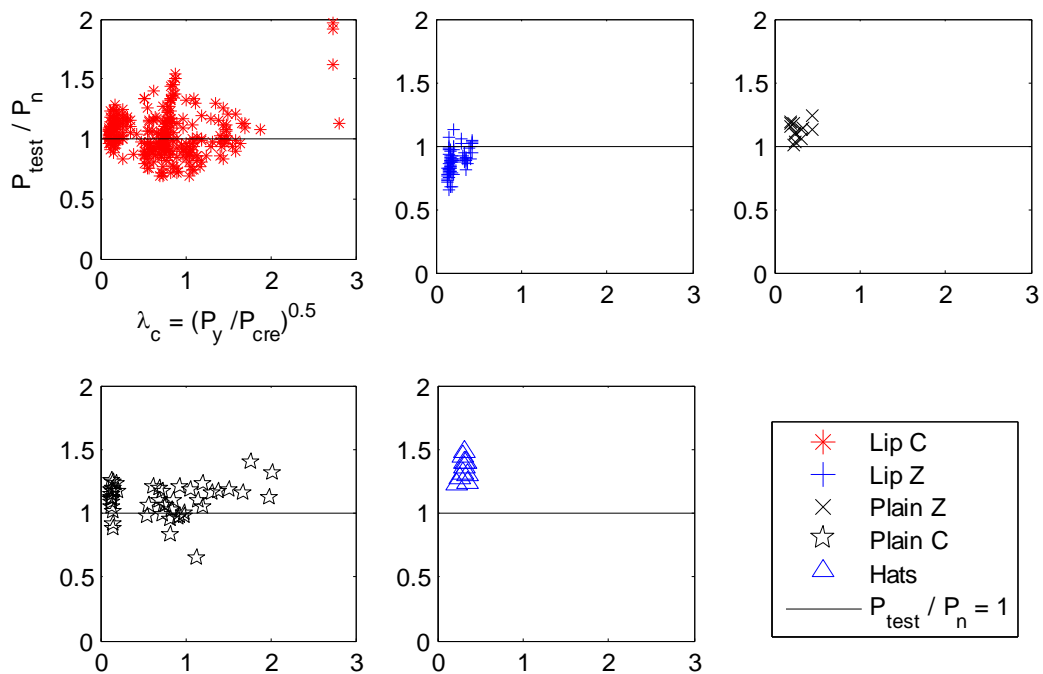


Figure 10. Main Specification test-to-predicted strength as a function of global slenderness

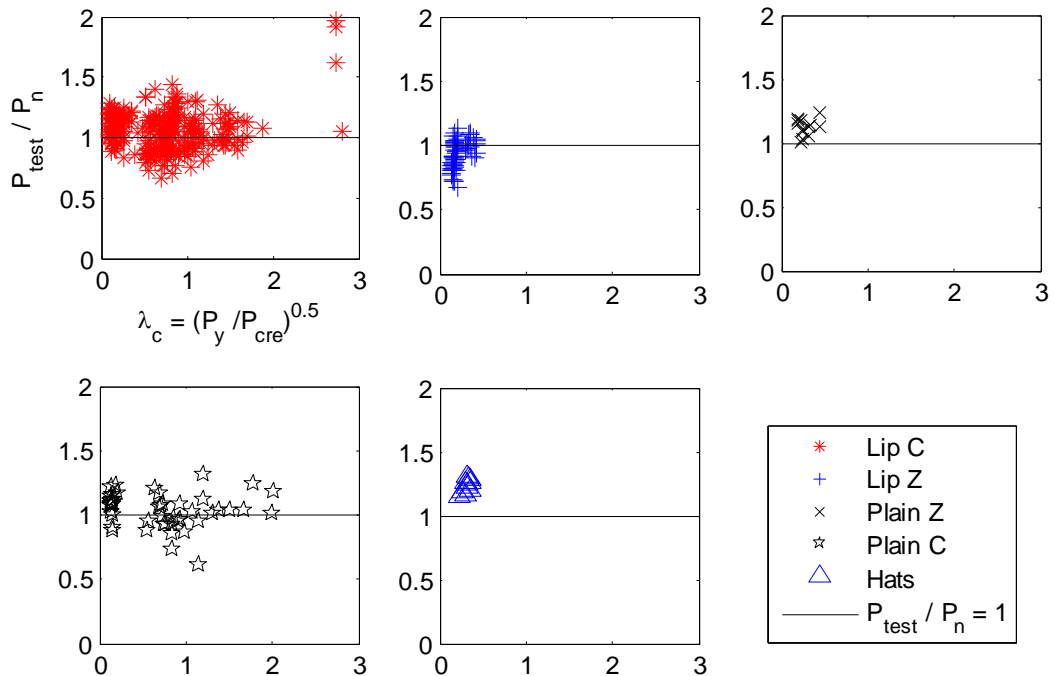


Figure 11. DSM test-to-predicted strength as a function of global slenderness

4.2.4 Partially and Fully Effective Sections

Table 6 presents resistance factors for columns without holes that are fully and partially effective respectively. For the Main Specification, it is noted that a column is considered to be fully effective when the effective area, A_e , is equal to the gross area, A_g . When the effective area, A_e , is less than the gross area, A_g , the column is considered to be partially effective. For DSM, a column is considered to be fully effective when the nominal axial strength for local buckling, $P_{n\ell}$, is equal to the nominal axial strength for flexural, torsional or flexural-torsional (global) buckling, P_{ne} . When $P_{n\ell}$ is less than P_{ne} , the column is considered to be partially effective.

The DSM resistance factor is 10 % higher than the Main Specification for partially effective cross-sections (compare $\phi_c = 0.89$ to $\phi_c = 0.81$ in Table 6), emphasizing that DSM provides improved strength prediction accuracy over a wide range of cold-formed steel columns sensitive to local buckling. The DSM and Main Specification resistance factors for fully effective sections are consistent (compare $\phi_c = 0.83$ to $\phi_c = 0.81$ in Table 6) because the same prediction equations are used in both approaches for global and distortional buckling.

Table 6. Resistance factors for partially and fully effective columns

AISI	Classification	Test-to-predicted statistics		ϕ LRFD	ϕ LSD	# of tests
		Mean (P_m)	COV (V_p)			
Main Spec	Fully effective [†]	1.04	0.19	0.81	0.65	104
	Fully effective	1.04	0.19	0.81	0.65	104
	Partially effective [†]	1.00	0.17	0.81	0.66	293
	Partially effective	1.02	0.17	0.82	0.66	335
DSM	Fully effective *	1.07	0.19	0.83	0.66	65
	Fully effective	1.04	0.19	0.81	0.65	109
	Partially effective *	1.04	0.13	0.89	0.72	325
	Partially effective	1.05	0.13	0.89	0.72	330

[†] Within Main Spec dimensional limits (see Appendix 1) * Within DSM prequalified limits (see Appendix 1)

Figure 12 presents a plot between the Main Specification test-to-predicted strength ratio versus the effective-area-to-gross-area ratio and Figure 13 presents a plot between the DSM test-to-predicted strength ratio versus the local buckling strength-to-global buckling strength ratio. From Figure 12, for the lipped C-sections, it can be observed that as the predictions are more conservative for fully effective sections ($A_e/A_g = 1$). A similar trend is also observed for DSM in Figure 13, and this trend is supported by the statistics in Table 6, wherein, the test-to-predicted strength mean, P_m , is higher for fully effective sections compared to partially effective sections for both the Main Specification and DSM.

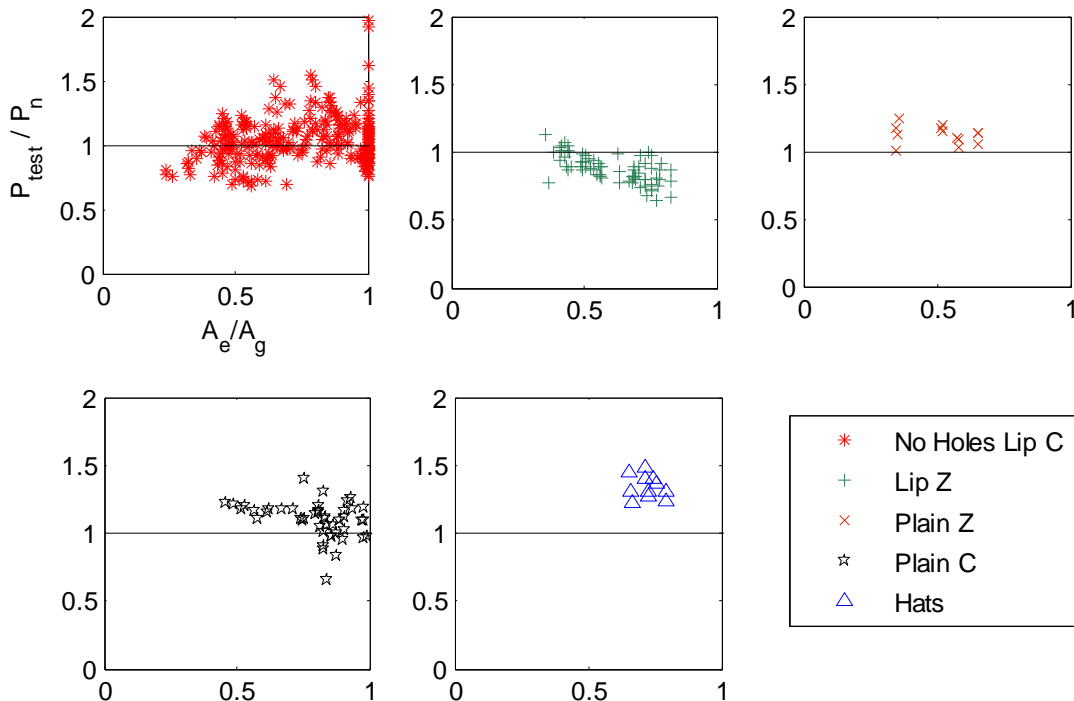


Figure 12. Main Specification test-to-predicted strength as a function of effective area-to-gross area

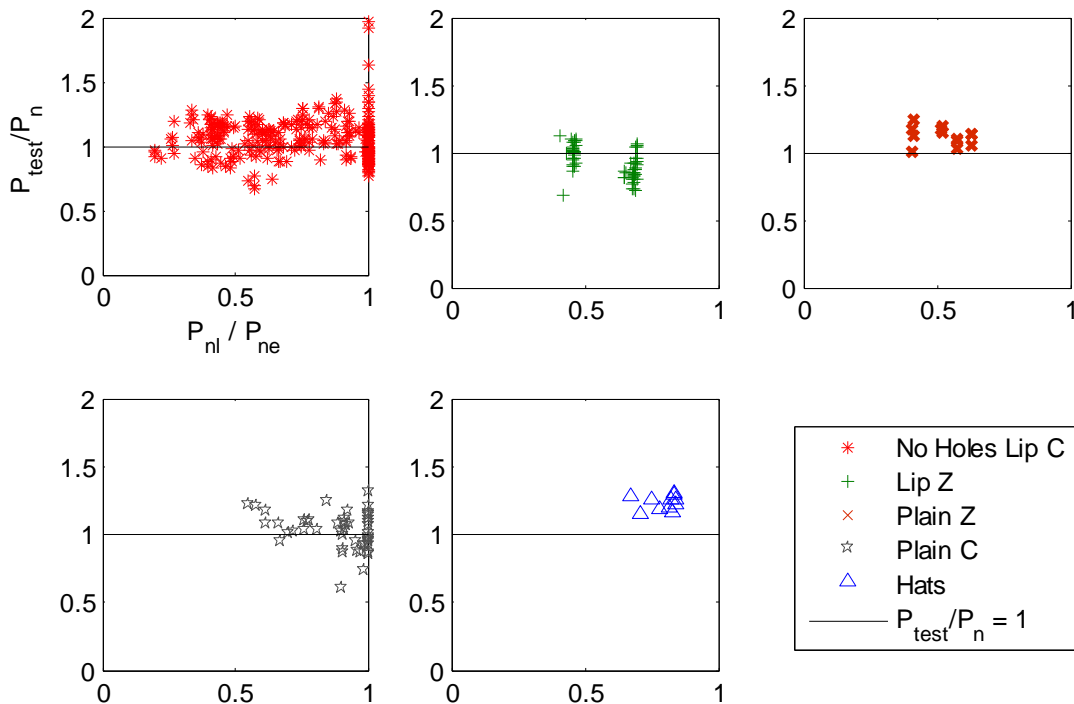


Figure 13. DSM test-to-predicted strength as a function of local-to-global buckling

4.2.5 Resistance Factors by Limit State

The AISI Main Specification and DSM relate column capacity to three limit states: global buckling or yielding of the cross-section, local-global buckling interaction, and distortional buckling. Grouping the column data by these limit states, and excluding columns with holes to provide a fair comparison between the Main Specification and DSM, the resulting resistance factors are provided in Table 7. The most accurate strength predictor is distortional buckling, with $\phi_c = 0.96$ for the Main Specification and $\phi_c = 0.94$ for DSM. Local-global buckling interaction is predicted much more accurately by DSM (compare $\phi_c = 0.87$ versus $\phi_c = 0.78$ in Table 7) which is consistent with the results in Table 6 for columns with partially effective cross-sections. The global buckling resistance factor is the same for DSM and the Main Specification

($\phi_c = 0.81$). An increase in the resistance factor for the distortional buckling limit state to $\phi_c = 0.95$ is a valid consideration for a future code revision, as is the replacement of the current Main Specification approach with DSM, which could lead to better prediction accuracy and a higher resistance factor. It is also found that the resistance factor for data within the Main Specification limits and the DSM prequalified limits is approximately the same as the resistance factor for data outside these limits. Thus the expansion of current limits for both Main Specification and DSM should be considered.

Table 7. Resistance factors by ultimate limit state

AISI	Classification	Test-to-predicted statistics		ϕ LRFD	ϕ LSD	# of tests
		Mean (P_m)	COV (V_p)			
Main Spec	Local [†]	0.98	0.17	0.78	0.63	235
	Local	1.00	0.19	0.79	0.63	265
	Global [†]	1.04	0.20	0.81	0.64	92
	Global	1.04	0.20	0.81	0.64	92
	Distortional [†]	1.09	0.10	0.96	0.79	70
	Distortional	1.09	0.10	0.96	0.79	82
DSM	Local *	1.03	0.14	0.87	0.70	235
	Local	1.03	0.14	0.87	0.70	236
	Global *	1.06	0.20	0.81	0.65	59
	Global	1.03	0.19	0.80	0.64	103
	Distortional *	1.07	0.09	0.94	0.78	96
	Distortional	1.08	0.09	0.95	0.78	100

[†] Within Main Spec dimensional limits (see Appendix 1) * Within DSM prequalified limits (see Appendix 1)

4.2.6 Comparison of Prediction Accuracy with Cross-section Dimensions

Figure 14 to Figure 23 present plots of the test-to-predicted strength ratio versus different column cross-section dimensions for both the Main Specification and DSM. Figure 14 and Figure 15 present the plot between the test-to-predicted strength ratio and the flange width-to-thickness ratio (B/t) for the Main Specification and DSM respectively while Figure 16 and

Figure 17 present the plot between the test-to-predicted strength ratio and the lip width-to-thickness ratio (D/t) for the Main Specification and DSM respectively. For the Main Specification, it can be observed that the strength predictions change from being conservative to unconservative as the flange width-to-thickness ratio (B/t) and the lip width-to-thickness ratio (D/t) increase. A similar trend can also be observed in Figure 18 which presents the plot of test-to-predicted strength ratio versus the web height-to-thickness (H/t) ratio for both the Main Specification.

From Figure 15, Figure 17 and Figure 19, and it can be observed that the DSM strength prediction accuracy does not vary as much as the Main Specification with the flange width-to-thickness ratio (B/t), lip width-to-thickness ratio (D/t) and web height-to-flange width ratio (H/B). From Figures 20 to 23, it can be observed that both the Main Specification and DSM strength prediction accuracy does not vary with the web height-to-flange width ratio (H/B) or the flange width-to-lip width (B/D). In all the figures, the spread away from $P_{test}/P_n = 1$ is greater for the Main Specification indicating that DSM is more accurate in predicting the strengths.

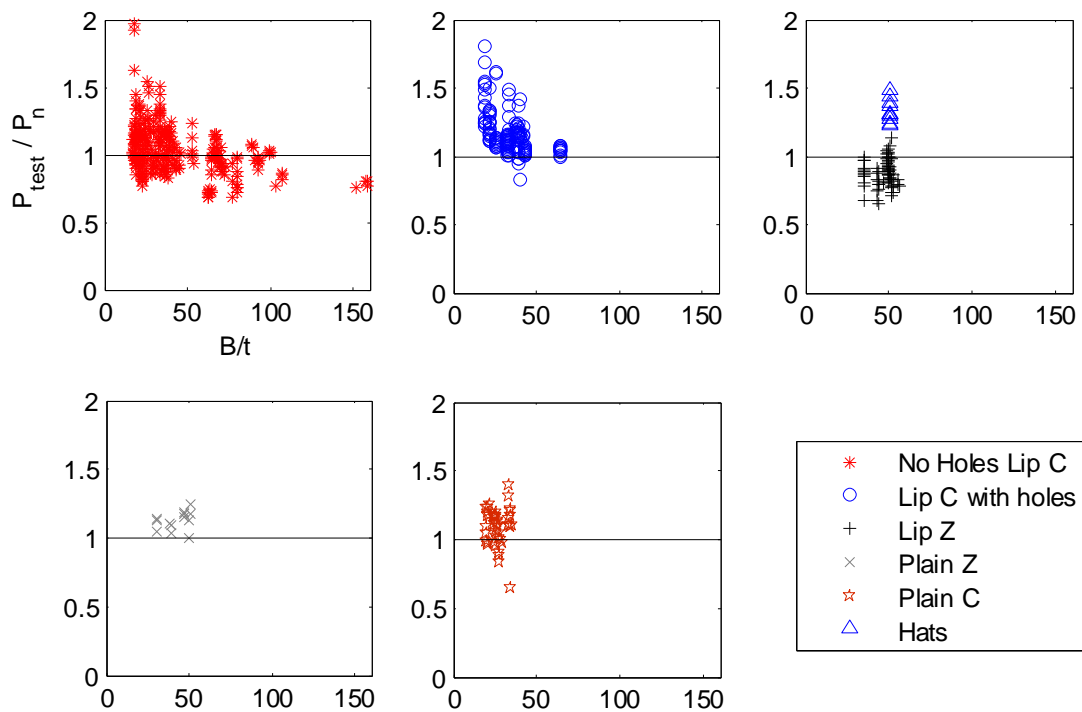


Figure 14. Main Specification test-to-predicted strength as a function of flange width-to-thickness (B/t)

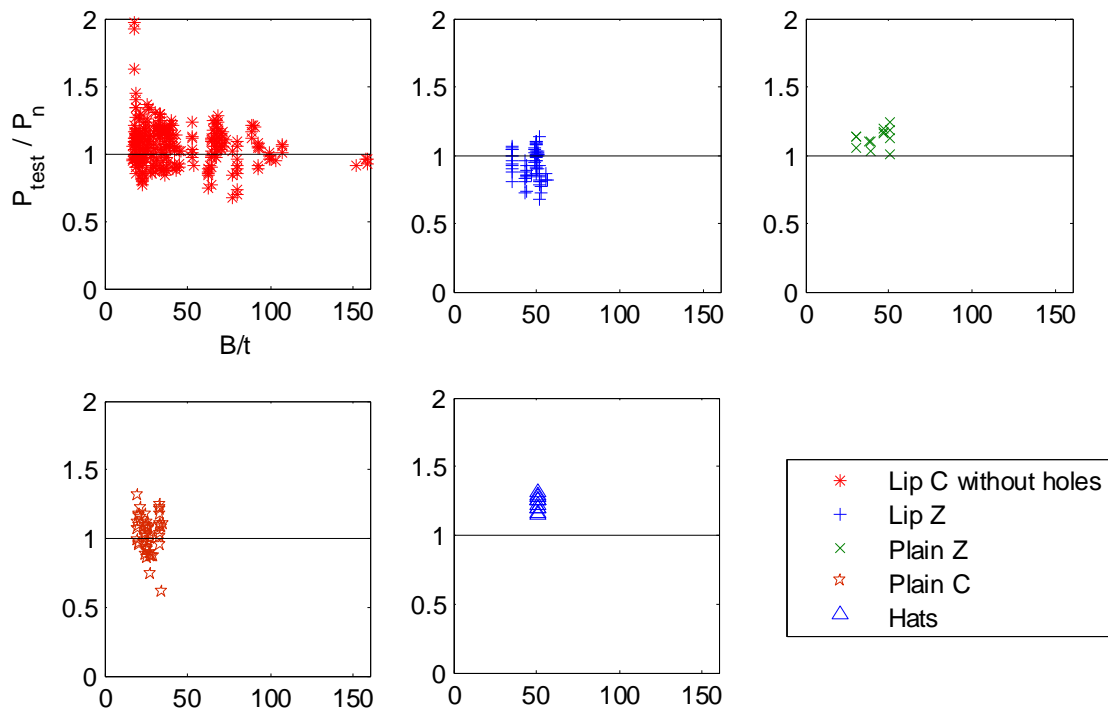


Figure 15. DSM test-to-predicted strength as a function of flange width-to-thickness (B/t)

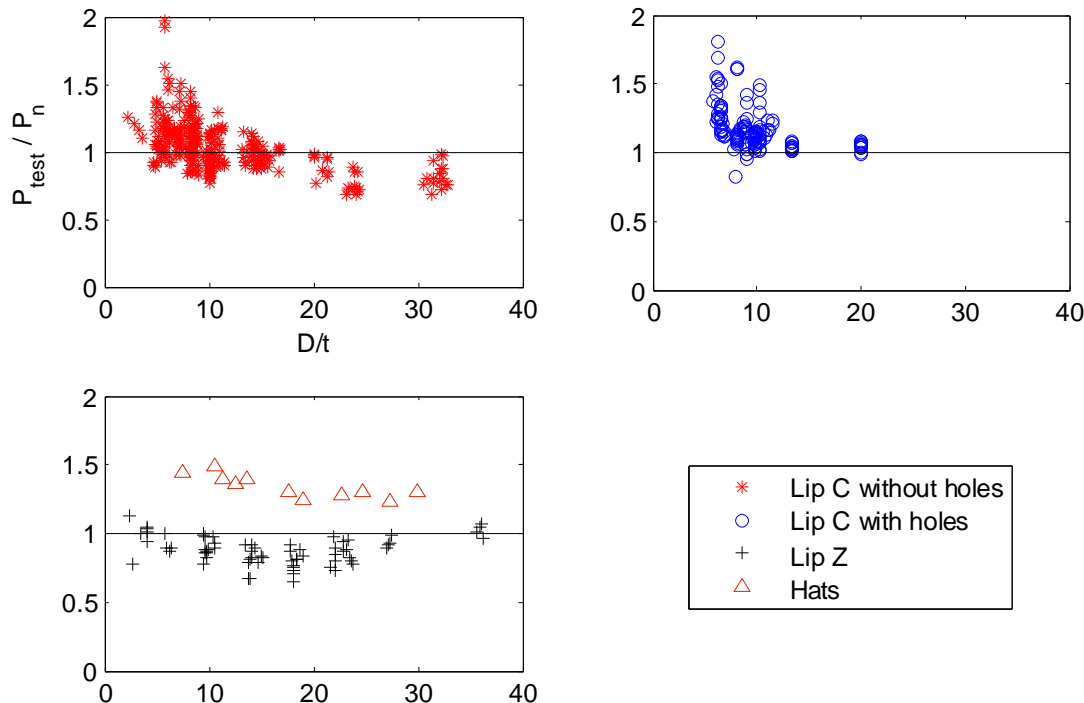


Figure 16. Main Specification test-to-predicted strength as a function of lip width-to-thickness (D/t)

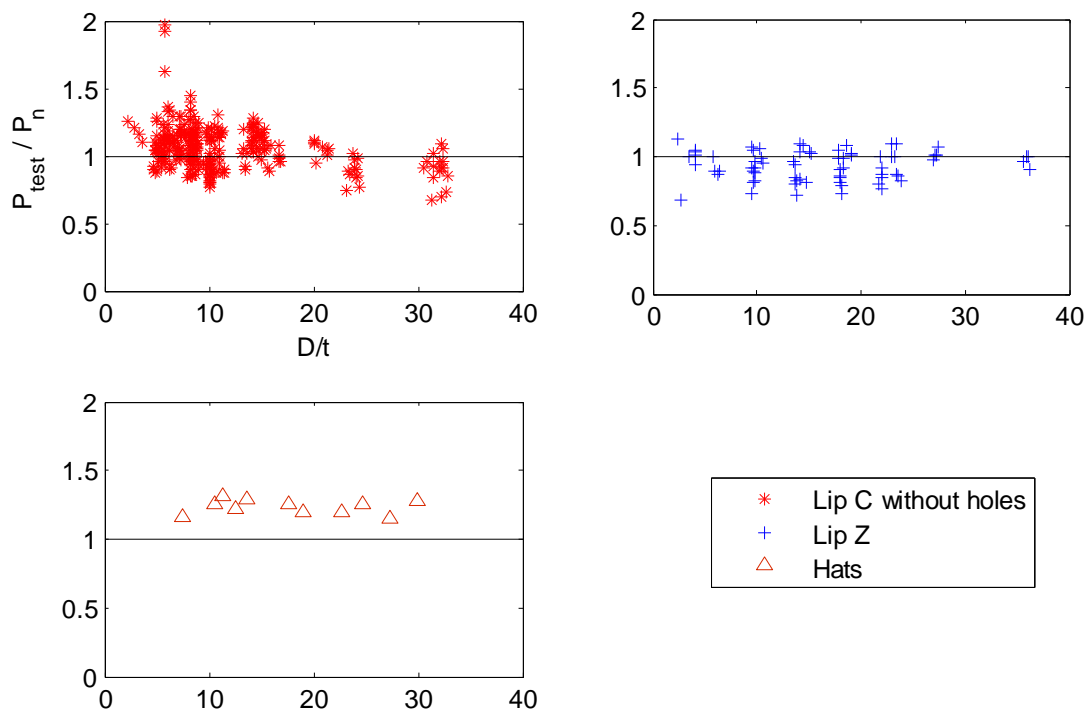


Figure 17. DSM test-to-predicted strength as a function of lip width-to-thickness (D/t)

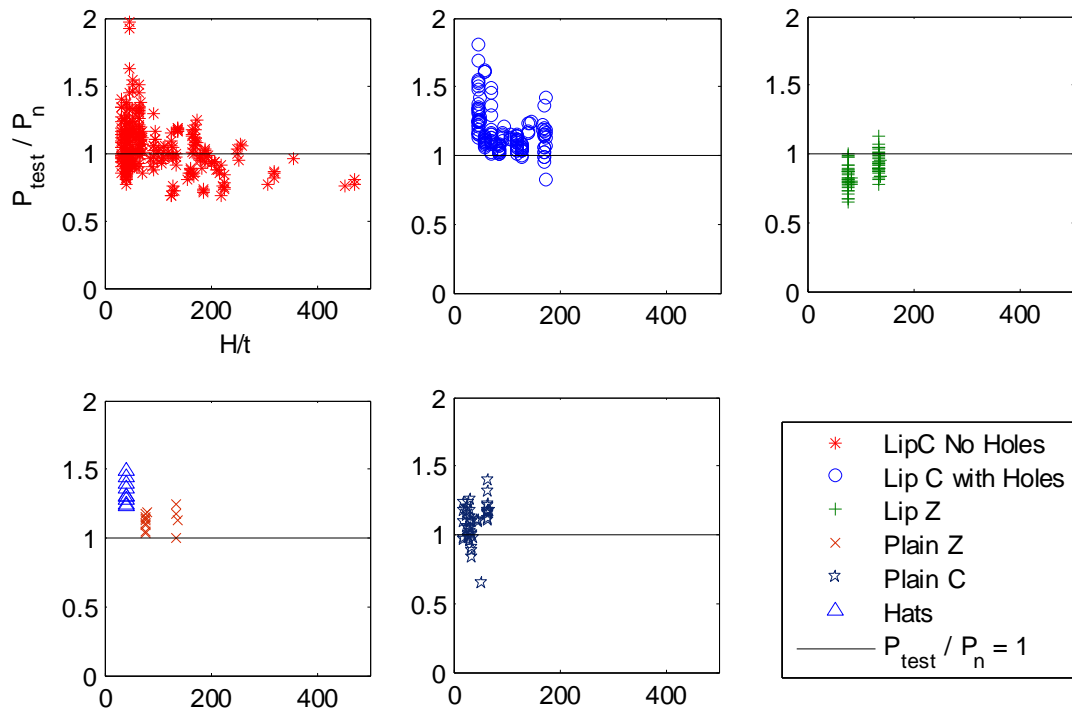


Figure 18. Main Specification test-to-predicted strength as a function of web height-to-thickness (H/t)

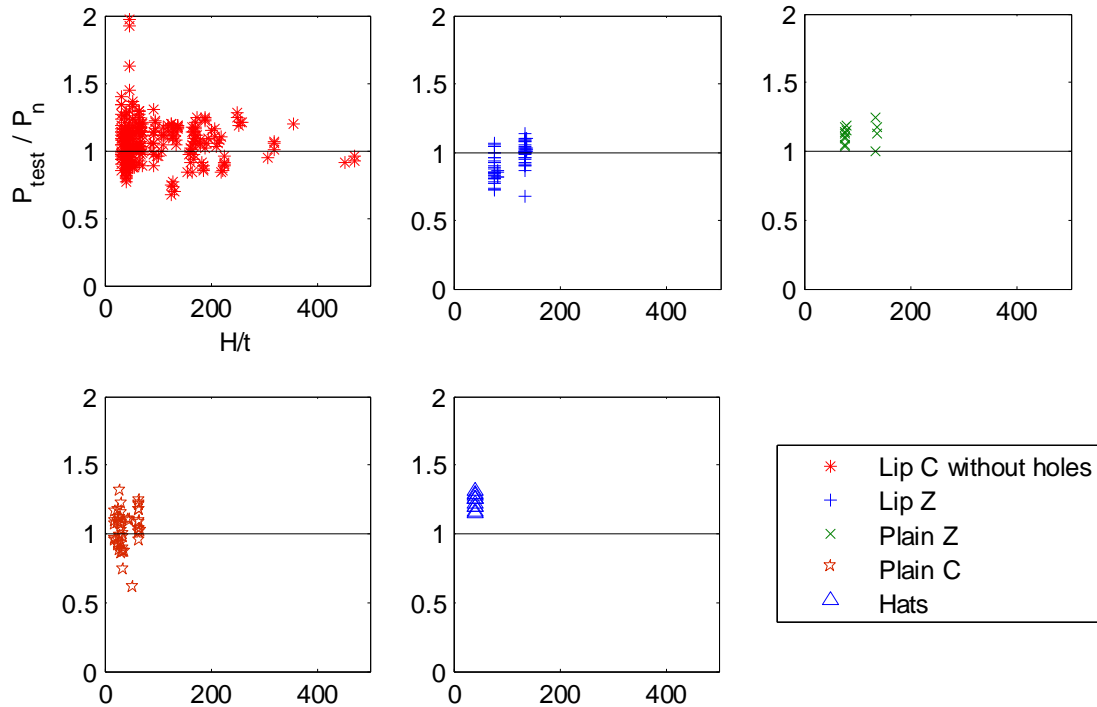


Figure 19. DSM test-to-predicted strength as a function of web height-to-thickness (H/t)

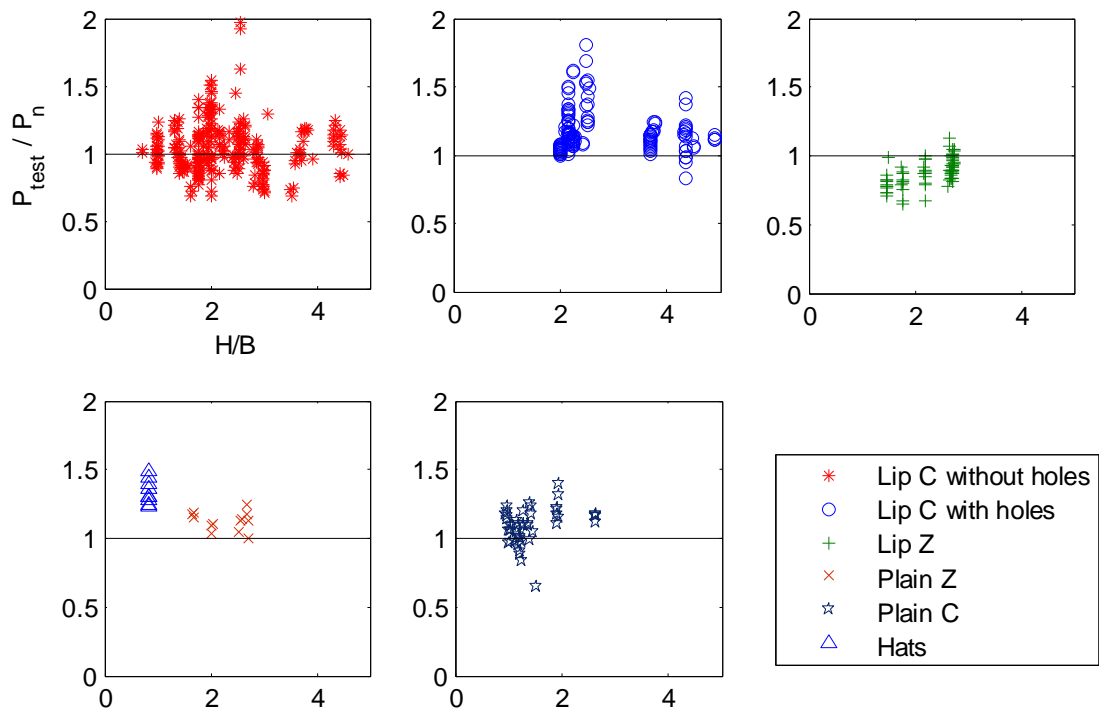


Figure 20. Main Specification test-to-predicted strength as a function of web height-to-flange width (H/B)

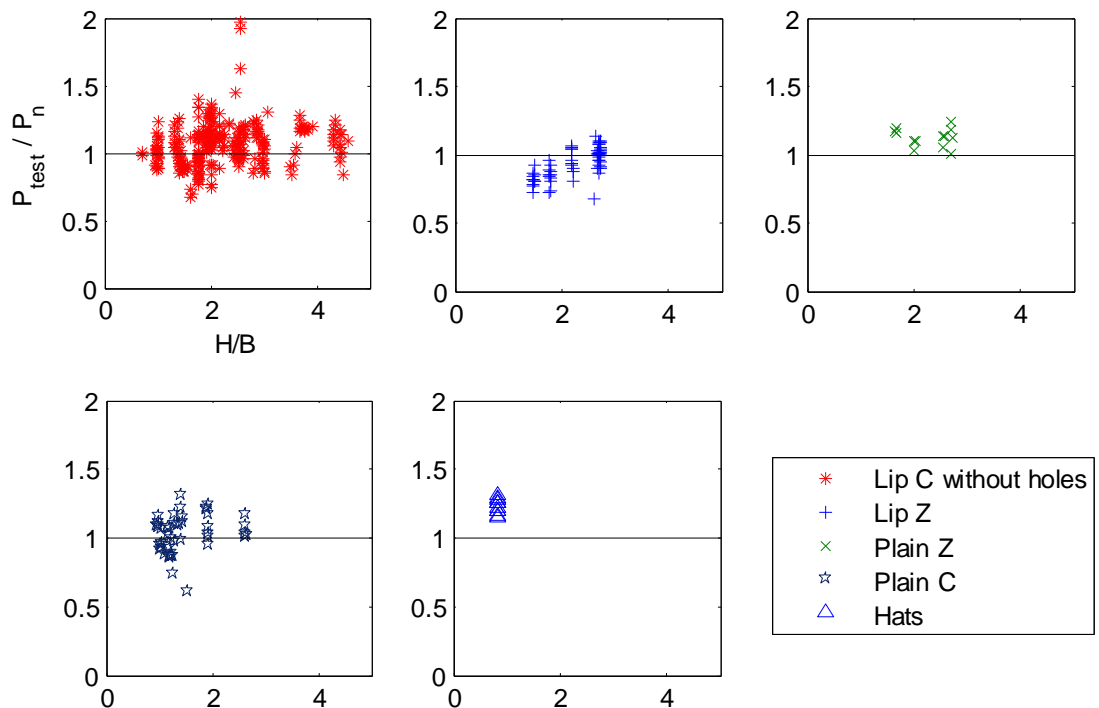


Figure 21. DSM test-to-predicted strength as a function of web height-to-flange width (H/B)

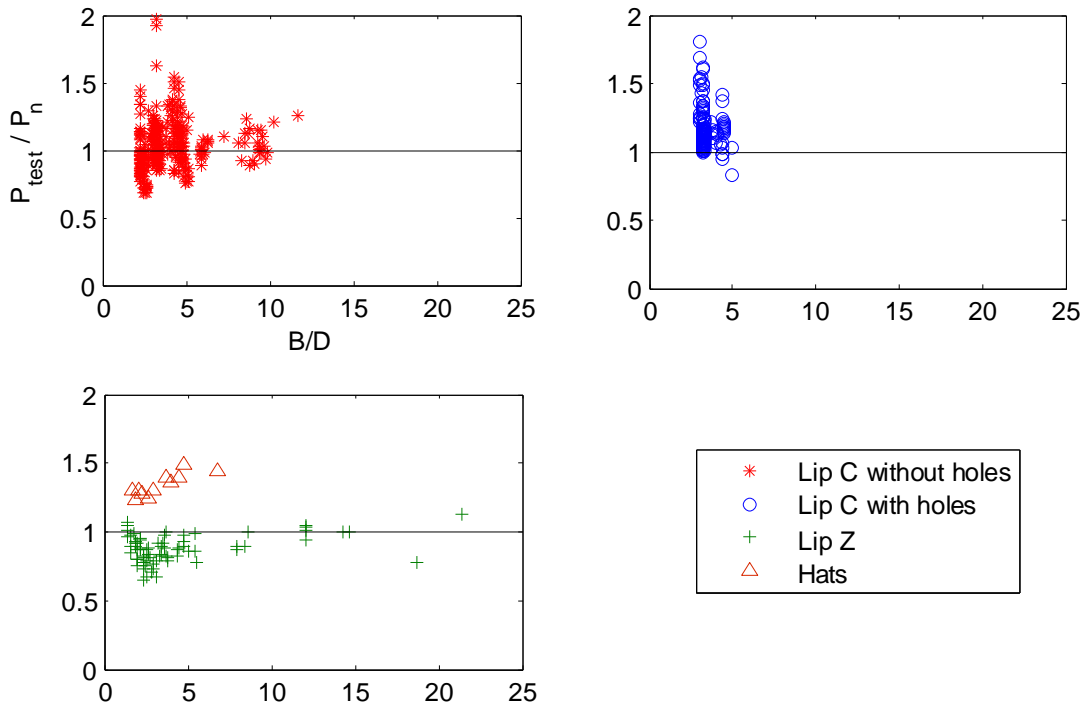


Figure 22. Main Specification test-to-predicted strength as a function of flange width-to-lip length (B/D)

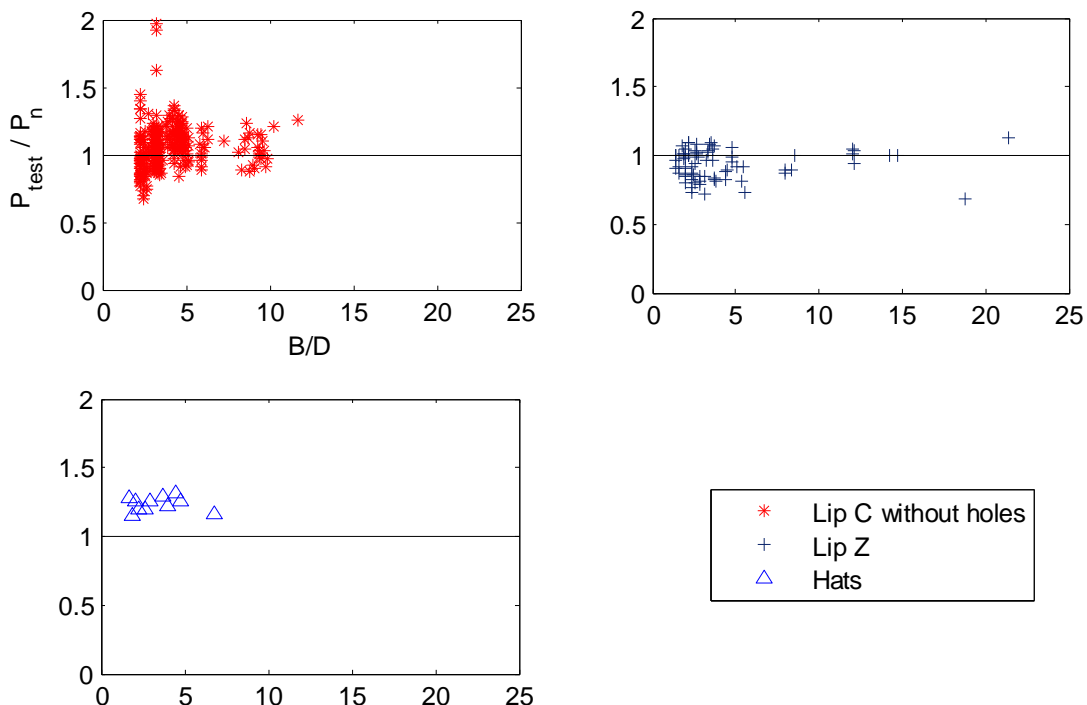


Figure 23. DSM test-to-predicted strength as a function of flange width-to-lip length (B/D)

4.2.7 Resistance Factors for Angle Columns

It was discussed earlier in Section 2.1.3 that Peköz recommended the use of an initial out-of-straightness of $L / 1000$ in order to account for the possibility of a reduction in the column strength due to the initial out-of-straightness (sweep). This study compares the results obtained for the predicted axial strength, P_n , for all plain angle columns calculated with and without the additional moment, $PL/1000$. The results from this study are summarized in Table 8.

It can be observed from Table 8 that the predicted strength of angle columns with the additional imperfection moment of $PL/1000$ is lower than the predicted strength of angle columns without the additional moment of $PL/1000$. This is because the additional moment of $PL/1000$ reduces the capacity of the member by approximately 47% for the angle columns considered in this study. Thus it can be seen that the addition of extra moment does not help in improving the accuracy of the capacity predicted by current provisions of the code. Thus, it was decided to calculate the capacity of all angle columns in this research without including the additional moment of $PL/1000$.

Figure 24 provides a comparison of the test-to-predicted strength ratio of plain angle columns as a function of slenderness with and without $PL/1000$. From the figure, it can be observed that for the same value of slenderness, the test-to-predicted strength ratio is higher when $PL/1000$ is added. This shows that the addition of the moment $PL/1000$ makes the prediction more conservative.

Table 8.Main Specification test-to-predicted strength ratiosfor angle columns.

Source	Cross-section Type	Member Name	P_{test} (kips)	P_{test}/P_n	P_{test}/P_n	λ_c
				(no PL/1000)	(with PL/1000)	
Popovic et al. (1999)	Fixed ended angles	LO24041	12.15	1.89	2.26	1.54
	Fixed ended angles	LO24071	9.34	1.46	1.97	1.55
	Fixed ended angles	LO24101	8.33	1.32	1.97	1.57
	Fixed ended angles	LO24131	7.04	1.14	1.83	1.59
	Fixed ended angles	LO24161	5.94	0.99	1.73	1.64
	Fixed ended angles	LO24191	5.02	1.07	1.81	1.77
	Fixed ended angles	LO38071	26.89	1.35	1.92	1.00
	Fixed ended angles	LO38101	21.35	1.18	1.82	1.06
	Fixed ended angles	LO38131	15.21	1.07	1.64	1.21
	Fixed ended angles	LO47071	32.45	1.20	1.80	0.85
	Fixed ended angles	LO47101	22.88	1.06	1.66	0.99
	Fixed ended angles	LO47131	19.04	1.15	1.78	1.20
Chodraui et al. (2005)	Pin-ended angles	L 60 x 2.38	7.20	1.23	1.48	1.72
	Pin-ended angles	L 60 x 2.38	6.30	1.08	1.43	1.73
	Pin-ended angles	L 60 x 2.38	5.40	0.93	1.34	1.74
	Pin-ended angles	L 60 x 2.38	5.40	1.12	1.64	1.97
Wilhoite et al. (1984)	Pin Ended Equal angles	1	16.31	1.60	1.99	1.89
	Pin Ended Equal angles	2	13.12	1.30	1.76	1.91
	Pin Ended Equal angles	3	13.52	1.34	1.82	1.91
	Pin Ended Equal angles	4	14.63	1.45	1.97	1.91
	Pin Ended Equal angles	5	10.89	1.16	1.67	1.97
	Pin Ended Equal angles	6	11.72	1.24	1.80	1.97
	Pin Ended Equal angles	7	13.32	1.41	2.05	1.97
Dhanalakshmi et al. (2001)	Fixed ended angles	EA20-0-0	20.27	2.22	2.34	1.58
	Fixed ended angles	EA40-0-0	11.14	4.08	4.38	2.95
	Fixed ended angles	EA60-0-0	6.68	6.53	7.02	4.90
Young B (2004)	Fixed ended angles	P1.2L250	5.35	9.75	10.60	5.06
	Fixed ended angles	P1.2L250R	5.30	9.66	10.50	5.06
	Fixed ended angles	P1.2L1000	4.20	7.59	10.22	5.06
	Fixed ended angles	P1.2L1500	3.42	6.03	9.17	5.01
	Fixed ended angles	P1.2L2000	2.83	5.22	8.83	5.08
	Fixed ended angles	P1.2L2500	2.61	4.37	8.14	4.93
	Fixed ended angles	P1.2L2500R	2.67	4.56	8.49	4.95
	Fixed ended angles	P1.2L3000	1.80	3.06	6.22	4.96
	Fixed ended angles	P1.2L3500	1.30	2.29	5.02	5.02
	Fixed ended angles	P1.5L250	8.90	7.51	8.17	3.72
	Fixed ended angles	P1.5L1000	6.97	5.76	7.78	3.70
	Fixed ended angles	P1.5L1500	5.66	4.69	7.18	3.69
	Fixed ended angles	P1.5L2000	3.93	3.40	5.80	3.74
	Fixed ended angles	P1.5L2500	3.53	3.01	5.62	3.75
	Fixed ended angles	P1.5L3000	2.94	2.60	5.33	3.77
	Fixed ended angles	P1.5L3500	2.58	2.16	4.76	3.74
	Fixed ended angles	P1.9L250	12.70	5.45	5.92	2.98
	Fixed ended angles	P1.9L250R	12.97	5.50	5.98	2.96
	Fixed ended angles	P1.9L1000	10.74	4.56	6.14	2.97
	Fixed ended angles	P1.9L1500	8.00	3.44	5.22	2.99
	Fixed ended angles	P1.9L2000	6.09	2.60	4.40	2.98
	Fixed ended angles	P1.9L2500	5.03	2.15	3.98	2.98
	Fixed ended angles	P1.9L3000	3.33	1.45	2.93	3.01
	Fixed ended angles	P1.9L3500	3.24	1.41	3.07	3.02

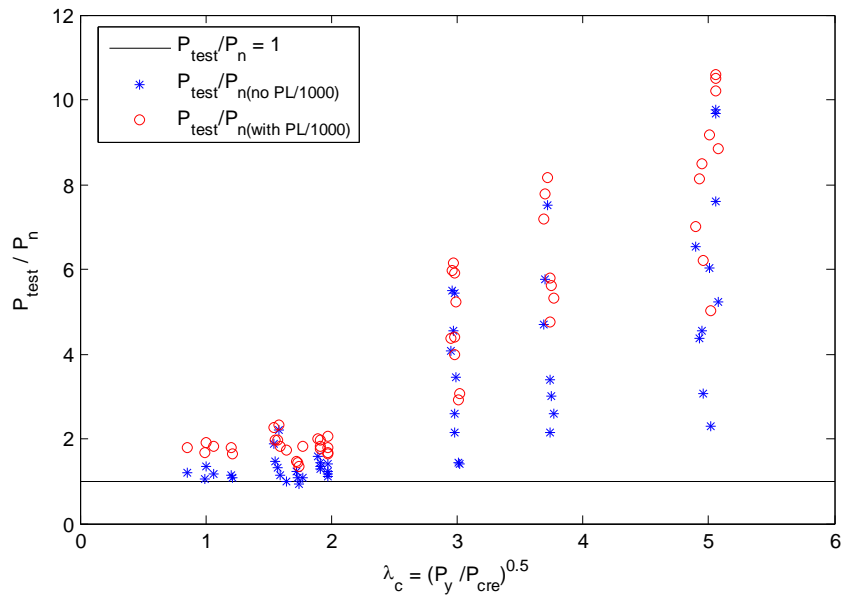


Figure 24. Test-to-predicted strength of plain angle columns with and without PL/1000.

Table 9 presents the resistance factors obtained for angle columns for strength predictions according to the Main Specification (see Section 2.1.3) without the additional moment of PL/1000. It can be seen that the resistance factor for lipped angle columns is about 35 % higher than the resistance factor for plain angle columns ($\phi_c = 0.93$ versus $\phi_c = 0.69$). The high values obtained for the test-to-predicted strength ratio mean indicates that the current provisions of the code under-predicts the strength of the angle section columns, or in other words, the prediction is very conservative. The low values for the resistance factor for angle columns indicate that the fundamental behavior of angle section columns is yet to be completely understood and there is a need for more research in future.

Table 9. Resistance factors for angle columns (Main Specification)

Type of Section	Test-to-predicted Statistics		Resistance Factor		# of tests
	Mean (P_m)	COV (V_p)	ϕ LRFD	ϕ LSD	
All Angles	2.76	0.76	0.62	0.39	75
Plain Angles	3.13	0.77	0.69	0.43	50
Lipped Angles	2.00	0.46	0.93	0.67	25

Table 10 provides resistance factors obtained for angle section columns with a global slenderness, $\lambda_c \leq 2$. This shows that as slenderness decreases, the code predicts the strength more accurately (also see Figure 24).

Table 10. Resistance factors for angle columns with $\lambda_c \leq 2$ (Main Specification)

Type of Section	Test-to-predicted Statistics		Resistance Factor		# of tests
	Mean (P_m)	COV (V_p)	ϕ LRF	ϕ LSD	
Angles with $\lambda_c \leq 2$ (without PL/1000)	1.35	0.26	0.93	0.73	38

Figure 25 plots the test-to-predicted strength ratio of angle section columns as a function of global slenderness. It can be seen that for both lipped and plain angle columns having slenderness lesser than 2, the test-to-predicted strength ratio approaches unity.

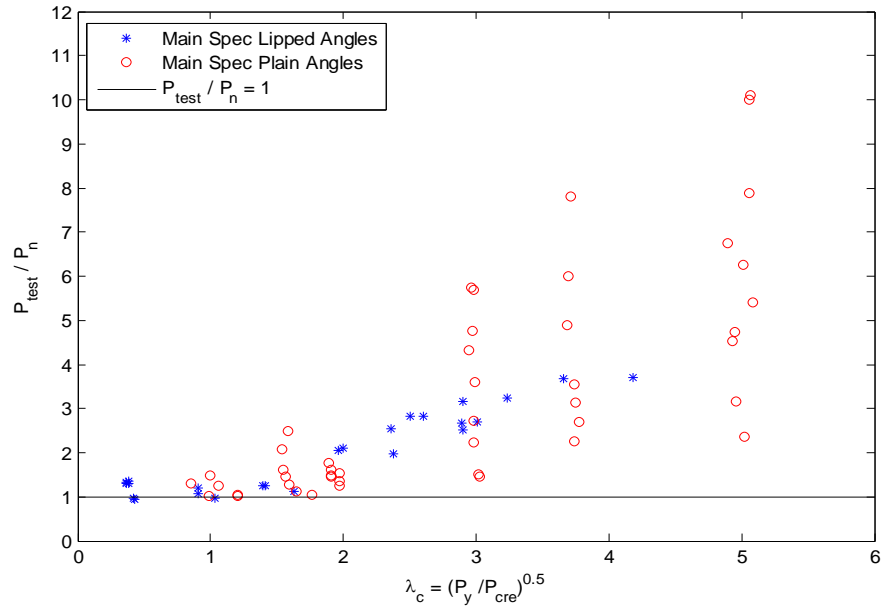


Figure 25. Main Specification test-to-predicted strength ratio as a function of slenderness

From Figure 25, it can also be observed that as slenderness increases, the test-to-predicted strength ratio increases showing that the current code provisions become conservative as angle

columns become more slender. It is also observed that for the same slenderness values, there are wide variations in the test-to-predicted strength ratio. Although the predicted strengths remain the same for members with the same slenderness, test results differ causing a difference in the test-to-predicted strength ratios.

Table 11 presents the results obtained for the resistance factors of angle sections using DSM. It can be observed that the resistance factor for angle columns using DSM is higher than that obtained using the Main Specification (Table 9). It can also be observed that the difference in the resistance factor between plain and lipped angle columns is 0.03, which is approximately 79% lower than the difference of 0.14 observed in Table 9. Although DSM, predicts the strength of angle columns more accurately than the Main Specification, the strengths predicted by both methods are still very low compared to the actual tested strengths. This indicates that the global capacity prediction equation (see Eq. (2)) is an inaccurate and conservative strength predictor for angle columns.

Table 11. Resistance Factors for angle columns (DSM)

Type of Section	Test-to-predicted Statistics		Resistance Factor		# of tests
	Mean (P_m)	COV (V_p)	ϕ LRFD	ϕ LSD	
All Angles	2.67	0.69	0.71	0.46	75
Plain Angles	3.02	0.69	0.81	0.53	50
Lipped Angles	1.97	0.49	0.84	0.60	25

Section 4.2.8 presents a derivation for the resistance factor with a modified expression for the coefficient of variation of load effect, V_Q , and the coefficient of variation of the resistance, V_R .

4.2.8 Resistance Factor using Modified Expressions for V_Q and V_R .

This section presents a derivation for the resistance factor wherein the Taylor Series expansion shown in Eq. (24) is not truncated at linear terms to obtain a first order approximation

for the mean and the variance. A quadratic term is included in the Taylor Series expansion which modifies the expressions for the coefficients of variation of the load effect and the resistance, V_Q and V_R respectively. The value of the resistance factor obtained using this quadratic term is compared against those obtained using a first order approximation.

It is assumed that the load effect, Q , and the resistance, R , have a lognormal probability distribution with parameters λ and ρ . Thus, failure, Z , which is also lognormal, can be expressed as

$$Z = \ln R - \ln Q, \quad (45)$$

with parameters, λ_z and ρ_z that can be expressed as follows:

$$\begin{aligned} \lambda_Z &= \lambda_R - \lambda_Q \\ \rho_Z^2 &= \rho_R^2 + \rho_Q^2. \end{aligned} \quad (46)$$

The probability of failure, p_f can then be expressed as

$$\begin{aligned} p_f &= 1 - \Phi\left(\frac{\lambda_Z}{\rho_Z}\right). \\ \text{Thus, } p_f &= 1 - \Phi\left(\frac{\lambda_R - \lambda_Q}{\sqrt{\rho_R^2 + \rho_Q^2}}\right) = 1 - \Phi(\beta). \end{aligned} \quad (47)$$

The reliability index, β , can be expressed as

$$\beta = \left(\frac{\lambda_R - \lambda_Q}{\sqrt{\rho_R^2 + \rho_Q^2}} \right). \quad (48)$$

A relationship between the mean value of the load effect, Q_m , the mean value of the resistance, R_m , the coefficient of variation of the load effect and the resistance, V_Q and V_R , and the parameters λ_Q , λ_R , ρ_Q and ρ_R is expressed by the following equations:

$$\lambda_R = \ln\left(\frac{R_m}{\sqrt{1+V_R^2}}\right) \quad (49)$$

$$\lambda_Q = \ln\left(\frac{Q_m}{\sqrt{1+V_Q^2}}\right) \quad (50)$$

$$\rho_R^2 = \ln(1+V_R^2) \quad (51)$$

$$\rho_Q^2 = \ln(1+V_Q^2) \quad (52)$$

Comparing Eqs. (51), (52) with Eq. (26), it can be observed that while in Eq. (26), the variance was equal to the square of the coefficient of variation, in Eqs. (51) and (52), the variance is equal to the logarithm of the coefficient of variation plus one. This represents the difference between the first order approximation method discussed Section 4.1 and the current method wherein the Taylor Series expansion is not truncated at linear terms. Using Eqs. (48) to (52), the value of the reliability index, β , is

$$\beta = \left(\frac{\ln\left[\frac{R_m}{Q_m} \sqrt{\frac{1+V_Q^2}{1+V_R^2}}\right]}{\sqrt{\ln((1+V_Q^2)(1+V_R^2))}} \right). \quad (53)$$

Substituting the ratio of the mean resistance to the mean load effect (R_m/Q_m) from Eq. (40), the coefficient of variation of resistance, V_R , and the coefficient of variation of the load effect, V_Q , from Eq. (35) in Eq. (53) and the following expression is obtained:

$$\beta = - \ln \left[\frac{1.10 P_m \left(\alpha_D \frac{D_n}{L_n} + \alpha_L \right)}{\phi \left(1.05 \frac{D_n}{L_n} + 1 \right)} \sqrt{ \frac{1 + \frac{\left(1.05 \frac{D_n}{L_n} \right)^2 0.10^2 + 0.25^2}{\left(\left(1.05 \frac{D_n}{L_n} \right) + 1.0 \right)^2}}{1 + 0.0125 + V_p^2} } \right] \quad (54)$$

Rearranging the terms in Eq. (54), we obtain the following expression for the resistance factor, ϕ :

$$\phi_c = \frac{1.10 P_m \left(\alpha_D \frac{D_n}{L_n} + \alpha_L \right)}{\left(1.05 \frac{D_n}{L_n} + 1 \right) \exp \left(\beta \sqrt{ \ln \left(\frac{1 + \frac{\left(1.05 \frac{D_n}{L_n} \right)^2 0.10^2 + 0.25^2}{\left(\left(1.05 \frac{D_n}{L_n} \right) + 1.0 \right)^2}}{1 + 0.0125 + V_p^2} \right)} \right)} \quad (55)$$

It can be observed that Eq. (55) is a function of the nominal dead-to-live load ratio (D_n/L_n), the load factors, α_D and α_L , the reliability index, β , the mean of the test results, P_m , and the coefficient of variance of the test results, V_p . The LRFD method uses the following values for nominal dead-to-live load ratio (D_n/L_n), the load factors, α_D and α_L , and the reliability index, β :

$D_n/L_n = 1/5$, $\alpha_D = 1.2$, $\alpha_L = 1.6$, $\beta = 2.5$. Substituting these values in Eq. (55), the resistance factor, ϕ_c , for LRFD is obtained as

$$\phi_c = 1.673 \sqrt{\frac{1.043}{V_p^2 + 1.012}} P_m e^{-2.5\sqrt{\ln(1.043V_p^2 + 1.056)}}. \quad (56)$$

Similarly, substituting the values $D_n/L_n = 1/3$, $\alpha_D = 1.25$, $\alpha_L = 1.5$, $\beta = 3.0$, in Eq. (55), the resistance factor ϕ_c , for LSD is obtained as

$$\phi_c = 1.562 \sqrt{\frac{1.035}{V_p^2 + 1.012}} P_m e^{-3.0\sqrt{\ln(1.035V_p^2 + 1.048)}}. \quad (57)$$

Table 12 presents the test-to-predicted statistics and resistance factors for columns with and without holes for the Main Specification. The resistance factors have been calculated for each type of column for both the LRFD (ϕ LRFD) and also the LSD (ϕ LSD). Thus, for all data whose dimensional properties are within the prescribed Main Specification limits, a total of 448 column tests, we find that the resistance factor according to the Main Specification for LRFD is 0.86. This value is about 0.01 (1.17 %) higher than the resistance factor calculated using the first order approximation (Table 2). This increase is due to the presence of the additional term in the COV in the Taylor Series expansion, which was neglected by the first order approximation.

Table 12. Resistance factors for columns with and without holes(Main Specification)

Type of Section	Test-to-predicted Statistics			Resistance Factor		# of tests
	Mean (P_m)	SD	COV (V_p)	ϕ LRFD	ϕ LSD	
Plain C	1.10	0.13	0.12	0.97	0.82	49
Lipped C	1.08	0.18	0.17	0.88	0.74	455
Lipped C (within Spec dimensional limits)	1.08	0.18	0.17	0.89	0.74	303
Plain Z	1.12	0.07	0.06	1.04	0.90	13
Lipped Z	0.88	0.10	0.11	0.77	0.66	72
Hat Sections	1.34	0.08	0.06	1.24	1.08	11
All Data (within Spec dimensional limits)	1.06	0.18	0.17	0.86	0.72	448
All Data	1.06	0.18	0.17	0.87	0.73	600

4.2.9 Comparison of Resistance Factors for LSD

This section compares the resistance factors obtained for different values of the nominal dead-to-live load ratio, (D_n/L_n) , and the reliability index, β , corresponding to the first order approximation. The load factors, α_D and α_L are kept constant at 1.25 and 1.5 respectively. Currently the AISI (AISI-S100 2007) specifies a value of 1/3 for (D_n/L_n) and 3.0 for β corresponding to LSD. The code (AISI-S100 2007) also specifies a value of 0.21 for the coefficient of variation of load effect, V_Q , for both LRFD and LSD. This however, fails to reflect the dependence of coefficient of variation of load effect, V_Q , on the dead-to-live load ratio, (D_n/L_n) as indicated by Eq. (35). Since the LRFD suggests a value of 1/5 for dead-to-live load ratio (D_n/L_n) (LSD considers 1/3), the value of V_Q must be different for LRFD and LSD. According to the provisions of the current code (AISI-S100 2007), with the use of 0.21 for the V_Q , the expression for the resistance factor is as follows:

$$\phi_c = 1.562P_m e^{-3.0 \sqrt{V_p^2 + 0.057}}. \quad (58)$$

It is to be noted that all the calculations corresponding to the resistance factor for LSD have been calculated using Eq. (58). However, according to the derivation, as shown in Eq. (44), the expression for calculating the resistance factor corresponding to LSD should be as follows:

$$\phi_c = 1.562P_m e^{-3.0 \sqrt{V_p^2 + 0.047}}. \quad (59)$$

Now, changing the dead-to-live load ratio (D_n/L_n) , to 1/5 and assuming a reliability index, β , of 3.0, the expression for calculating the resistance factor is as follows:

$$\phi_c = 1.591 P_m e^{-3.0 \sqrt{V_p^2 + 0.055}}. \quad (60)$$

Now, the dead-to-live load ratio (D_n/L_n) is assumed to 1/5 and reliability index, β , is assumed to be 2.5. Thus the expression for calculating the resistance factor is as follows:

$$\phi_c = 1.591 P_m e^{-2.5 \sqrt{V_p^2 + 0.055}}. \quad (61)$$

Let the resistance factors obtained using the Eqs. (58), (59), (60) and (61) be called as ϕ LSD (Current), ϕ LSD (i), ϕ LSD (ii) and ϕ LSD (iii) respectively. Table 13 presents the resistance factors for columns with and without holes for the Main Specification corresponding to ϕ LRFD, ϕ LSD (Current), ϕ LSD (i), ϕ LSD (ii) and ϕ LSD (iii).

Table 13. Comparison of resistance factors for all columns for LSD (Main Specification)

Type of Section	Test-to-predicted Statistics			Resistance factor				# of tests
	Mean	SD	COV	ϕ LRFD	ϕ LSD (current)	ϕ LSD (i)	ϕ LSD (ii)	
Plain C	1.10	0.13	0.12	0.95	0.77	0.82	0.80	0.91
Lipped C	1.08	0.18	0.17	0.87	0.70	0.74	0.72	0.84
Lipped C (within Spec dimensional limits)	1.08	0.18	0.17	0.87	0.70	0.74	0.72	0.84
Plain Z	1.12	0.07	0.06	1.02	0.84	0.89	0.87	0.98
Lipped Z	0.88	0.10	0.11	0.76	0.62	0.66	0.64	0.73
Hat Sections	1.34	0.08	0.06	1.21	1.00	1.07	1.03	1.16
All Data (within Spec dimensional limits)	1.06	0.18	0.17	0.85	0.68	0.72	0.70	0.81
All Data	1.06	0.18	0.17	0.85	0.69	0.72	0.71	0.82
								600

It can be observed from Table 13 that ϕ LSD (current) has the lowest resistance factor values for all types of sections. The resistance factor for ϕ LSD (i), which represents the derived value of the resistance factor corresponding to the first order approximation without substituting the value of $V_Q = 0.21$, increases from 0.68 to 0.72 for all data with dimensions within the prescribed Main Specification limits. ϕ LSD (ii), which corresponds to Eq. (60) having a dead-to-live load ratio (D_n/L_n) of 1/5, has a lower resistance factor value of 0.70 when compared to ϕ LSD (i), but is higher than ϕ LSD (current). ϕ LSD (iii), which has a dead-to-live load ratio (D_n/L_n) of 1/5 and a lower reliability index of 2.5, has the highest resistance factor value of 0.81 for all data

with dimensions within the prescribed Main Specification limits. However, even this value of 0.81 is lower than that of ϕ LRFD. This can be attributed to the fact that the LRFD method follows different values for the load factors, α_D and α_L , which are 1.2 and 1.6 respectively.

Chapter 5: Conclusions

5.1 Summary and Conclusions

This study analyzed a total of 675 members using both the Main Specification and the DSM. The test-to-predicted strength ratio (P_{test}/P_n) according to both methods was found and the resistance factors corresponding to both the LRFD and the LSD were calculated. Of the 675 members, 161 had holes and 75 were angle sections and thus only the Main Specification was employed to calculate the resistance factors corresponding to those members. Of the 600 members, it was found that 448 members had dimensional properties within the prescribed Main Specification limits. The resistance factor for these 448 members, according to the LRFD, was found to be 0.85 and 0.68 corresponding to the LSD.

For the sections with holes, only 51 of the 161 members had dimensions within the prescribed Main Specification limits. The strength prediction of columns with holes by the Main Specification was found to be typically conservative with high test-to-predicted strength ratios. The conservative nature of the Main Specification predictions for members with holes led to high resistance factor values. For members with the prescribed Main Specification limits, the resistance factor corresponding to LRFD was found to be 1.01, while it was 0.83 corresponding to the LSD. The resistance factor for holes whose dimensions were outside the prescribed Main Specification limits was found to be lower (0.97 for LRFD).

A total of 439 members did not have any perforations. Of them, 397 members were found to be within prescribed Main Specification limits while 390 of them were within the prescribed

DSM limits. For all members within the prescribed limits, DSM was found to have a higher resistance factor of 0.87 (LRFD) compared to 0.83 (LRFD) for Main Specification.

For data within the prescribed Main Specification limits, the resistance factor was found to be the same for both fully and partially effective columns (0.81 for LRFD). For data within the prequalified DSM limits, the resistance factor for partially effective columns was found to be 0.89 for LRFD, approximately 10 % greater than the resistance factor for fully effective sections (0.83 for LRFD). This is due to the more accurate strength predictions by DSM for columns sensitive to local buckling.

It was also observed that for both Main Specification and DSM, the resistance factor for columns that failed by distortional buckling is higher than those that failed by local-global interaction or global buckling (yielding). For data within the prescribed Main Specification limits, the resistance factor for columns that failed by distortional buckling is 0.96 (LRFD) and for those that failed by local-global interaction and global buckling, it is 0.78 and 0.81 respectively. For all data within the DSM prequalified limits, the resistance factor for columns that failed by distortional buckling is 0.94 (LRFD) and 0.81 for global buckling. Consistent with what was observed in the classification on the basis of cross-section slenderness, the resistance factor for DSM for local-global interaction mode of failure is 0.87, approximately 11% higher than that observed for the Main Specification.

The resistance factor obtained for angle columnswas low relative to the other cross-sections considered in this study (0.62 for LRFD). It was observed that the resistance factor for lipped angle columns (ϕ LRFD = 0.93) is higher than the resistance factor for plain angle columns (ϕ LRFD = 0.69). Thus it can be said that the current code provisions predict the strength of lipped

angle columns better than plain angle columns but overall the predictions are still extremely conservative and there appears to be something fundamentally skewed with the equations that predict the capacity of angle columns. It is also observed that the strength predictions are more accurate for angle section columns with a global slenderness, $\lambda_c \leq 2$, and as slenderness increases, the predictions become more and more conservative. The low values for the resistance factor for angle columns reflect the fact that the predictions are not accurate which clearly implies that the behaviour of angle sections, particularly plain angle sections, is yet to be completely understood, thereby leaving scope for more research.

It was found that the inclusion of an additional moment of $(P L / 1000)$ for angle columns reduces the predicted capacity of the column. Given that the predicted strength for plain angle column was already conservative, the addition of the moment further reduces the predicted strength thereby making the results even more conservative. Thus it is observed that the addition of an extra moment does not help in improving the accuracy of the capacity predicted by current provisions of the code and further research must be done in order to better predict the strength of angle columns.

The method with a modified coefficient of variation for calculating the resistance factor produced an increase of about 2%. This increase was due to the presence of an additional term in coefficient of variation in the Taylor Series expansion, which was otherwise neglected by the first order approximation.

The calibration of the Canadian resistance factor, which uses the LSD method, was also addressed by deriving the resistance factors with different values of dead-to-live load ratios and

reliability indices. A dead-to-live load ratio (D_n/L_n) of 1/5 and a reliability index of 2.5, with load factors, α_D and α_L , as 1.25 and 1.5 respectively, produced the highest resistance factor.

5.2 Recommendations for Code Revisions

This research began with the aim of investigating if the LRFD resistance factor for CFS compression members can be increased above its current value of $\phi_c = 0.85$ as established by the 1991 Specification (AISI 1991). This research has shown that this is possible if the resistance factors are provided on the basis of limit states. Distortional buckling mode of failure is predicted very accurately and consequently has a high resistance factor value. For data within the prescribed Main Specification limits, the resistance factor for columns that failed by distortional buckling is 0.96 (LRFD) and for DSM it is 0.94 (LRFD). For failure by local buckling, DSM has a higher resistance factor value of 0.87 compared to 0.78 for the Main Specification and this means that DSM is a more accurate strength predictor of columns sensitive to local buckling. For global buckling, the resistance factor is approximately the same for both DSM and the Main Specification and is 0.81. Thus, the provision of separate resistance factors on the basis of limit states with a higher resistance factor of $\phi_c = 0.95$ for columns that fail by distortional buckling must be considered. Given that DSM consistently produces higher resistance factors, replacing the Main Specification with DSM must be considered in order to achieve a higher resistance factor.

The resistance factor for data within the Main Specification limits and the DSM prequalified limits was found to be approximately the same as the resistance factor for data outside the limits. Thus the expansion of current limits for both the Main Specification and DSM should be

considered. Tables 14 and 15 present the new recommended limits for the Main Specification and DSM respectively. The recommended changes to be made to the existing limits are presented in bold.

Table 14. Modified Main Specification limits.

Type	Ratio	Limit (in.)
Stiffened compression element with longitudinal edge connected to web/flange	Flat-width-to-thickness (w/t)	w/t ≤ 160
Stiffened compression element with both longitudinal edges connected stiffened elements	Flat-width-to-thickness (w/t)	w/t ≤ 500
Unstiffened compression element	Flat-width-to-thickness (w/t)	w/t ≤ 60
Uniformly compressed stiffened element with circular holes	Depth of hole-to-flat width (d_h/w)	0.5 ≥ $d_h/w \geq 0$
	Flat-width-to-thickness (w/t)	w/t ≤ 60
Uniformly compressed stiffened element with non circular holes	Center-to-center hole spacing (s)	s ≥ 24
	Clear distance from hole at ends (s_{end})	$s_{end} \geq 10$
	Depth of the hole (d_h)	$d_h \leq 2.5$
	Length of the hole (L_h)	$L_h \leq 4.5$
	Depth of hole-to-out-to-out-width(d_h/w_o)	$d_h/w_o \leq 0.5$
Uniformly compressed stiffened element with simple lip edge stiffener	Lip Angle (θ)	140° ≥ $\theta \geq 40^\circ$

Table 15. Modified DSM prequalified limits.

Modified DSM Prequalified Limits			
Ratio	Lipped C-section	Lipped Z-section	Hat section
Web height-to-thickness (H/t)	H/t < 472	H/t < 137	H/t < 50
Flange width-to-thickness (B/t)	B/t < 159	B/t < 56	B/t < 51
Lip width-to-thickness (D/t)	4 < D/t < 33	0 < D/t < 36	4 < D/t < 29.9
Web height-to-flange width (H/B)	0.7 < H/B < 5.0	1.5 < H/B < 2.7	1.0 < H/B < 1.2
Lip width-to-flange width (D/B)	0.05 < D/B < 0.41	0.00 < D/B < 0.73	0.13 < D/B < 0.6
Lip Angle (θ)	40° ≤ θ ≤ 151°	$\theta = 50^\circ$	---

It was also observed that the test-to-predicted ratios for plain and lipped angle columns exhibited a high coefficient of variation and become increasingly conservative with increasing global slenderness. It was also found that the inclusion of the additional out-of-straightness moment makes the predictions more conservative. Thus, its inclusion must be reconsidered. Overall, the predictions were found to be extremely conservative and there appears to be something fundamentally skewed with the equations that predict the capacity of angle columns. Thus more research on the mechanics of angle compression members is needed to improve existing design methods.

The resistance factor value of 0.80 recommended by the Main Specification (AISI-S100 2007) for LSD is found to be higher than the computed value of 0.68. The current value of $V_Q=0.21$, as suggested by the Main Specification (AISI-S100 2007) was found to be wrong and must be revised. This value, when corrected, was found to increase the resistance factor to 0.72. However, even this is higher than the current resistance factor value of 0.80. Thus, a reduction in the resistance factor value for LSD must be considered.

5.3Future Work

Potential code modifications were identified during this research that can improve column strength prediction accuracy and design efficiency.

1. Define LRFD resistance factors by limit state for DSM:

$$\phi_c P_n = \min(\phi_{ce} P_{ne}, \phi_{cl} P_{nl}, \phi_{cd} P_{nd}),$$

where $\phi_{ce}=0.80$, $\phi_{cl}=0.90$, and $\phi_{cd}=0.95$.

Defining resistance factors by limit state allows us to take advantage of DSM's strength prediction accuracy for columns with partially effective cross-sections. Higher resistance factor are supported by the calculations and data in this report - local-global buckling interaction goes to 0.90 and distortional buckling goes to 0.95. The increased resistance factors for locally slender columns come with a small price - a resistance factor of 0.80 for columns with fully effective cross-sections. This is a slightly unsavory result (supported by the data) that can be thought of as an acceptable compromise considering that most cold-formed steel columns designed with AISI-S100-07 are partially effective.

For comparison, the recommended Main Specification resistance factors (derived with the same data used to evaluate DSM) are also presented:

$$\phi_c P_n = \min(\phi_{ce} A F_n, \phi_{cl} A_e F_n, \phi_{cd} P_{nd})$$

where $\phi_{ce}=0.80$, $\phi_{cl}=0.80$, and $\phi_{cd}=0.95$.

The lower Main Specification resistance factor for the local buckling limit state reflects the observation made in this report that the Main Specification is less accurate than DSM.

2. Move the AISI Direct Strength Method into the Main Specification.

DSM was demonstrated throughout this research to be a more accurate predictor of column capacity than the Main Specification. Improved prediction accuracy facilitates higher resistance factors, see Recommendation #1.

3. Lower the LSD resistance factor to $\phi_c=0.70$ to provide a uniform probability of failure consistent with $\beta=3.0$.

Alternatively, the current LSD resistance factor of $\phi_c=0.80$ can be maintained by lowering β from 3.0 to 2.5 and decreasing the D/L ratio from 1/3 to 1/5 (see Section 4.2.9 of this report). DSM resistance factors by LSD limit state could also be considered.

4. The LSD load effects coefficient of variation, V_Q , could be decreased from 0.21 to 0.19 in AISI-S100-07, Chapter F, Section F1.1.

As demonstrated in Eq. (35) of this report, the coefficient of variation of the load effects is a function of dead to live load ratio. For D/L=1/5, $V_Q=0.21$. For D/L=1/3, $V_Q=0.19$. This reduction in COV is beneficial and will increase the calculated LSD resistance factor (and available column capacity) by approximately 5%.

References

- Abdel-Rahman, N., and Sivakumaran, K. S. (1998). "Effective design width for perforated cold-formed steel compression members." *Canadian Journal of Civil Engineering*, 25, 315-330.
- AISC. (1986). "Load and resistance factor design specification for structural steel buildings." American Institute of Steel Construction, Chicago, IL.
- AISC. (1993). "Load and resistance factor design specification for structural steel buildings." American Institute of Steel Construction, Chicago, IL.
- AISI-S100. (2007). "North American specification for the design of cold-formed steel structural members." American Iron and Steel Institute, Washington, D.C.
- AISI. (1986). "Cold-formed steel design manual." American Iron and Steel Institute, Washington, DC.
- AISI. (1991). "LRFD cold-formed steel design manual." American Iron and Steel Institute, Washington, DC.
- AISI. (1996). "Cold-formed steel design manual." American Iron and Steel Institute, Washington, DC.
- AISI. (2001). "North American Specification for the Design of Cold-Formed Steel Structural Members and Commentary." American Iron and Steel Institute, Washington, D.C.
- AISI. (2004). "Supplement to the North American specification for the design of cold-formed steel structural members, Appendix 1." American Iron and Steel Institute, Washington, D.C.
- Chodraui, G. M. B., Shifferaw, Y., Malite, M., and Schafer, B. W. "Cold-formed steel angles under axial compression." *Eighteenth International Specialty Conference on Cold-Formed Steel Structures: Recent Research and Developments in Cold-Formed Steel Design and Construction*, Orlando, FL, United States, 285-300.
- Dat, D. T. (1980). "The strength of cold-formed steel columns." Cornell University Department of Structural Engineering Report No. 80-4, Ithaca, NY.
- Desmond, T. P., Pekoz, T., and Winter, G. (1981). "Edge stiffeners for thin-walled members." *ASCE Journal of Structural Division*, 107(2), 329-353.
- DeWolf, J. T., Pekoz, T., and Winter, T. (1974). "Local and overall buckling of cold-formed Members." *ASCE Journal of Structural Division*, 100(10), 2017-2036.
- Hsiao, L.-E., Yu, W.-W., and Galambos, T. V. (1990). "AISI LRFD method for cold-formed steel structural members." *ASCE Journal of structural engineering New York, N.Y.*, 116(2), 500-517.
- Loh, T. S., and Peköz, T. (1985). "Combined axial load and bending in cold-formed steel Members." Cornell University Department of Structural Engineering Report, Ithaca, NY.
- Loughlan, J. (1979). "Mode interaction in lipped channel columns under concentric or eccentric loading," Ph.D. Thesis, University of Strathclyde, Glasgow.
- Mathworks. (2009). "Matlab 7.8.0 (R2009a)." Mathworks, Inc., www.mathworks.com.
- Miller, T. H., and Peköz, T. (1994). "Unstiffened strip approach for perforated wall studs." *ASCE Journal of Structural Engineering*, 120(2), 410-421.
- Moen, C. D., and Schafer, B. W. (2008). "Experiments on cold-formed steel columns with holes." *Thin-Walled Structures*, 46, 1164-1182.

- Moen, C. D., and Schafer, B. W. (2010). "Direct strength design of cold-formed steel columns with holes." *2010 Annual Technical Session and Meeting, Structural Stability Research Council*, Orlando, FL.
- Moldovan, A. (1994). "Compression tests on cold-formed steel columns with monosymmetrical section." *Thin-Walled Structures*, 20(1-4 pt 2), 241-252.
- Mulligan, G. P. (1983). "The influence of local buckling on the structural behavior of singly-symmetric cold-formed steel columns," Ph.D. Thesis, Cornell University, Ithaca, NY.
- Ortiz-Colberg, R. A. (1981). "The load carrying capacity of perforated cold-formed steel columns," M.S. Thesis, Cornell University, Ithaca, NY.
- Peköz, T., and Sümer Ö. (1992). "Design provisions for cold-formed steel columns and beam columns." American Iron and Steel Institute, Washington, DC.
- Peköz, T. B. (1987). "Development of a unified approach to the design of cold-formed steel members." American Iron and Steel Institute, Washington, DC.
- Polyzois, D., and Charnvarnichborikarn, P. (1993). "Web-flange interaction in cold-formed steel z-section columns." *ASCE Journal of Structural Engineering*, 119(9), 2607-2628.
- Popovic, D., Hancock, G. J., and Rasmussen, K. J. R. (1999). "Axial compression tests on cold-formed angles." *ASCE Journal of Structural Engineering*, 125(5), 515-523.
- Pu, Y., Godley, M. H. R., Beale, R. G., and Lau, H. H. (1999). "Prediction of ultimate capacity of perforated lipped channels." *ASCE Journal of Structural Engineering*, 125(5), 510-514.
- Ravindra, M. K., and Galambos, T. V. (1978). "Load and resistance factor design for steel." *ASCE Journal of Structural Division*, 104(9), 1337-1353.
- Schafer, B. W. (2000). "Distortional buckling of cold-formed steel columns." American Iron and Steel Institute, Washington, D.C.
- Schafer, B. W. (2002). "Local, distortional, and Euler buckling of thin-walled columns." *ASCE Journal of Structural Engineering*, 128(3), 289-299.
- Schafer, B. W., and Ádàny, S. "Buckling analysis of cold-formed steel members using CUFSM: conventional and constrained finite strip methods." *Eighteenth International Specialty Conference on Cold-Formed Steel Structures*, Orlando, FL.
- Shanmugam, N. E., and Dhanalakshmi, M. (2001). "Design for openings in cold-formed steel channel stub columns." *Thin-Walled Structures*, 39, 961-981.
- Sivakumaran, K. S. (1987). "Load capacity of uniformly compressed cold-formed steel section with punched web." *Canadian Journal of Civil Engineering*, 14, 550-558.
- Thomasson, P. O. (1978). "Thin-walled C-shaped panels in axial compression." *Swedish Council for Building Research*, Report: ISBN-91-540-2820-5, Sweden.
- Von Karman, T., Sechler, E. F., and Donnell, L. H. (1932). "Strength of thin plates in compression." *American Society of Mechanical Engineers -- Transactions -- Applied Mechanics*, 54(2), 53-56.
- Weng, C. C., and Pekoz, T. (1990). "Compression tests of cold-formed steel columns." *ASCE Journal of Structural Engineering*, 116(5), 1230-1246.
- Young, B. (2004). "Tests and design of fixed-ended cold-formed steel plain angle columns." *ASCE Journal of Structural Engineering*, 130(12), 1931-1940.
- Young, B., and Chen, J. (2008). "Column tests of cold-formed steel non-symmetric lipped angle sections." *Journal of Constructional Steel Research*, 64(7-8), 808-815.
- Young, B., and Hancock, G. J. (2003). "Compression tests of channels with inclined simple edge stiffeners." *ASCE Journal of Structural Engineering*, 129(10), 1403-1411.

- Young, B., and Rasmussen, K. J. R. (1998a). "Design of lipped channel columns." *ASCE Journal of structural engineering*, 124(2), 140-148.
- Young, B., and Rasmussen, K. J. R. (1998b). "Tests of fixed-ended plain channel columns." *ASCE Journal of Structural Engineering*, 124(2), 131-139.

Appendix 1

Appendix 1 presents the cross-section dimensions, boundary conditions, test results and calculated capacities according to the AISI Main Specification and DSM. Tables that summarize these results use symbols to represent the cross-section dimensions and boundary conditions. The following table presents the symbol, its meaning and its units as used in Table A4.

Table A1.Symbols used in Table A4 and its meaning.

Symbol	Meaning	Units
L	Length	in.
Bnd Cond	Boundary Conditions	NA
0	Weak Axis Pinned	
1	Strong Axis Pinned	
2	Fixed-Fixed	
L Hole	Length of hole	in.
H Hole	Height of hole	in.
S	Spacing	in.
f_y	Yield Stress	ksi
t	thickness	in.
H1	Web height	in.
B1, B2	Flange width	in.
D1, D2	Lip width	in.
R	Outer radius	in.
P_{test}	Tested Capacity	kips
P_{crl}	Local elastic buckling capacity	kips
P_{crd}	Distortional elastic buckling capacity	kips
P_{cre}	Global elastic buckling capacity	kips
A_e	Effective area at buckling stress, F_n	sq. in.

Tables A2 and A3 present the Main Specification and the DSM Prequalified limits respectively.

Table A2.Main Specification limits

Main Specification Limits (Section B1.1, B2.2 and B4)		
Type	Ratio	Limit (in.)
Stiffened compression element with longitudinal edge connected to web/flange	Flat-width-to-thickness (w/t)	w/t ≤ 60
Stiffened compression element with both longitudinal edges connected stiffened elements	Flat-width-to-thickness (w/t)	w/t ≤ 500
Unstiffened compression element	Flat-width-to-thickness (w/t)	w/t ≤ 60
Uniformly compressed stiffened element with circular holes	Depth of hole-to-flat width (d_h/w) Flat-width-to-thickness (w/t)	0.5 ≥ $d_h/w \geq 0$ w/t ≤ 60
Uniformly compressed stiffened element with non circular holes	Center-to-center hole spacing (s) Clear distance from hole at ends (s_{end}) Depth of the hole (d_h) Length of the hole (L_h) Depth of hole-to-out-to-out-width(d_h/w_0)	s ≥ 24 $s_{end} \geq 10$ $d_h \leq 2.5$ $L_h \leq 4.5$ $d_h/w_0 \leq 0.5$
Uniformly compressed stiffened element with simple lip edge stiffener	Lip Angle (θ)	140° ≥ $\theta \geq 40^\circ$

Table A3.DSM prequalified limits

DSM Prequalified Limits for	Type of Cross-section		
	Lipped C-section	Lipped Z-section	Hat section
Web height-to-thickness (H/t)	H/t < 472	H/t < 137	H/t < 50
Flange width-to-thickness (B/t)	B/t < 159	B/t < 56	B/t < 20
Lip width-to-thickness (D/t)	4 < D/t < 33	0 < D/t < 36	4 < D/t < 6
Web height-to-flange width (H/B)	0.7 < H/B < 5.0	1.5 < H/B < 2.7	1.0 < H/B < 1.2
Lip width-to-flange width (D/B)	0.05 < D/B < 0.41	0.00 < D/B < 0.73	D/B = 0.13
Lip Angle (θ)	$\theta = 90^\circ$	$\theta = 50^\circ$	---

Table A4 presents details of each test including column dimensions, boundary conditions and test results.

Table A4.Column test details

Author	Specimen Name	Cross section Name	Hole type	L	Bnd Cond	L Hole	H Hole	Spacing S	Hole Offset	f _y	t	H1	B1	B2	D1	D2	R	P _{test}
Thomasson 1978	A71	Lipped Cee	NaN	105.90	0.00	NaN	NaN	NaN	NaN	56.70	0.03	11.78	3.95	3.95	0.77	0.77	0.08	3.60
	A74	Lipped Cee	NaN	105.90	0.00	NaN	NaN	NaN	NaN	57.30	0.03	11.80	3.97	3.97	0.81	0.81	0.08	3.65
	A75	Lipped Cee	NaN	105.90	0.00	NaN	NaN	NaN	NaN	57.70	0.03	11.78	3.96	3.96	0.79	0.79	0.08	3.49
	A76	Lipped Cee	NaN	105.90	0.00	NaN	NaN	NaN	NaN	41.80	0.03	11.81	3.94	3.94	0.80	0.80	0.09	3.26
	A101	Lipped Cee	NaN	105.90	0.00	NaN	NaN	NaN	NaN	67.30	0.04	11.80	3.96	3.96	0.80	0.80	0.10	8.30
	A102	Lipped Cee	NaN	105.90	0.00	NaN	NaN	NaN	NaN	66.70	0.04	11.80	3.96	3.96	0.79	0.79	0.10	7.88
	A103	Lipped Cee	NaN	105.90	0.00	NaN	NaN	NaN	NaN	66.70	0.04	11.78	3.96	3.96	0.77	0.77	0.10	8.35
	A104	Lipped Cee	NaN	105.90	0.00	NaN	NaN	NaN	NaN	68.90	0.04	11.74	3.92	3.92	0.77	0.77	0.10	7.76
	A151	Lipped Cee	NaN	105.90	0.00	NaN	NaN	NaN	NaN	55.40	0.06	11.78	3.94	3.94	0.80	0.80	0.12	17.21
	A152	Lipped Cee	NaN	105.90	0.00	NaN	NaN	NaN	NaN	55.00	0.06	11.81	3.94	3.94	0.80	0.80	0.12	15.71
	A153	Lipped Cee	NaN	105.90	0.00	NaN	NaN	NaN	NaN	57.30	0.05	11.81	3.93	3.93	0.82	0.82	0.11	16.02
	A154	Lipped Cee	NaN	105.90	0.00	NaN	NaN	NaN	NaN	57.00	0.06	11.84	3.95	3.95	0.92	0.92	0.11	16.40
	A156	Lipped Cee	NaN	105.90	0.00	NaN	NaN	NaN	NaN	55.30	0.06	11.79	3.93	3.93	0.80	0.80	0.11	15.50

Table A5.Main Specification and DSM results

Author	Specimen Name	P_{cre}	P_{crl}	P_{crd}	A_e	P_{test}/P_n	P_{test}/P_n	
						DSM	Main Spec	
Thomasson 1978	A71	26.91	0.36	2.38	0.13	0.96	0.80	
	A74	27.63	0.36	2.47	0.13	0.96	0.80	
	A75	27.22	0.36	2.42	0.13	0.92	0.77	
	A76	28.17	0.40	2.65	0.15	0.91	0.75	
	A101	39.99	1.16	5.31	0.25	1.05	0.85	
	A102	39.86	1.16	5.28	0.25	1.00	0.81	
	A103	39.68	1.16	5.22	0.25	1.06	0.86	
	A104	39.63	1.26	4.95	0.26	0.95	0.76	
	A151	59.79	4.25	11.53	0.53	1.10	0.93	
	A152	58.74	4.02	10.99	0.52	1.04	0.88	
	A153	57.02	3.61	11.52	0.50	1.11	0.91	
	A154	61.31	3.85	13.00	0.53	1.07	0.86	
	A156	57.50	3.82	11.93	0.51	1.05	0.88	
	Mulligan 1983	GM1	60.85	4.84	13.04	0.38	1.04	0.90
	GM2	39.52	6.26	12.39	0.37	1.11	1.06	
	GM3	16.46	5.11	11.49	0.44	1.08	0.97	
	GM4	16.35	4.88	11.56	0.43	1.14	1.00	
	GM5	44.75	5.86	14.18	0.43	1.17	1.04	
	GM6	52.18	2.76	8.27	0.38	1.14	0.94	
	GM7	29.90	2.76	7.94	0.41	1.14	0.92	
	GM8	19.01	2.57	7.35	0.42	1.16	0.93	
	GM9	32.40	3.39	9.67	0.46	1.24	1.00	
	GM10	41.05	9.18	12.37	0.44	0.88	0.94	
	GM11	121.74	4.02	12.16	0.44	1.08	0.97	
	GM12	68.68	3.99	11.02	0.43	1.06	0.97	
	GM13	68.63	3.99	10.34	0.43	1.05	0.98	
Loughlan 1979	L1	9.46	2.82	9.25	0.21	0.75	0.69	
	L2	19.93	2.58	9.56	0.18	0.77	0.72	
	L3	17.06	2.84	10.47	0.19	0.70	0.71	
	L4	24.85	3.16	11.72	0.19	0.67	0.69	
	L5	37.22	2.90	12.12	0.18	0.73	0.75	
	L6	9.92	1.83	7.31	0.20	1.02	0.88	
	L7	13.98	1.86	7.66	0.19	0.97	0.85	
	L8	21.57	1.87	8.16	0.18	0.98	0.86	
	L9	18.43	2.05	10.32	0.19	0.92	0.87	
	L10	26.43	2.06	11.13	0.18	0.91	0.87	
	L11	41.38	2.28	11.87	0.19	0.84	0.80	
	L12	10.95	1.58	6.47	0.21	0.88	0.74	
	L13	15.67	1.59	6.84	0.20	0.85	0.71	
	L14	23.42	1.58	7.04	0.19	0.86	0.72	
	L15	19.72	1.56	9.03	0.19	1.09	0.98	
	L16	29.03	1.72	10.45	0.20	1.02	0.93	
	L17	42.91	1.59	11.09	0.18	1.06	0.97	
	L18	10.85	1.16	4.94	0.20	0.91	0.74	
	L19	15.58	1.17	5.22	0.19	0.90	0.73	
	L20	24.92	1.28	6.09	0.19	0.84	0.69	
	L21	20.77	1.27	7.76	0.19	0.89	0.78	
	L22	29.54	1.27	8.37	0.19	0.96	0.84	
	L23	45.38	1.29	9.64	0.18	0.85	0.75	
	L24	18.66	12.33	24.51	0.57	1.31	1.29	
	L25	37.00	14.43	35.57	0.66	1.05	0.97	
	L26	53.20	15.15	38.05	0.67	0.99	0.90	
	L27	80.56	14.58	39.08	0.65	0.97	0.87	
	L28	19.65	9.99	19.28	0.58	1.04	1.01	
	L29	28.32	10.49	20.32	0.58	1.00	0.95	
	L30	42.66	10.61	21.19	0.57	0.99	0.92	
	L31	38.68	11.06	29.37	0.66	1.18	1.05	
	L32	54.47	11.08	30.40	0.65	1.11	0.97	
	L33	84.33	11.21	32.50	0.64	1.11	0.96	

Author	Specimen Name	P_{cre}	P_{crl}	P_{crd}	A_c	P_{test}/P_n	P_{tes}/P_n
						DSM	Main Spec
Mulligan 1983	60x30	481.72	11.03	19.94	0.27	1.15	1.18
	90x30	808.24	6.70	16.36	0.28	1.16	1.11
	120x30	1322.84	4.57	10.99	0.29	1.19	1.09
	60x60	469.09	12.68	33.20	0.36	1.03	1.11
	60x60	458.31	13.18	34.27	0.37	1.06	1.13
	120x60	1545.28	5.90	29.47	0.37	1.14	1.05
	120x60	1511.21	5.87	27.68	0.36	1.20	1.14
	180x60	1916.77	3.27	19.37	0.38	1.22	1.02
	180x60	1288.67	3.20	15.49	0.37	1.24	1.03
	240x60	2588.63	2.21	14.57	0.38	1.28	1.03
	240x60	969.13	2.20	8.83	0.37	1.18	0.95
	240x60	2618.28	2.27	14.91	0.38	1.24	1.00
	60x90	296.46	7.76	22.49	0.37	0.98	1.00
	60x90	290.53	7.75	22.54	0.36	1.01	1.03
	90x90	583.45	7.28	21.70	0.36	0.96	1.02
	90x90	578.21	7.51	22.08	0.37	0.96	1.01
	180x90	3368.59	6.74	63.39	0.56	1.04	0.95
	180x90	3383.49	6.75	63.13	0.56	1.05	0.96
	180x90	2239.34	3.97	28.61	0.32	0.91	0.89
	180x90	2306.23	4.61	22.57	0.45	1.11	1.07
	180x90	2358.67	4.74	24.43	0.47	1.16	1.08
	270x90	3007.27	2.59	16.23	0.45	1.20	1.06
	270x90	1858.79	2.66	12.90	0.45	1.21	1.07
	360x90	3702.02	1.65	9.17	0.45	1.19	0.96
Miller and Peköz 1994	LC-1	11.93	36.26	39.22	0.49	1.08	1.08
	LC-2	12.35	36.27	41.19	0.49	0.96	0.96
	LC-3	12.45	37.40	42.17	0.50	0.99	0.98
	LC-4	6.24	1.75	2.39	0.20	1.13	1.03
	LC-6	6.53	1.72	2.60	0.20	0.93	0.83
	LC-7	6.13	1.77	2.62	0.20	1.09	0.99
	LC-10	38.39	36.63	41.43	0.47	1.11	1.17
	LC-14	1.78	1.84	2.68	0.27	1.05	1.12
	LC-15	7.03	1.78	2.61	0.20	0.97	0.85
	LC-17	11.81	35.76	40.27	0.50	1.21	1.21
	LC-18	12.03	36.11	40.53	0.50	1.06	1.06
	LC-19	3.57	36.11	40.53	0.50	1.92	1.92
	LC-21	12.54	35.21	40.24	0.49	1.11	1.11
	LC-22	13.26	36.11	40.97	0.50	1.03	1.03
	LC-23	13.10	35.56	40.49	0.50	1.00	0.99
	LC-24	39.26	36.11	40.98	0.48	1.16	1.23
	LC-25	26.31	1.78	2.67	0.16	1.07	1.07
	LC-30	3.57	36.11	40.53	0.50	1.97	1.97
	LC-31	3.55	35.56	40.06	0.50	1.63	1.62
Young and Rasmussen 1998a	L36F0280	975.13	15.14	40.16	0.31	1.17	1.12
	L36F1000	77.78	15.44	25.10	0.34	1.13	1.06
	L36F1500	35.63	15.42	24.66	0.35	1.17	1.12
	L36F2000	20.11	15.09	23.64	0.36	1.20	1.20
	L36F2500	13.53	15.45	23.95	0.38	1.19	1.26
	L36F3000	9.95	15.46	24.36	0.40	1.01	1.10
	L48F0300	1126.24	16.41	39.30	0.30	1.18	1.29
	L48F1000	102.36	16.37	23.56	0.32	1.16	1.26
	L48F1500	46.21	16.45	23.49	0.34	1.24	1.32
	L48F2000	26.65	16.87	23.30	0.38	1.29	1.34
	L48F2500	17.42	16.76	22.52	0.42	1.27	1.30
	L48F3000	12.64	16.62	23.32	0.45	1.14	1.20
	P36F0280	583.44	9.47	10.26	0.20	1.17	1.17
	P36F1000	47.11	9.69	9.75	0.22	1.09	1.17
	P36F1500	21.78	9.23	9.26	0.24	1.02	1.18
	P36F2000	13.01	9.68	9.70	0.27	1.04	1.17
	P36F2500	8.94	9.65	9.66	0.31	1.04	1.16
	P36F3000	6.24	9.46	9.47	0.35	1.02	1.12
	P48F0300	771.32	7.83	8.54	0.20	1.22	1.22
	P48F1000	70.89	7.82	7.88	0.21	1.21	1.21
	P48F1500	32.27	7.67	7.70	0.23	1.09	1.21
	P48F1850	21.98	8.16	8.18	0.26	0.96	1.10
	P48F2150	16.55	7.84	7.86	0.27	1.01	1.16
	P48F2500	12.50	7.82	7.83	0.29	1.04	1.18
	P48F3000	9.09	7.84	7.85	0.33	1.25	1.40
	P48F3500	6.98	7.85	7.85	0.36	1.18	1.31

Author	Specimen Name	P_{cre}	P_{crl}	P_{crd}	A_e	P_{test}/P_n	P_{test}/P_n
						DSM	Main Spec
Young and Hancock 2003	ST15A30	49.13	16.62	12.88	0.32	1.06	1.09
	ST15A45	50.36	16.62	15.83	0.33	1.02	1.12
	ST15A60	49.51	16.93	18.17	0.33	1.01	1.14
	ST15A90	46.58	16.94	21.34	0.34	1.20	1.32
	ST15A120	43.58	16.58	19.49	0.33	1.29	1.45
	ST15A135	40.68	15.71	16.55	0.31	1.19	1.37
	ST15A150	39.44	15.91	15.18	0.31	1.29	1.51
	ST19A30	61.35	21.33	21.38	0.46	1.14	1.17
	ST19A45	63.36	34.88	27.55	0.49	1.09	1.18
	ST19A60	63.13	34.73	31.27	0.50	1.13	1.27
	ST19A90	59.07	32.98	34.61	0.50	1.23	1.33
	ST19A120	55.93	33.10	34.55	0.50	1.33	1.46
	ST19A135	52.11	32.78	30.32	0.48	1.34	1.50
	ST19A150	51.01	32.33	28.11	0.48	1.37	1.54
	ST24A30	83.83	38.83	41.53	0.67	1.03	1.04
	ST24A45	88.10	67.86	49.22	0.69	1.05	1.16
	ST24A60	84.89	67.73	54.93	0.70	1.11	1.27
	ST24A90	83.73	69.17	65.14	0.71	1.08	1.22
	ST24A120	76.27	64.53	57.02	0.68	1.15	1.33
	ST24A135	70.41	50.36	54.42	0.67	1.26	1.37
	ST24A150	69.38	47.07	52.80	0.67	1.28	1.37
	LT15A30	83.29	6.58	7.31	0.32	1.11	1.11
	LT15A45	82.52	16.93	8.61	0.33	1.03	1.03
	LT15A60	84.73	18.39	10.49	0.34	0.98	0.98
	LT15A90	81.21	17.37	10.60	0.33	0.97	0.98
	LT15A120	79.80	18.23	10.26	0.34	1.06	1.06
	LT15A135	76.24	7.96	8.58	0.32	1.15	1.15
	LT15A150	75.73	7.54	8.30	0.31	1.15	1.15
	LT19A30	100.67	11.30	32.95	0.47	0.91	0.93
	LT19A45	105.41	14.69	15.76	0.49	1.01	1.01
	LT19A60	105.39	16.32	17.26	0.50	1.03	1.03
	LT19A90	104.10	35.99	18.89	0.50	0.97	0.98
	LT19A120	101.62	17.34	18.33	0.50	1.11	1.13
	LT19A135	97.12	14.19	16.19	0.48	1.12	1.12
	LT19A150	96.07	13.11	15.76	0.47	1.23	1.23
	LT24A30	130.74	20.00	20.89	0.69	0.92	0.92
	LT24A45	133.32	24.13	24.91	0.71	0.90	0.90
	LT24A60	135.26	29.35	31.02	0.73	0.88	0.89
	LT24A90	138.97	33.96	35.90	0.76	0.88	0.92
	LT24A120	133.75	29.90	32.61	0.73	1.02	1.05
	LT24A135	127.18	23.16	28.99	0.70	1.04	1.06
	LT24A150	129.17	21.97	29.03	0.70	1.05	1.05
Moen and Schafer 2008	362-1-24-NH	128.73	4.95	10.18	0.17	1.22	1.16
	362-2-24-NH	127.97	5.16	10.15	0.18	1.20	1.10
	362-3-24-NH	128.16	5.51	10.41	0.18	1.13	1.05
	362-1-48-NH	31.72	5.77	9.75	0.20	1.06	0.97
	362-2-48-NH	31.09	5.80	9.62	0.20	1.11	1.02
	362-3-48-NH	31.31	5.52	9.34	0.19	1.14	1.05
	600-1-24-NH	257.06	3.57	7.11	0.22	1.16	1.16
	600-2-24-NH	249.45	3.56	6.95	0.22	1.18	1.18
	600-3-24-NH	250.31	3.58	7.11	0.22	1.19	1.19
	600-1-48-NH	62.16	3.49	6.17	0.23	1.17	1.16
	600-2-48-NH	60.57	3.48	6.05	0.22	1.18	1.17
	600-3-48-NH	61.12	3.47	5.99	0.23	1.18	1.18

Author	Specimen Name	P_{cre}	P_{crl}	P_{crd}	A_e	P_{test}/P_n	P_{test}/P_n
						DSM	Main Spec
Ortiz-Colberg 1981	L2	9.03	10.70	18.38	0.31	1.17	1.29
	L3	49.15	10.70	20.63	0.27	1.07	1.11
	L6	9.03	10.70	18.38	0.29	1.17	1.37
	L7	9.03	10.70	18.38	0.27	1.17	1.45
	L9	23.56	10.70	19.19	0.28	0.97	1.03
	L10	23.68	10.70	19.20	0.26	1.05	1.19
	L14	23.44	10.70	19.19	0.29	1.00	1.01
	S4	648.76	10.83	30.03	0.26	1.15	1.15
	S7	661.97	10.92	32.31	0.24	1.00	1.08
	S6	653.97	11.09	30.60	0.24	1.05	1.11
	S8	652.21	11.08	30.55	0.23	1.03	1.16
	S5	654.10	11.22	30.78	0.26	1.09	1.12
	S3	650.39	11.28	30.74	0.27	1.12	1.10
	S14	983.85	39.89	69.20	0.45	0.97	1.17
	S15	984.81	39.89	69.19	0.42	0.95	1.21
	L16	20.35	39.69	47.30	0.47	1.12	1.31
	L17	20.27	39.69	47.29	0.43	0.98	1.24
	L19	72.58	39.69	50.06	0.42	0.88	1.15
	L22	26.13	39.69	47.60	0.43	1.18	1.50
	L26	26.13	39.69	47.60	0.47	1.14	1.34
	L27	72.58	39.69	50.06	0.45	0.96	1.17
	L28	72.58	39.69	50.06	0.46	1.10	1.32
	L32	13.34	39.69	46.93	0.47	1.15	1.34
	L1	9.03	10.70	18.38	0.31	1.36	1.49
	L5	49.15	10.70	20.63	0.27	1.09	1.12
	L8	9.03	10.70	18.38	0.29	0.99	1.16
	L18	26.13	39.69	47.60	0.46	1.06	1.25
	L20	26.13	39.69	47.60	0.46	1.11	1.30
	L21	26.13	39.69	47.60	0.47	0.96	1.13
	L23	26.13	39.69	47.60	0.43	0.93	1.19
	L24	26.13	39.69	47.60	0.47	0.98	1.15
	L31	26.13	39.69	47.60	0.46	1.07	1.26
Ortiz-Colberg 1981	L4	49.15	10.70	20.63	0.30	1.14	1.06
	L11	23.56	10.70	19.19	0.31	0.89	0.85
	L12	49.15	10.70	20.63	0.30	1.14	1.07
	L13	9.03	10.70	18.38	0.33	1.12	1.16
	L15	26.13	39.69	47.60	0.53	1.29	1.33
	L25	13.55	39.69	46.94	0.55	1.15	1.15
	L29	72.58	39.69	50.06	0.52	1.08	1.14
	L30	72.58	39.69	50.06	0.52	1.10	1.16
	S1	660.35	10.94	32.57	0.28	1.20	1.11
	S2	649.99	10.91	30.21	0.28	1.20	1.12
	S12	1008.67	38.84	68.37	0.51	1.11	1.17

Author	Specimen Name	P_{cre}	P_{crl}	P_{crd}	A_e	P_{test}/P_n	P_{test}/P_n	
						DSM	Main Spec	
Pu et al. 1999	M-1.2-2-10-1	818.76	8.57	33.72	0.32	1.03	1.04	
	M-1.2-2-10-2	818.76	8.57	33.72	0.32	1.04	1.05	
	M-1.2-2-10-3	818.76	8.57	33.72	0.32	1.04	1.05	
	M-1.2-2-15-1	818.76	8.57	33.72	0.32	0.99	1.01	
	M-1.2-2-15-2	818.76	8.57	33.72	0.32	1.00	1.02	
	M-1.2-2-15-3	818.76	8.57	33.72	0.32	1.02	1.03	
	M-1.2-2-20-1	818.76	8.57	33.72	0.31	0.99	1.01	
	M-1.2-2-20-2	818.76	8.57	33.72	0.31	1.00	1.02	
	M-1.2-2-20-3	818.76	8.57	33.72	0.31	0.99	1.01	
	M-1.2-1-15-1	818.76	8.57	33.72	0.32	1.02	1.04	
	M-1.2-1-15-2	818.76	8.57	33.72	0.32	1.02	1.04	
	M-1.2-1-15-3	818.76	8.57	33.72	0.32	1.03	1.05	
	C-1.2-1-30-1	818.76	8.57	33.72	0.32	1.05	1.07	
	C-1.2-1-30-2	818.76	8.57	33.72	0.32	1.06	1.08	
	C-1.2-1-30-3	818.76	8.57	33.72	0.32	1.06	1.07	
	M-0.8-2-10-1	560.76	2.54	18.70	0.17	1.09	1.06	
	M-0.8-2-10-2	560.76	2.54	18.70	0.17	1.06	1.04	
	M-0.8-2-10-3	560.76	2.54	18.70	0.17	1.07	1.04	
	M-0.8-2-15-1	560.76	2.54	18.70	0.17	1.08	1.06	
	M-0.8-2-15-2	560.76	2.54	18.70	0.17	1.09	1.07	
	M-0.8-2-15-3	560.76	2.54	18.70	0.17	1.07	1.04	
	M-0.8-2-20-1	560.76	2.54	18.70	0.17	1.07	1.04	
	M-0.8-2-20-2	560.76	2.54	18.70	0.17	1.01	0.99	
	M-0.8-2-20-3	560.76	2.54	18.70	0.17	1.02	1.01	
	M-0.8-1-15-1	560.76	2.54	18.70	0.17	1.06	1.04	
	M-0.8-1-15-2	560.76	2.54	18.70	0.17	1.07	1.04	
	M-0.8-1-15-3	560.76	2.54	18.70	0.17	1.05	1.03	
	C-0.8-1-30-1	560.76	2.54	18.70	0.17	1.10	1.08	
	C-0.8-1-30-2	560.76	2.54	18.70	0.17	1.08	1.06	
	C-0.8-1-30-3	560.76	2.54	18.70	0.17	1.10	1.08	
	Pu et al. 1999	U-1.2-0-0-1	818.76	8.57	33.72	0.35	1.05	0.96
		U-1.2-0-0-2	818.76	8.57	33.72	0.35	1.05	0.96
		U-1.2-0-0-3	818.76	8.57	33.72	0.35	1.06	0.96
		U-0.8-0-0-1	560.76	2.54	18.70	0.19	1.10	0.97
		U-0.8-0-0-2	560.76	2.54	18.70	0.19	1.12	0.99
		U-0.8-0-0-3	560.76	2.54	18.70	0.19	1.09	0.96

Author	Specimen Name	P_{cre}	P_{crl}	P_{crd}	A_e	P_{test}/P_n	P_{test}/P_n
						DSM	Main Spec
Sivakumaran 1987	A-2-1	748.44	21.12	66.98	0.37	1.03	1.07
	A-2-2	748.44	21.12	66.98	0.37	1.03	1.07
	A-2-3	748.44	21.12	66.98	0.37	1.04	1.07
	A-4-1	748.44	21.12	66.98	0.34	0.98	1.10
	A-4-2	748.44	21.12	66.98	0.34	0.99	1.10
	A-4-3	748.44	21.12	66.98	0.34	0.99	1.10
	A-6-1	748.44	21.12	66.98	0.32	0.94	1.13
	A-6-2	748.44	21.12	66.98	0.32	0.93	1.12
	A-6-3	748.44	21.12	66.98	0.32	0.95	1.14
	B-2-1	748.44	21.12	66.98	0.35	1.01	1.12
	B-2-2	748.44	21.12	66.98	0.35	1.02	1.12
	B-2-3	748.44	21.12	66.98	0.35	1.03	1.13
	B-4-1	748.44	21.12	66.98	0.34	0.98	1.10
	B-4-2	748.44	21.12	66.98	0.34	0.98	1.10
	B-4-3	748.44	21.12	66.98	0.34	0.99	1.11
	B-6-1	748.44	21.12	66.98	0.33	0.92	1.06
	B-6-2	748.44	21.12	66.98	0.33	0.94	1.08
	B-6-3	748.44	21.12	66.98	0.33	0.95	1.09
	C-1-1	748.44	21.12	66.98	0.21	0.87	1.61
	C-1-2	748.44	21.12	66.98	0.21	0.88	1.61
	C-1-3	748.44	21.12	66.98	0.21	0.88	1.61
	D-0-1	748.44	21.12	66.98	0.39	1.02	0.99
	D-0-2	748.44	21.12	66.98	0.39	1.02	0.99
	D-0-3	748.44	21.12	66.98	0.39	1.05	1.02
	A-2-1	435.11	5.54	19.37	0.31	1.17	1.06
	A-2-2	435.11	5.54	19.37	0.31	1.17	1.06
	A-2-3	435.11	5.54	19.37	0.31	1.17	1.06
	A-4-1	435.11	5.54	19.37	0.28	1.17	1.14
	A-4-2	435.11	5.54	19.37	0.28	1.15	1.12
	A-4-3	435.11	5.54	19.37	0.28	1.16	1.12
	A-6-1	435.11	5.54	19.37	0.27	1.05	1.10
	A-6-2	435.11	5.54	19.37	0.27	0.99	1.04
	A-6-3	435.11	5.54	19.37	0.27	1.03	1.07
	B-2-1	435.11	5.54	19.37	0.29	1.15	1.11
	B-2-2	435.11	5.54	19.37	0.29	1.15	1.11
	B-2-3	435.11	5.54	19.37	0.29	1.18	1.14
	B-4-1	435.11	5.54	19.37	0.28	1.13	1.11
	B-4-2	435.11	5.54	19.37	0.28	1.12	1.09
	B-4-3	435.11	5.54	19.37	0.28	1.08	1.05
	B-6-1	435.11	5.54	19.37	0.28	1.04	1.03
	B-6-2	435.11	5.54	19.37	0.28	1.02	1.01
	B-6-3	435.11	5.54	19.37	0.28	1.01	1.01
	C-1-1	435.11	5.54	19.37	0.27	1.14	1.15
	C-1-2	435.11	5.54	19.37	0.27	1.12	1.14
	C-1-3	435.11	5.54	19.37	0.27	1.10	1.12
	D-0-1	435.11	5.54	19.37	0.33	1.18	1.00
	D-0-2	435.11	5.54	19.37	0.33	1.18	1.01
	D-0-3	435.11	5.54	19.37	0.33	1.16	0.98

Author	Specimen Name	P_{cre}	P_{crl}	P_{crd}	A_e	P_{test}/P_n	P_{test}/P_n
						DSM	Main Spec
Moen and Schafer 2008	362-1-24-H	120.12	5.68	11.33	0.16	1.12	1.16
	362-2-24-H	114.90	5.13	10.33	0.16	1.20	1.21
	362-3-24-H	131.02	5.56	11.03	0.17	1.09	1.15
	362-1-48-H	29.03	5.55	9.80	0.18	1.08	1.10
	362-2-48-H	28.84	5.47	9.65	0.17	1.11	1.13
	362-3-48-H	29.73	5.73	10.07	0.18	1.11	1.14
	600-1-24-H	240.57	3.20	6.43	0.18	1.23	1.23
	600-2-24-H	238.97	3.00	3.24	0.18	1.25	1.24
	600-3-24-H	240.83	3.38	6.69	0.19	1.18	1.18
	600-1-48-H	64.20	3.39	6.03	0.20	1.17	1.17
	600-2-48-H	60.34	3.38	5.88	0.19	1.24	1.24
	600-3-48-H	63.98	3.42	5.96	0.20	1.17	1.17
	Miller and Peköz 1994	1-12	1051.34	35.36	58.95	0.32	1.02
		1-13	1085.04	34.81	58.88	0.32	0.94
		1-17	155.05	1.65	3.12	0.13	1.07
		1-19	171.45	1.68	3.22	0.13	1.13
		2-11	1118.19	34.93	60.00	0.34	0.87
		2-12	1100.41	35.21	60.02	0.34	0.86
		2-13	1104.29	35.63	60.55	0.34	0.86
		2-14	210.68	1.71	3.12	0.13	1.17
		2-15	210.66	1.65	3.04	0.12	1.17
		2-16	210.04	1.70	3.11	0.13	1.15
		2-17	1417.74	35.21	65.16	0.34	0.89
		2-18	1214.14	35.77	62.50	0.34	0.86
		2-19	1249.32	36.90	64.37	0.34	0.84
		2-20	982.92	1.70	5.25	0.13	1.11
		2-21	977.73	1.68	5.17	0.13	1.16
		2-22	998.47	1.79	5.48	0.13	1.16
		2-23	1021.56	1.79	5.54	0.13	1.19
		2-24	237.41	1.76	3.26	0.13	1.16
		2-25	240.07	1.76	3.26	0.13	1.16
		2-26	240.87	1.72	3.20	0.13	1.20
	LC-5	6.65	1.72	2.59	0.17	1.00	1.05
	LC-9	17.12	35.17	41.06	0.32	0.87	1.37
	LC-11	43.72	34.57	42.34	0.33	0.95	1.48
	LC-12	7.04	1.69	2.59	0.17	0.92	0.95
	LC-13	27.24	1.66	2.32	0.13	1.03	1.03
	LC-20	13.29	34.87	41.93	0.34	1.16	1.81
	LC-28	1.87	1.63	2.46	0.20	1.08	1.42
	LC-29	4.36	34.87	41.93	0.33	0.98	1.54
	LC-32	7.54	1.69	2.53	0.16	0.97	0.99
	LC-33	13.27	34.87	41.93	0.33	1.08	1.69
	LC-35	1.88	1.69	2.53	0.20	1.03	1.37
	LC-36	1.89	1.69	2.53	0.20	0.74	0.99
	LC-37	7.53	1.69	2.53	0.16	1.01	1.03
	LC-38	7.10	1.74	2.67	0.17	1.03	1.06
	LC-39	26.54	1.61	2.25	0.12	0.83	0.83
	LC-40	13.30	34.87	41.93	0.34	0.87	1.35
	LC-41	4.40	35.96	42.90	0.34	0.97	1.52

Author	Specimen Name	P_{cre}	P_{crl}	P_{crd}	A_e	P_{test}/P_n	P_{test}/P_n
						DSM	Main Spec
Miller and Peköz 1994	1-1	1078.71	35.32	59.72	0.47	1.11	1.15
	1-2	1088.16	36.05	60.76	0.48	1.09	1.13
	1-3	1059.24	35.36	58.67	0.47	1.11	1.15
	1-4	215.70	1.87	3.09	0.15	0.83	0.83
	1-5	226.06	1.91	3.46	0.16	1.00	1.00
	1-6	220.88	1.84	3.10	0.15	1.13	1.13
	1-7	879.85	48.70	65.90	0.54	0.96	1.01
	1-8	904.50	49.79	68.43	0.55	0.95	1.01
	1-9	915.22	48.65	66.20	0.54	1.06	1.11
	1-10	1273.60	34.52	62.03	0.47	1.15	1.19
	1-11	1216.21	34.94	61.15	0.47	1.19	1.23
	1-14	220.51	1.72	3.16	0.15	1.21	1.21
	1-15	206.86	1.61	2.95	0.14	1.25	1.25
	1-16	204.10	1.84	3.28	0.15	1.18	1.18
	2-1	911.65	35.63	57.41	0.47	0.93	0.97
	2-2	901.85	35.27	57.01	0.47	1.05	1.08
	2-3	909.51	35.35	57.08	0.47	1.04	1.07
	2-4	911.65	35.63	57.41	0.47	0.90	0.93
	2-5	909.51	35.35	57.08	0.47	1.04	1.07
	2-6	203.19	1.75	3.12	0.15	1.14	1.14
	2-7	209.58	1.74	3.16	0.15	1.12	1.12
	2-8	202.00	1.72	3.11	0.15	1.06	1.06
	2-9	204.72	1.73	3.12	0.15	1.09	1.09
	2-10	204.10	1.72	3.11	0.15	1.17	1.17
Abdel-Rahman and Sivakumaran 1998	A-C	1031.27	11.50	19.39	0.45	1.12	1.12
	A-S	1032.74	11.50	19.42	0.44	1.13	1.13
	A-O	826.77	11.50	18.29	0.44	1.15	1.15
	A-R	826.77	11.50	18.29	0.44	1.12	1.12
	B-C	1273.96	9.36	36.52	0.26	1.04	1.08
	B-S	1273.96	9.36	36.52	0.26	1.04	1.08
	B-O	884.92	9.36	30.47	0.26	1.03	1.07
	B-R	884.92	9.36	30.47	0.26	1.05	1.09
Polyzois, D. et al. 1993	38-0.0-1	196.75	8.27	8.59	0.27	1.14	1.14
	38-0.0-2	199.74	8.35	8.67	0.27	1.05	1.05
	38-0.0-3	201.21	8.29	8.61	0.27	1.13	1.13
	51.0.0-1	409.30	7.63	8.06	0.28	1.03	1.03
	51.0.0-2	408.40	7.63	8.06	0.28	1.09	1.09
	51.0.0-3	410.63	7.60	8.03	0.28	1.10	1.10
	63-0.0-1	683.74	6.40	6.76	0.28	1.15	1.15
	63-0.0-2	685.17	6.40	6.76	0.28	1.19	1.19
	63-0.0-3	692.54	6.34	6.70	0.28	1.18	1.18
	68-0.0-1 a	781.25	4.67	5.01	0.27	1.18	1.18
	68-0.0-2 .	767.17	4.70	5.04	0.27	1.00	1.00
	68-0.0-1 a	192.06	4.65	4.73	0.28	1.13	1.13
	68-0.0-2"	191.24	4.69	4.77	0.28	1.24	1.24
	68-0.0-P	958.59	5.02	5.74	0.29	1.13	1.13

Author	Specimen Name	P_{cre}	P_{crl}	P_{crd}	A_e	P_{test}/P_n	P_{test}/P_n
						DSM	Main Spec
Polyzois, D. et al. 1993	68-0.0-2 b	951.38	5.28	133.71	0.29	0.68	0.78
	68-3.8-1 f	952.16	5.73	6.50	0.31	1.00	1.00
	68-3.8-2	958.66	5.80	6.57	0.31	1.00	1.00
	68-6.4-1	1043.42	6.86	12.38	0.36	0.87	0.87
	68-6.4-2	1094.31	6.85	12.40	0.36	0.90	0.90
	68-0.0-1 b	225.61	6.32	6.63	0.33	1.01	1.01
	68-0.0-2 b	227.00	6.25	6.57	0.33	0.94	0.94
	68-3.8-1	224.57	6.28	6.59	0.33	1.04	1.04
	68-3.8-2	227.19	6.23	6.54	0.33	1.03	1.03
	68-6.4-1	252.63	6.77	9.57	0.37	0.90	0.90
	68-6.4-2	253.94	6.74	8.48	0.36	1.00	1.00
	38-6.4-1	639.05	14.37	30.20	0.40	1.05	0.97
	38-6.4-2	659.13	14.38	30.56	0.40	0.96	0.89
	38-6.4-3	648.40	14.29	29.55	0.39	1.07	1.00
	38-12.7-1	781.89	15.11	44.95	0.46	0.94	0.78
	38-12.7-2	802.65	15.13	55.31	0.47	1.04	0.87
	38-12.7-3	764.38	15.11	45.06	0.46	0.80	0.67
	38-19.1-1	899.47	15.81	72.88	0.46	0.91	0.80
	38-19.1-2	915.28	15.79	73.24	0.46	0.99	0.87
	38-19.1-3	907.57	15.88	73.12	0.46	1.04	0.92
	38-25.4-1	1045.39	16.59	89.02	0.44	1.00	0.97
	38-25.4-2	1067.62	16.48	88.54	0.44	0.92	0.90
	38-25.4-3	1051.15	16.43	88.53	0.43	0.87	0.85
	51-6.4-1	1007.50	15.27	34.06	0.40	0.88	0.88
	51-6.4-2	997.61	15.47	33.67	0.40	0.89	0.89
	51-6.4-3	992.44	15.40	34.24	0.40	0.83	0.83
	51-12.7-1	1154.07	16.32	54.42	0.45	0.84	0.80
	51-12.7-2	1157.65	16.22	54.66	0.45	0.72	0.68
	51-12.7-3	1132.12	16.36	54.00	0.44	0.96	0.91
	51-19.1-1	1337.84	16.82	77.29	0.50	0.73	0.65
	51-19.1-2	1349.38	16.86	77.64	0.50	0.92	0.81
	51-19.1-3	1343.62	16.82	76.85	0.50	0.86	0.75
	51-25.4-1	1500.16	17.39	99.32	0.49	0.80	0.75
	51-25.4-2	1415.45	14.35	86.92	0.44	0.86	0.80
	51-25.4-3	1536.49	17.65	99.82	0.49	0.85	0.80
	63-6.4-1	1400.44	16.53	36.43	0.41	0.73	0.78
	63-6.4-2	1402.80	16.39	36.92	0.41	0.81	0.86
	63-6.4-3	1379.47	16.17	30.02	0.41	0.92	0.99
	63-12.7-1	1471.01	14.10	52.83	0.42	0.81	0.79
	63-12.7-2	1584.71	17.39	62.05	0.47	0.84	0.83
	63-12.7-3	1572.63	17.34	61.59	0.46	0.82	0.81
	63-19.1-1	1775.51	18.16	91.18	0.53	0.79	0.71
	63-19.1-2	1779.03	17.91	90.74	0.53	0.85	0.76
	63-19.1-3	1785.47	17.91	90.46	0.53	0.81	0.73
	63-25.4-1	1864.55	15.30	106.06	0.46	0.87	0.83
	63-25.4-2	2000.96	18.66	122.42	0.52	0.77	0.73

Author	Specimen Name	P_{cre}	P_{crl}	P_{crd}	A_e	P_{test}/P_n	P_{test}/P_n
						DSM	Main Spec
Polyzois, D. et al. 1993	63-25.4-3	1905.34	15.27	106.47	0.47	0.82	0.78
	68-12.7-1	1206.54	7.10	21.46	0.42	0.99	0.92
	68-12.7-2	1220.41	7.18	21.84	0.42	0.95	0.89
	68-19.1-1	1441.73	7.39	39.56	0.50	1.03	0.84
	68-19.1-2	1455.74	7.41	39.89	0.50	1.02	0.83
	68-25.4-1	1590.12	7.56	53.68	0.50	1.01	0.83
	68-25.4-2	1590.98	7.55	53.62	0.50	1.02	0.84
	68-31.8-1	1730.90	7.74	79.46	0.49	1.10	0.96
	68-31.8-2	1724.82	7.93	80.99	0.49	1.01	0.88
	68-38.1-1	1886.51	8.14	85.20	0.48	1.08	0.99
	68-38.1-2	1894.31	8.15	85.43	0.48	1.01	0.93
	68-50.8-1	2291.99	8.74	114.78	0.44	1.00	1.07
	68-50.8-2	2251.14	8.61	112.59	0.44	0.91	0.97
	68-12.7-1	286.76	7.18	15.74	0.42	1.06	0.98
	68-12.7-2	294.82	7.12	15.02	0.42	0.92	0.86
	68-19.1-1	335.05	7.35	21.48	0.49	1.10	0.91
	68-19.1-2	335.47	7.38	21.94	0.49	1.09	0.89
	68-25.4-1	379.89	7.61	29.92	0.51	1.08	0.89
	68-25.4-2	376.60	7.59	29.69	0.51	0.99	0.81
	68-31.8-1	414.32	7.85	38.62	0.50	1.00	0.87
	68-31.8-2	415.00	7.85	38.65	0.50	1.09	0.94
	68-38.1-1	466.33	8.10	40.88	0.49	0.98	0.89
	68-38.1-2	462.57	8.15	41.13	0.49	1.01	0.92
	68-50.8-1	556.20	8.61	48.47	0.45	0.96	1.01
	68-50.8-2	555.61	8.59	48.20	0.45	1.00	1.05
Young 2004	P1.2L250	0.74	0.88	NaN	0.21	9.01	10.11
	P1.2L250R	0.74	0.88	NaN	0.21	8.93	10.01
	P1.2L1000	0.75	0.75	NaN	0.21	7.42	7.87
	P1.2L1500	0.76	0.76	NaN	0.21	5.92	6.26
	P1.2L2000	0.73	0.72	NaN	0.21	5.13	5.41
	P1.2L2500	0.80	0.79	NaN	0.22	4.32	4.53
	P1.2L2500R	0.79	0.77	NaN	0.21	4.50	4.72
	P1.2L3000	0.79	0.76	NaN	0.22	3.04	3.17
	P1.2L3500	0.77	0.73	NaN	0.21	2.28	2.37
	P1.5L250	1.60	1.89	NaN	0.27	6.96	7.82
	P1.5L1000	1.63	1.64	NaN	0.27	5.64	5.99
	P1.5L1500	1.63	1.61	NaN	0.27	4.62	4.88
	P1.5L2000	1.56	1.52	NaN	0.27	3.37	3.54
	P1.5L2500	1.58	1.52	NaN	0.27	2.99	3.13
	P1.5L3000	1.52	1.44	NaN	0.27	2.61	2.71
	P1.5L3500	1.60	1.48	NaN	0.28	2.19	2.25
	P1.9L250	3.16	3.72	NaN	0.34	5.05	5.69
	P1.9L250R	3.19	3.76	NaN	0.34	5.11	5.75
	P1.9L1000	3.18	3.19	NaN	0.34	4.48	4.76
	P1.9L1500	3.14	3.09	NaN	0.34	3.40	3.59
	P1.9L2000	3.15	3.04	NaN	0.34	2.60	2.72
	P1.9L2500	3.15	2.96	NaN	0.34	2.16	2.24
	P1.9L3000	3.07	2.67	NaN	0.34	1.49	1.51
	P1.9L3500	3.07	1.98	NaN	0.34	1.56	1.47

Author	Specimen Name	P_{cre}	P_{crl}	P_{crd}	A_e	P_{test}/P_n	P_{test}/P_n
						DSM	Main Spec
Young and Chen 2008	U1.0L250	108.52	4.88	NaN	0.14	0.97	0.95
	U1.0L250R	113.86	5.03	NaN	0.14	0.99	0.97
	U1.0L625	18.73	5.06	NaN	0.16	1.01	0.97
	U1.0L1000	7.45	4.88	NaN	0.20	1.19	1.11
	U1.0L1500	3.52	4.93	NaN	0.24	1.91	1.98
	U1.0L2000	2.21	5.07	NaN	0.25	2.71	2.69
	U1.0L2500	1.48	4.91	NaN	0.25	3.72	3.69
	U1.0L3000	1.13	4.91	NaN	0.25	3.73	3.70
	U1.5L250	177.35	16.90	NaN	0.25	1.15	1.31
	U1.5L250R	182.80	17.13	NaN	0.25	1.16	1.32
	U1.5L625	29.46	17.09	NaN	0.28	1.08	1.20
	U1.5L1000	12.16	16.95	NaN	0.33	1.11	1.24
	U1.5L1500	6.02	16.59	NaN	0.37	2.13	2.11
	U1.5L2000	3.83	16.12	NaN	0.37	2.87	2.83
	U1.5L2500	2.88	16.78	NaN	0.38	3.21	3.17
	U1.5L3000	2.28	16.18	NaN	0.37	3.27	3.23
	U1.9L250	213.43	33.20	NaN	0.34	1.06	1.31
	U1.9L250R	214.80	33.53	NaN	0.34	1.11	1.37
	U1.9L625	37.41	33.25	NaN	0.39	0.92	1.08
	U1.9L1000	15.87	33.83	NaN	0.43	1.13	1.24
	U1.9L1500	7.91	32.59	NaN	0.47	2.08	2.05
	U1.9L2000	5.53	33.09	NaN	0.48	2.59	2.55
	U1.9L2500	4.52	33.69	NaN	0.48	2.86	2.82
	U1.9L3000	3.62	32.30	NaN	0.47	2.57	2.53
	U1.9L3000R	3.64	32.86	NaN	0.47	2.71	2.66
Moldovan 1994	PI-I	545.64	15.31	16.62	0.35	1.00	1.01
	PI-2	516.22	15.31	16.55	0.35	0.89	0.91
	PI-3	559.63	15.33	16.65	0.35	0.87	0.88
	P4-1	805.94	11.30	12.34	0.39	1.10	1.10
	P4-2	846.26	11.80	12.92	0.39	1.09	1.09
	P4-3	814.13	12.04	13.15	0.39	1.11	1.11
	P6-1	1219.28	47.56	51.91	0.73	1.14	1.18
	P6-2	1261.20	46.60	50.91	0.74	1.21	1.26
	P9-1	1884.62	44.21	50.03	0.94	1.07	1.11
	P9-2	1757.25	39.79	45.03	0.89	1.02	1.05
	P9-3	1700.81	44.64	50.51	0.92	1.07	1.12
	PII-I	1928.87	92.86	105.07	1.20	1.08	1.17
	PII-2	1939.22	95.92	108.54	1.20	1.15	1.24
	P14-1	3069.43	67.88	79.54	1.32	1.08	1.14
	P14-2	2929.79	74.08	86.66	1.36	1.12	1.20
	P14-3	2929.79	74.08	86.66	1.36	1.09	1.16
	P17-1	1328.95	41.07	103.35	0.59	0.96	0.97
	P17-2	1359.00	41.80	105.98	0.59	0.95	0.96
	P20-1	1706.89	38.38	122.20	0.70	0.88	0.91
	P20-2	1704.34	42.96	128.84	0.73	0.94	0.97
	P23-1	2917.37	168.41	269.36	1.20	1.23	1.23
	P23-2	2917.37	168.41	269.36	1.20	1.18	1.18
	P26-1	3889.90	159.12	309.27	1.49	1.07	1.07
	P26-2	3918.93	157.67	290.62	1.52	1.04	1.04
	P26-3	4263.86	146.80	287.82	1.55	1.00	1.00
	P29-1	2703.29	34.17	160.26	0.87	1.02	1.01
	P29-2	2726.54	32.70	156.68	0.85	1.02	1.01

Author	Specimen Name	P_{cre}	P_{crl}	P_{crd}	A_e	P_{test}/P_n	P_{test}/P_n
						DSM	Main Spec
Moldovan 1994	P2-1	20.03	19.26	19.32	0.41	0.85	0.95
	P2-2	19.63	19.37	19.43	0.41	0.92	1.03
	P3-1	13.05	13.93	13.97	0.36	0.87	0.99
	P3-2	12.10	11.91	11.94	0.34	0.86	0.98
	P5-1	11.76	10.49	10.51	0.42	0.61	0.65
	P7-1	47.44	59.45	59.78	0.82	0.98	0.98
	P7-2	54.36	55.48	55.78	0.81	1.16	1.19
	P8-1	18.07	59.45	59.57	0.89	1.11	1.05
	P8-2	17.73	59.53	59.66	0.88	1.31	1.23
	P10-1	49.71	40.82	40.99	0.97	0.74	0.83
	P10-2	45.93	42.35	42.52	0.97	0.97	1.10
	P12-1	97.43	106.43	106.99	1.32	1.06	1.09
	P12-2	101.59	104.30	104.85	1.32	1.05	1.10
	P13-1	57.46	95.55	95.83	1.31	0.94	0.97
	P13-2	55.79	96.72	97.00	1.31	0.96	0.97
	P15-1	111.95	76.51	76.91	1.46	0.92	1.06
	P15-2	104.53	75.96	76.36	1.44	0.92	1.06
	P16-1	190.08	75.49	76.20	1.43	0.95	1.06
	P16-2	196.34	78.86	79.60	1.45	0.88	0.98
	P18-1	62.61	43.77	38.05	0.59	0.91	0.92
	P18-2	73.69	46.21	51.85	0.64	0.87	0.86
	P19-1	20.23	45.55	50.04	0.63	0.90	0.90
	P19-2	19.02	35.11	41.21	0.59	0.91	0.91
	P21-1	56.79	32.63	43.34	0.66	0.87	0.90
	P21-2	56.96	33.66	43.41	0.66	0.90	0.92
	P22-1	31.81	36.29	46.95	0.71	0.88	0.89
	P22-2	35.37	40.35	49.71	0.74	0.89	0.90
	P24-1	200.66	169.47	133.62	1.20	1.04	1.04
	P25-1	60.77	165.83	129.76	1.20	0.98	0.97
	P25-2	59.55	165.45	128.54	1.19	1.04	1.04
	P27-1	56.52	95.77	125.61	1.26	1.44	1.44
	P27-2	143.68	130.49	126.67	1.45	0.97	0.97
	P27-3	142.40	129.19	127.65	1.45	0.87	0.87
	P28-1	110.42	134.19	122.87	1.46	0.85	0.85
	P28-2	109.15	131.07	125.11	1.47	0.92	0.91
	P30-1	76.22	33.59	49.80	0.90	0.90	0.90
	P30-2	76.22	33.59	49.80	0.90	0.92	0.92
Dat 1980	PBC 14 (I) A3	89.97	49.21	63.08	0.53	0.95	0.96
	PBC 14 (I) A5	43.12	49.21	58.69	0.53	1.02	1.02
	PBC 14 (I) A9	20.19	49.21	56.54	0.53	0.96	0.96
	PBC 14 (I) A11	13.78	49.21	55.93	0.53	0.97	0.97
	PBC 14 (I) A13	10.78	49.21	55.65	0.53	1.11	1.11
	PBC 14 (I) A14	8.28	49.21	55.42	0.53	1.13	1.13
	PBC 14 (II) A1	148.73	49.21	68.58	0.53	0.85	0.86
	PBC 14 (II) A2	89.97	49.21	63.08	0.53	0.79	0.80
	PBC 14 (II) A4	60.23	49.21	60.29	0.53	0.81	0.81

Author	Specimen Name	P_{cre}	P_{crl}	P_{crd}	A_e	P_{test}/P_n	P_{test}/P_n
						DSM	Main Spec
Dat 1980	PBC 14 (II) A6	43.12	49.21	58.69	0.53	0.76	0.76
	PBC 14 (II) A7	32.39	49.21	57.68	0.53	0.77	0.77
	PBC 14 (II) A8	25.22	49.21	57.01	0.53	0.85	0.85
	PBC 14 (II) A10	16.53	49.21	56.19	0.53	0.80	0.80
	PBC 14 (II) A12	11.66	49.21	55.74	0.53	0.94	0.94
	RFC 14 (I) B2	89.97	49.21	63.08	0.52	0.86	0.87
	RFC 14 (I) B4	43.12	49.21	58.69	0.53	0.91	0.91
	RFC 14 (I) B5	25.22	49.21	57.01	0.53	0.96	0.96
	RFC 14 (I) B6	25.22	49.21	57.01	0.53	0.93	0.93
	RFC 14 (I) B9	10.12	49.21	55.59	0.53	0.99	0.99
	RFC 14 (I) B10	10.12	49.21	55.59	0.53	0.90	0.90
	RFC 14 (I) B11	9.10	49.21	55.50	0.53	1.13	1.13
	RFC 14 (II) B1	89.97	49.21	63.08	0.52	0.82	0.83
	RFC 14 (II) B3	43.12	49.21	58.69	0.53	0.82	0.82
	RFC 14 (II) B7	25.22	49.21	57.01	0.53	0.84	0.84
	RFC 14 (II) B8	16.53	49.21	56.19	0.53	0.86	0.86
	PBC 13 (I) C3	53.54	91.60	91.49	0.66	1.14	1.14
	PBC 13 (I) C4	31.31	91.60	88.87	0.66	1.10	1.09
	PBC 13 (I) C5	20.52	91.60	87.60	0.66	0.99	0.99
	PBC 13 (I) C6	12.11	91.60	86.62	0.66	0.94	0.94
	PBC 13 (I) C7	8.14	91.60	86.15	0.66	1.08	1.08
	PBC 13 (II) C1	111.71	91.60	98.34	0.66	1.34	1.34
	PBC 13 (II) C2	111.71	91.60	98.34	0.66	0.90	0.90
	RFC 13 (I) D6	53.54	91.60	91.49	0.66	1.27	1.27
	RFC 13 (I) D7	40.22	91.60	89.92	0.66	1.14	1.14
	RFC 13 (I) D8	31.31	91.60	88.87	0.66	1.17	1.17
	RFC 13 (I) D9	25.07	91.60	88.14	0.66	1.12	1.12
	RFC 13 (I) D10	20.52	91.60	87.60	0.66	1.00	0.99
	RFC 13 (I) D11	17.11	91.60	87.20	0.66	0.93	0.93
	RFC 13 (I) D12	14.48	91.60	86.89	0.66	0.97	0.97
	RFC 13 (I) D13	10.76	91.60	86.46	0.66	0.96	0.96
	RFC 13 (II) D3	111.71	91.60	98.34	0.66	1.34	1.34
	RFC 13 (II) D4	111.71	91.60	98.34	0.66	0.85	0.85
	RFC 13 (II) D5	74.78	91.60	93.99	0.66	1.39	1.39
Desmond et al. 1981	E-21.4-0	779.94	19.65	22.39	0.42	1.25	1.25
	E-21.4-1.33	856.54	26.61	33.66	0.47	1.10	1.10
	E-21.4-6.69	1350.04	61.69	114.45	0.56	1.09	1.09
	E-23.9-0.0	1239.31	38.86	44.85	0.84	1.21	1.21
	E-23.9-0.48	1277.91	43.31	51.58	0.87	1.16	1.16
	E-23.9-2.87	1518.50	103.92	111.97	1.00	1.13	1.24
	E-23.9-5.26	1838.19	109.58	177.97	1.09	1.08	1.17
	E-45.6A-8.87	472.77	43.65	45.48	0.64	1.31	1.40
	E-45.6A-11.1	455.12	44.81	52.97	0.68	1.30	1.40
	E-45.6A-16.5	429.90	44.61	62.00	0.77	1.20	1.24
	E-45.6A-22.1	436.74	36.83	70.66	0.75	1.26	1.30
	E-45.6A-27.4	475.73	28.62	77.32	0.73	1.28	1.31

Author	Specimen Name	P_{cre}	P_{crl}	P_{crd}	A_e	P_{test}/P_n	P_{test}/P_n
						DSM	Main Spec
Desmond et al. 1981	E-45.6-5.00	484.86	40.61	49.52	0.55	1.17	1.45
	E-45.6-8.05	470.73	42.93	64.61	0.62	1.26	1.49
	E-45.6-10.1	476.05	43.95	73.55	0.67	1.22	1.37
	E-45.6-15	561.15	44.83	97.25	0.75	1.26	1.31
	E-45.6-20.1	779.21	40.59	128.15	0.73	1.19	1.28
	E-45.6-24.8	1107.43	33.17	170.46	0.70	1.16	1.23
Popovic et al. 1999	LO24041	8.35	8.32	NaN	0.30	2.03	2.09
	LO24071	8.23	7.76	NaN	0.30	1.62	1.62
	LO24101	8.06	4.73	NaN	0.30	1.60	1.47
	LO24131	7.86	2.96	NaN	0.30	1.60	1.27
	LO24161	7.45	1.87	NaN	0.31	1.65	1.12
	LO24191	5.34	1.34	NaN	0.34	1.72	1.05
	LO38071	35.25	13.88	NaN	0.54	1.66	1.49
	LO38101	27.35	6.87	NaN	0.54	1.71	1.25
	LO38131	17.17	4.32	NaN	0.54	1.56	1.02
	LO47071	62.97	15.86	NaN	0.66	1.49	1.31
	LO47101	31.20	7.88	NaN	0.66	1.42	1.03
	LO47131	19.37	4.90	NaN	0.66	1.58	1.04
Wilhoite et al. 1984	1	13.20	13.11	NaN	0.53	1.72	1.77
	2	13.09	12.58	NaN	0.53	1.42	1.45
	3	13.09	12.58	NaN	0.53	1.46	1.49
	4	13.09	12.58	NaN	0.53	1.58	1.61
	5	11.82	11.78	NaN	0.55	1.27	1.26
	6	11.82	11.78	NaN	0.55	1.36	1.35
	7	11.82	11.78	NaN	0.55	1.55	1.54
Shanmugam and Dhanalakshmi 2001	EA20-0-0	11.91	14.56	NaN	0.34	2.21	2.48
Chodraui et al. 2006	EA40-0-0	3.65	4.53	NaN	0.38	3.80	4.32
	EA60-0-0	1.39	1.74	NaN	0.41	5.88	6.75
	L 60 x 2.38	7.63	7.68	NaN	0.36	1.21	1.23
	L 60 x 2.39	7.58	7.40	NaN	0.36	1.08	1.08
	L 60 x 2.40	7.51	7.10	NaN	0.37	0.94	0.93
	L 60 x 2.41	5.82	5.81	NaN	0.39	1.19	1.12

Appendix 2

The following are the primary MATLAB functions used in the calculation of nominal capacity of lipped C-section and lipped Z-section columns.

- 1) Start file: To input data and to call other functions to evaluate the member capacity.
- 2) cztemplate (): Create the actual test specimen using the provided out-to-out dimensions.
- 3) specgeom (): Converts the out-to-out dimensions into xy coordinates for use in CUFSM.
- 4) cutwp_prop2 (): Calculates the sections properties.
- 5) strip (): Uses the finite strip method to produce the elastic buckling curve.
- 6) mainspec_compression (): Calculates compressive strength of CFS members using the AISI Main Specification.
- 7) ftb (): Calculates the three roots of the classical cubic buckling equation.
- 8) Stiffel_simplelip (): Calculates the effective width of the “elements”.
- 9) LocDisBuckling (): Picks out points on the elastic buckling curve corresponding to local and distortional buckling.
- 10) Buckling (): Using DSM equations, this function evaluates the nominal axial strengths for local, distortional and flexural, torsional or flexural-torsional buckling, $P_{n\ell}$, P_{nd} , P_{ne} respectively.

The code for each of the above functions is provided below.

Start File:

```
%load input data
in_data = load('-mat', 'lough_3');
data = in_data.lough_3;

% prop: [matnum Ex Ey vx vy G] 6 x nmats
prop=[100 29500.00 29500.00 0.30 0.30 11346.15];
%CROSS-SECTION DIMENSIONS
%          Z
%
%          A
%
%          X
%
%          D2 /           I           \ D1
%          RT2 / S2 ____ S |   ____ S1 _\ RT1
%          \   |           /           /
%          B2 \           |           / B1
%          \   |           /           /
%          F2 \ _____ / F1 ____ ABAQUS Y AXIS
%          RB2     H     RB1

for index = 1:size(data,1)

    member = index %to display current member

    %column length
    L=data(index,1); %inches;

    %base thickness
    tbase = data(index,9); %inches;

    %[H      B1      B2      D1      D2      F1      F2      S1      S2      RB1
    %RB2      RT1      RT2      t      tbare]
    dimensions = data(index,10:22);
    dims = [dimensions tbase tbase];

    %column effective width factors
    if data(index,2) == 0
        kx = 0.5; ky = 1; kphi = 0.5; %(Weak Axis Pinned)
    elseif data(index,2) == 1
        kx = 1; ky = 0.5; kphi = 0.5; %(Strong Axis Pinned)
    elseif data(index,2) == 2
        kx = 0.5; ky = 0.5; kphi = 0.5; %(Fixed, Fixed)
    end;

    %hole dimensions
    Lhole = data(index,4); %2.24;

    dh = data(index,5); %1.49; %hole depth (or diameter)
    S = data(index,6); %47.76; %hole spacing
    Send= 0; %20.87; %clear spacing from end of hole
    delta=data(index,7); %transverse hole offset
```

```

if data(index,3) == 0
    holetype = 0; % no hole
elseif data(index,3) == 1
    holetype = 1; % circular
else
    holetype = 2; % noncircular
end;

Fy = data(index,8); %steel yield stress

E=29500; %elastic modulus

nu=0.3; %Poisson's ratio

%number of elements around the cross section
%[D1 RT1 B1 RB1 H RB2 B2 RT2 D2]
n=[2 2 4 2 16 2 4 2 2];

%convert out-to-out dimensions to centerline dimensions
CorZ=2 % 1 - channel, 2 - Zee

%constraints: [node#e dofe coeff node#k dofk]
% e=dof to be eliminated k=kept dof dofe_node = coeff*dofk_nodek
springs=0; constraints= 0;
GBTcon.glob=0; GBTcon.dist=0; GBTcon.local=0; GBTcon.other=0;

% lengths to be analyzed
lengths=[1.00 2.00 2.5 3.00 3.5 4.00 4.5 5.00 6.00 7.00 8.00 9.00...
          10.00 11.00 12.00 13.00 14.00 15.00 20.00 25.0 30.00 35.0 40.00...
          50.00 60.00 70.00 80.00 90.00 100.00 200.00];

%calculate node and element matrices
[node,elem]=cztemplate(CorZ,dims,n);

[A] = GlobalBuckling(elem,node,L,E,nu,kx,ky,kphi);
node(:,8) = 1/A;

[curve,shapes,clas]=strip(prop,node,elem,lengths,1,springs, ...
                           constraints,GBTcon);

%critical elastic buckling load (distortional buckling)
% Pcrd = data(index,23);
% calculate column strength
[A,Pcre,Ae,Fn,Pn,Pnd,Pcrl,Pcrd,Pcrd_dboost,loc_halfwave, ...
  dist_halfwave,answ]=mainspec_compression(node,elem,kx,ky,kphi,E, ...
  nu,Fy,holetype,L,dims,CorZ,n,dh,Lhole,S,Send,curve,lengths);

Pnfinal=min([Pn Pnd]); %min of local-global interaction and dist

PnDSM = min(answ); % [answ] = [Pne Pnl Pnd];
outDSM(index,:)= [A Pcre Pcrl loc_halfwave Pcrd dist_halfwave...
  Pcrd_dboost answ PnDSM];
outMainSpec(index,:)= [Py Ae Fn Pnfinal];
end;

```

cztemplate():

```
function [node,elem]=cztemplate(CorZ,dims,n)

%Ben Schafer
%August 23, 2000
%CorZ=determines sign conventions for flange 1=C 2=Z
%modified by Cris Moen October 18, 2006
%CorZ=determines sign conventions for flange 1=C 2=Z
%convert out to out dimensions to centerline xy coordinates around the
%section
%modified by Karthik Ganesan, December, 2008.

[geom]=specgeom(dims);

%for S9R5 element, one element is made up of two subelements
n=n*2;

if CorZ==2
    cz=-1;
else
    cz=1;
end
%channel template

H=dims(1);
B1=dims(2);
B2=dims(3);
D1=dims(4);
D2=dims(5);
F1=dims(6)*pi/180;
F2=dims(7)*pi/180;
S1=dims(8)*pi/180;
S2=dims(9)*pi/180;
RB1=dims(10);
RB2=dims(11);
RT1=dims(12);
RT2=dims(13);
t=dims(14);
tbare=dims(15);

r1=RB2-t/2;
r2=RT2-t/2;
r3=RB1-t/2;
r4=RT2-t/2;

geom([7 8 9 10],2)=cz*geom([7 8 9 10],2);

%stop

% figure(1)
% plot(geom(:,2),geom(:,3),'.')
% stop

%number of elements between the geom coordinates
```

```

%n=4;
%for i=1:size(geom,1)-1
count=1;
for i=1:size(geom,1)-1

if (RB1==0 | RB2==0 | RT1==0 | RT2==0)

%node(count,:)=[count geom(i,2:3) 1 1 1 1 1.0];
%count=count+1;
    start=geom(i,2:3);
    stop=geom(i+1,2:3);

if max(i==[1 3 5 7 9]) %use linear interpolation

if i==1
    node(count,:)=[count start 1 1 1 1 1.0];
    count=count+1
end

for j=1:n(i)
    node(count,:)=[count start+(stop-start)*j/n(i) 1 1 1 1 1.0];
    count=count+1;
end
end

else

node(count,:)=[count geom(i,2:3) 1 1 1 1 1.0];
count=count+1;
start=geom(i,2:3);
stop=geom(i+1,2:3);

if max(i==[1 3 5 7 9]) %use linear interpolation
for j=1:n(i)-1
    node(count,:)=[count start+(stop-start)*j/n(i) 1 1 1 1 1.0];
    count=count+1;
end
else%we are in a corner and must be fancier

for j=1:n(i)-1
if i==2
    r=r2;, xc=geom(i+1,2)+r2*sin(pi/2-F2);,
    zc=geom(i+1,3)+r2*cos(pi/2-F2);, qstart=S2;, dq=(pi-F2-S2)*j/n(i);
end
if i==4
    r=r1;, xc=geom(i+1,2)+r1;, zc=geom(i+1,3);, qstart=pi-
F2;, dq=F2*j/n(i);
end
if i==6
    r=r3;, xc=(geom(i,2)+r3)*cz;, zc=geom(i,3);,
    qstart=(1==cz)*pi;, dq=cz*F1*j/n(i);
end
if i==8
if cz==-1

```

```

r=r4;, xc=(geom(i,2)-r4*sin(pi/2-F1));, zc=geom(i,3)-
r4*cos(pi/2-F1);, qstart=pi+S1;, dq=(pi-F1-S1)*(n(i)-j)/n(i);
else
    r=r4;, xc=(geom(i,2)+r4*sin(pi/2-F1));, zc=geom(i,3)-
r4*cos(pi/2-F1);, qstart=3/2*pi-(pi/2-F1);, dq=cz*(pi-F1-S1)*j/n(i);
end

end

x2=xc+r*cos(qstart+dq);
z2=zc-r*sin(qstart+dq); %note sign on 2nd term is negative
due to z sign convention (down positive)
node(count,:)=[count x2 z2 1 1 1 1 1.0];
count=count+1;
end

end
end
end

i=10;
node(count,:)=[count geom(i,2:3) 1 1 1 1 1.0];

if (RB1==0 | RB2==0 | RT1==0 | RT2==0)

    node(length(node),:)=[];
end

% figure(1)
% plot(node(:,2), node(:,3), '-.-')

for i=1:size(node,1)-1
    elem(i,:)=[i i i+1 tbare 100];
end

```

specgeom ():

```
function [geomfinal]=specgeom(dims)

%CDM
%October 25, 2006
%Takes out to out dimensions and corner angles of a channel and converts
%them to xy coordinates for use in CUFSM

%dims=[H      B1      B2      D1      D2      F1      F2      S1      S2      RB1      RB2      RT1      RT2      t]

H=dims(1);
B1=dims(2);
B2=dims(3);
D1=dims(4);
D2=dims(5);
F1=dims(6)*pi/180;
F2=dims(7)*pi/180;
S1=dims(8)*pi/180;
S2=dims(9)*pi/180;
RB1=dims(10);
RB2=dims(11);
RT1=dims(12);
RT2=dims(13);
t=dims(14);

%channel orientation - web is horizontal
%left half of xy coordinates defined
xoW=-H/2;
yoW=0;

x1W=xoW+RB1*tan(F1/2);
y1W=yoW+t/2;

x2W=x1W-(RB1-t/2)*tan(F1/2)-(RB1-t/2)*tan(F1/2)*cos(F1);
y2W=y1W+(RB1-t/2)*(1-cos(F1));

x3W=xoW-B1*cos(F1);
y3W=yoW+B1*sin(F1);

IW=pi-F1-S1;
x4W=x3W+RT1*tan(IW/2)*cos(F1)+t/2*cos(pi/2-F1); %correct
y4W=y3W-RT1*tan(IW/2)*sin(F1)+t/2*sin(pi/2-F1); %correct

x5W=x3W+RT1*tan(IW/2)*cos(S1)+t/2*cos(pi/2-S1); %correct
y5W=y3W+RT1*tan(IW/2)*sin(S1)-t/2*sin(pi/2-S1); %correct

x6W=x3W+D1*cos(S1)+t/2*sin(S1);
y6W=y3W+D1*sin(S1)-t/2*cos(S1);

%right half of coordinates defined
xoE=H/2;
```

```

y0E=0;

x1E=x0E-RB2*tan(F2/2);
y1E=y0E+t/2;

x2E=x1E+2*(RB2-t/2)*sin(F2/2)*cos(F2/2);
y2E=y1E+2*(RB2-t/2)*sin(F2/2)*sin(F2/2);

x3E=x0E+B2*cos(F2);
y3E=y0E+B2*sin(F2);

IE=pi-F2-S2;

x4E=x3E-RT2*tan(IE/2)*cos(F2)-t/2*cos(pi/2-F2); %correct
y4E=y3E-RT2*tan(IE/2)*sin(F2)+t/2*sin(pi/2-F2); %correct

x5E=x3E-RT2*tan(IE/2)*cos(S2)-t/2*cos(pi/2-S2); %correct
y5E=y3E+RT2*tan(IE/2)*sin(S2)-t/2*sin(pi/2-S2); %correct

x6E=x3E-D2*cos(S2)-t/2*sin(S2);
y6E=y3E+D2*sin(S2)-t/2*cos(S2);

%transform into CUFSM format
geom=[ x1W y1W
       x2W y2W
       x4W y4W
       x5W y5W
       x6W y6W
       x1E y1E
       x2E y2E
       x4E y4E
       x5E y5E
       x6E y6E];

%rotate coordinates so that web is vertical
sigma=-3*pi/2;
transx=[cos(sigma) -sin(sigma)];
transy=[-sin(sigma) cos(sigma)];

geomxrot=geom*transx';
geomyrot=geom*transy';

geomfinal=[[6 7 8 9 10 5 4 3 2 1]' -geomxrot-t/2 geomyrot];
geomfinal=sortrows(geomfinal,1);

%save geomfinal
% figure(1)
% plot(geomfinal(:,2),geomfinal(:,3),'.')


```

cutwp_prop2

```
function [A,xc,yc,Ix,Iy,Ixy,theta,I1,I2,J,xs,ys,Cw,B1,B2,wn] =
cutwp_prop2(coord,ends)

%Function modified for use in CUFSM by Ben Schafer in 2004 with permission
%of Sarawit. removed elastic buckling calcs and kept only section
%properties
%
%August 2005: additional modifications, program only handles
%singly-branched open sections, or single cell closed sections, arbitrary
%section designation added for other types.
%
%December 2006 bug fixes to B1 B2
%
% Compute cross section properties
%-----
% Written by:
%     Andrew T. Sarawit
%     last revised:   Wed 10/25/01

% Function purpose:
%     This function computes the cross section properties: area, centroid,
%     moment of inertia, torsional constant, shear center, warping
%     constant,
%     B1, B2, elastic critical buckling load and the deformed buckling
%     shape
%
% Dictionary of Variables
%     KL1          == effective unbraced length for bending about the 1-
% axis
%     KL2          == effective unbraced length for bending about the 2-
% axis
%     KL3          == effective unbraced length for twisting about the
% 3-axis
%     force        == type of force applied
%     == 'Pe'      : elastic critical axial force
%     == 'Me1'    : elastic critical moment about the 1-axis
%     == 'Me2'    : elastic critical moment about the 2-axis
%     exy(1:2)    == Pe eccentricities coordinates
%                 exy(1) = ex
%                 exy(2) = ey
%
% Output Information:
%     A            == cross section area
%     xc           == X coordinate of the centroid from origin
%     yc           == Y coordinate of the centroid from origin
%     Ix           == moment of inertia about centroid X axes
%     Iy           == moment of inertia about centroid Y axes
%     Ixy          == product of inertia about centroid
%     Iz           == polar moment of inertia about centroid
%     theta        == rotation angle for the principal axes
%     I1           == principal moment of inertia about centroid 1 axes
%     I2           == principal moment of inertia about centroid 2 axes
%     J            == torsional constant
```

```

%
%           xs          == X coordinate of the shear center from origin
%           ys          == Y coordinate of the shear center from origin
%           Cw          == warping constant
%           B1          == int(y*(x^2+y^2),s,0,L)    *BWS, x,y=prin. crd.
%           B2          == int(x*(x^2+y^2),s,0,L)
%                           where: x = x1+s/L*(x2-x1)
%                               y = y1+s/L*(y2-y1)
%                               L = lenght of the element
%           Pe(i)       == buckling mode i's elastic critical buckling load
%           dcoord      == node i's coordinates of the deformed buckling
shape
%
%                           coord(i,1,mode) = X coordinate
%                           coord(i,2,mode) = Y coordinate
%                           where: mode = buckling mode number
%

nele = size(ends,1);
node = ends(:,1:2); node = node(:);
nnode = 0; j = 0;

while ~isempty(node)
    i = find(node==node(1));
    node(i) = [];
if size(i,1)==2
    j = j+1;
end
    nnod = nnod+1;
end

% classify the section type
if j == nele
    section = 'close'; %single cell
elseif j == nele-1
    section = 'open'; %singly-branched
else
%connected
    section = 'open'; %multi-branched
%disconnected
end

% if the section is close re-order the element
if strcmp(section,'close')
    xnele = (nele-1);
for i = 1:xnele
    en = ends; en(i,2) = 0;
    [m,n] = find(ends(i,2)==en(:,1:2));
if n==1
        ends(i+1,:) = en(m,:);
        ends(m,:) = en(i+1,:);
elseif n == 2
        ends(i+1,:) = en(m,[2 1 3]);
        ends(m,:) = en(i+1,[2 1 3]);
end
end
end

```

```

% find the element properties
for i = 1:nele
    sn = ends(i,1); fn = ends(i,2);
% thickness of the element
    t(i) = ends(i,3);
% compute the coordinate of the mid point of the element
    xm(i) = mean(coord([sn fn],1));
    ym(i) = mean(coord([sn fn],2));
% compute the dimension of the element
    xd(i) = diff(coord([sn fn],1));
    yd(i) = diff(coord([sn fn],2));
% compute the length of the element
    L(i) = norm([xd(i) yd(i)]);
end

% compute the cross section area
A = sum(L.*t);
% compute the centroid
xc = sum(L.*t.*xm)/A;
yc = sum(L.*t.*ym)/A;

if abs(xc/sqrt(A)) < 1e-12
    xc = 0;
end
if abs(yc/sqrt(A)) < 1e-12
    yc = 0;
end

% compute the moment of inertia
Ix = sum((yd.^2/12+(ym-yc).^2).*L.*t);
Iy = sum((xd.^2/12+(xm-xc).^2).*L.*t);
Ixy = sum((xd.*yd/12+(xm-xc).*(ym-yc)).*L.*t);

if abs(Ixy/A^2) < 1e-12
    Ixy = 0;
end

% compute the rotation angle for the principal axes
theta = angle(Ix-Iy-2*Ixy*li)/2;

% transfer the section coordinates to the centroid principal coordinates
coord12(:,1) = coord(:,1)-xc;
coord12(:,2) = coord(:,2)-yc;
coord12 = [cos(theta) sin(theta); -sin(theta) cos(theta)]*coord12';
coord12 = coord12';

% find the element properties
for i = 1:nele
    sn = ends(i,1); fn = ends(i,2);
% compute the coordinate of the mid point of the element
    xm(i) = mean(coord12([sn fn],1));
    ym(i) = mean(coord12([sn fn],2));
% compute the dimension of the element
    xd(i) = diff(coord12([sn fn],1));
    yd(i) = diff(coord12([sn fn],2));

```

```

end

% compute the principal moment of inertia
I1 = sum((yd.^2/12+ym.^2).*L.*t);
I2 = sum((xd.^2/12+xm.^2).*L.*t);

if strcmp(section,'close')
% compute the torsional constant for close-section
for i = 1:nele
    sn = ends(i,1); fn = ends(i,2);
    p(i) = ((coord(sn,1)-xc)*(coord(fn,2)-yc)-(coord(fn,1)-
    xc)*(coord(sn,2)-yc))/L(i);
end
J = 4*sum(p.*L/2)^2/sum(L./t);
xs = NaN; ys = NaN; Cw = NaN; B1 = NaN; B2 = NaN; Pe = NaN; dcoord = NaN;
wn=NaN;
elseif strcmp(section,'open')
% compute the torsional constant for open-section
J = sum(L.*t.^3)/3;

% compute the shear center and initialize variables
nnode = size(coord,1);
w = zeros(nnode,2); w(ends(1,1),1) = ends(1,1);
wo = zeros(nnode,2); wo(ends(1,1),1) = ends(1,1);
Iwx = 0; Iwy = 0; wno = 0; Cw = 0;

for j = 1:nele
    i = 1;
    while
        (any(w(:,1)==ends(i,1))&any(w(:,1)==ends(i,2))) | (~any(w(:,1)==ends(i,1))) & (~
        any(w(:,1)==ends(i,2)))
            i = i+1;
    end
    sn = ends(i,1); fn = ends(i,2);
    p = ((coord(sn,1)-xc)*(coord(fn,2)-yc)-(coord(fn,1)-xc)*(coord(sn,2)-
    yc))/L(i);
    if w(sn,1)==0
        w(sn,1) = sn;
        w(sn,2) = w(fn,2)-p*L(i);
    elseif w(fn,1)==0
        w(fn,1) = fn;
        w(fn,2) = w(sn,2)+p*L(i);
    end
    Iwx = Iwx+(1/3*(w(sn,2)*(coord(sn,1)-xc)+w(fn,2)*(coord(fn,1)-
    xc))+1/6*(w(sn,2)*(coord(fn,1)-xc)+w(fn,2)*(coord(sn,1)-xc)))*t(i)* L(i);
    Iwy = Iwy+(1/3*(w(sn,2)*(coord(sn,2)-yc)+w(fn,2)*(coord(fn,2)-
    yc))+1/6*(w(sn,2)*(coord(fn,2)-yc)+w(fn,2)*(coord(sn,2)-yc)))*t(i)* L(i);
end

if (Ix*Iy-Ixy^2)~=0
    xs = (Iy*Iwy-Ixy*Iwx)/(Ix*Iy-Ixy^2)+xc;
    ys = -(Ix*Iwx-Ixy*Iwy)/(Ix*Iy-Ixy^2)+yc;
else
    xs = xc; ys = yc;
end

```

```

if abs(xs/sqrt(A)) < 1e-12
    xs = 0;
end
if abs(ys/sqrt(A)) < 1e-12
    ys = 0;
end

% compute the unit warping
for j = 1:nele
    i = 1;
    while
        (any(wo(:,1)==ends(i,1))&any(wo(:,1)==ends(i,2))) | (~any(wo(:,1)==ends(i,1)))
        &(~any(wo(:,1)==ends(i,2))))
            i = i+1;
    end
    sn = ends(i,1); fn = ends(i,2);
    po = ((coord(sn,1)-xs)*(coord(fn,2)-ys)-(coord(fn,1)-
    xs)*(coord(sn,2)-ys))/L(i);
    if wo(sn,1)==0
        wo(sn,1) = sn;
        wo(sn,2) = wo(fn,2)-po*L(i);
    elseif wo(ends(i,2),1)==0
        wo(fn,1) = fn;
        wo(fn,2) = wo(sn,2)+po*L(i);
    end
    wno = wno+1/(2*A)*(wo(sn,2)+wo(fn,2))*t(i)* L(i);
end
wn = wno-wo(:,2);

% compute the warping constant
for i = 1:nele
    sn = ends(i,1); fn = ends(i,2);
    Cw = Cw+1/3*(wn(sn)^2+wn(sn)*wn(fn)+wn(fn)^2)*t(i)* L(i);
end

% transfer the shear center coordinates to the centroid principal coordinates
s12 = [cos(theta) sin(theta); -sin(theta) cos(theta)]*[xs-xc; ys-yc];
% compute the polar radius of gyration of cross section about shear center
ro = sqrt((I1+I2)/A+s12(1)^2+s12(2)^2);

% compute B1 and B2
B1 = 0; B2 = B1;
for i = 1:nele
    sn = ends(i,1); fn = ends(i,2);
    x1 = coord12(sn,1); y1 = coord12(sn,2);
    x2 = coord12(fn,1); y2 = coord12(fn,2);
    B1 =
    B1+((y1+y2)*(y1^2+y2^2)/4+(y1*(2*x1^2+(x1+x2)^2)+y2*(2*x2^2+(x1+x2)^2))/12)*L
    (i)*t(i);
    B2 =
    B2+((x1+x2)*(x1^2+x2^2)/4+(x1*(2*y1^2+(y1+y2)^2)+x2*(2*y2^2+(y1+y2)^2))/12)*L
    (i)*t(i);
end
B1 = B1/I1-2*s12(2);
B2 = B2/I2-2*s12(1);

```

```

if abs(B1/sqrt(A)) < 1e-12
    B1 = 0;
end
if abs(B2/sqrt(A)) < 1e-12
    B2 = 0;
end
elseif strcmp(section,'arbitrary')
% compute the torsional constant based on an open-section
    J = sum(L.*t.^3)/3;
    xs = NaN; ys = NaN; Cw = NaN; B1 = NaN; B2 = NaN; Pe = NaN; dcoord = NaN;
wn=NaN;
end

```

strip():

```

function
[curve,shapes,clas]=strip(prop,node,elem,lengths,eigflag,springs,constraints,
GBTcon);

%last updated October 2006 BWS
%INPUTS
%prop: [matnum Ex Ey vx vy G] 6 x nmats
%node: [node# x z dofx dofy dofrot stress] nnodes x 8;
%elem: [elem# nodei nodej t matnum] nelems x 5;
%lengths: lengths to be analyzed
%eigflag: eigensolver to be used, 1=use eig, 2=use eigs (1 is far more
robust)
%springs: [node# d.o.f. kspring kflag] where 1=x dir 2= z dir 3 = y dir 4 = q
dir (twist) flag says if k is a foundation stiffness or a total stiffness
%constraints: [node#e dofe coeff node#k dofk] e=dof to be eliminated k=kept
dof dofe_node = coeff*dofk_nodek
%GBTcon: GBTcon.glob,GBTcon.dist, GBTcon.local, GBTcon.other vectors of 1's
% and 0's referring to the inclusion (1) or exclusion of a given mode from
% the analysis, GBTcon.basis=1 for natural modal basis, 2 for axial modal
basis but 0 modes
% partially orthogonal, 3 for axial modal basis, but 0 modes fully
orthogonal, i.e, null of GDL
%
%FUNCTIONS CALLED IN THIS ROUTINE
% \analysis\addspring.m : add springs to K
% \analysis\assemble.m : assemble global K, Kg
% \analysis\elemprop.m : element properties
% \analysis\kglocal.m : element kg matrix
% \analysis\klocal.m : element k matrix
% \analysis\trans.m : transform k, kg matrix
% \analysis\cFSM\base_unit_length : cFSM base vectors
% \analysis\cFSM\base_update.m' : cFSM base vectors with selected basis,
%                               orthogonalization, and normalization
% \analysis\cFSM\constr_user : user defined constraints in cFSM style
% \analysis\cFSM\mode_select : selection of modes for constraint matrix R
%
```

```

%GUI WAIT BAR FOR FINITE STRIP ANALYSIS
wait_message=waitbar(0,'Performing Finite Strip Analysis');
%
%NUMBER OF HALF SINE WAVES ALONG THE LENGTH IS HARDCODED AS 1
m = 1;
%
%MATRIX SIZES
nnodes = length(node(:,1));
nelems = length(elem(:,1));
ndof= 4*nnodes;
nlenghts = length(lengths);
%
%GENERATE STRIP WIDTH AND DIRECTION ANGLE
[elprop]=elemprop(node,elem,nnodes,nelems);
%
%SET SWITCH FOR cFSM ANALYSIS AND CLASSIFICATION
if sum(GBTcon.glob)+sum(GBTcon.dist)+sum(GBTcon.local)+sum(GBTcon.other)>0
%turn on modal classification analysis
    cFSM_analysis=1;
    clas=[];
%generate unit length natural base vectors
    [b_v_ul,ngm,ndm,nlm]=base_unit_length(m,node,elem,prop);
else
%no modal classification constraints are engaged
    cFSM_analysis=0;
    clas=[];
end
%
%
%BOUNDARY CONDITIONS AND USER DEFINED CONSTRAINTS
%d_constrained=Ruser*d_unconstrained, d=nodal DOF vector (note by BWS June 5
2006)
Ruser=constr_user(node,constraints);
Ru0=null(Ruser)';
%Number of boundary conditions and user defined constraints = nu0
nu0=length(Ru0(1,:));
%
%
-----  

----  

%LOOP OVER ALL THE LENGTHS TO BE INVESTIGATED
l=0; %length_index = one
while l<nlenghts
    l=l+1; %length index = length index + one
%
%
%ZERO OUT THE GLOBAL MATRICES
    K=sparse(zeros(nnodes*4,nnodes*4));
    Kg=sparse(zeros(nnodes*4,nnodes*4));
%
%
%ASSEMBLE THE GLOBAL STIFFNESS MATRICES
for i=1:nelems
%Generate element stiffness matrix (k) in local coordinates
    t=elem(i,4);
    a=lengths(l);

```

```

b=elprop(i,2);
matnum=elem(i,5);
row=find(matnum==prop(:,1));
Ex=prop(row,2);
Ey=prop(row,3);
vx=prop(row,4);
vy=prop(row,5);
G=prop(row,6);
[k_1]=klocal(Ex,Ey,vx,vy,G,t,a,b,m);
%Generate geometric stiffness matrix (kg) in local coordinates
    Ty1=node(elem(i,2),8)*t;
    Ty2=node(elem(i,3),8)*t;
    [kg_1]=kglocal(a,b,m,Ty1,Ty2);
%Transform k and kg into global coordinates
    alpha=elprop(i,3);
    [k,kg]=trans(alpha,k_1,kg_1);
%Add element contribution of k to full matrix K and kg to Kg
    nodei=elem(i,2);
    nodej=elem(i,3);
    [K,Kg]=assemble(K,Kg,k,kg,nodei,nodej,nnodes);
end
%
%ADD SPRING CONTRIBUTIONS TO STIFFNESS
if ~isempty(springs) %springs variable exists
    [K]=addspring(K,springs,nnodes,a);
end
%
%GENERATION OF cFSM CONSTRAINT MATRIX
if cFSM_analysis==1
%SET UP THE VECTOR TO CONSIDER LENGTH-DEPENDENCY ON BASE VECTORS
%AND PERFORM ORTHOGONALIZATION IF GBT-LIKE MODES ARE ENFORCED

b_v=base_update(GBTcon.basis,0,b_v_ul,a,m,node,elem,prop,ngm,ndm,nlm); %no
normalization is enforced
%assign base vectors to constraints

b_v=mode_select(b_v,ngm,ndm,nlm,GBTcon.glob,GBTcon.dist,GBTcon.local,GBTcon.o
ther);
Rmode=b_v;
else
%no modal constraints are activated therefore
    Rmode=eye(4*nnodes);%activate modal constraints
end
%
%CREATE FINAL CONSTRAINT MATRIX
%Determine the number of modal constraints, nm0
nm0=0;
Rm0=null(Rmode');
nm0=length(Rm0(1,:));
R0=Rm0;
if nu0>0
    R0(:,(nm0+1):(nm0+nu0))=Ru0;
end
R=null(R0');
%
%INTRODUDCE CONSTRAINTS AND REDUCE K MATRICES TO FREE PARTS ONLY
Kff=R'*K*R;

```

```

Kgff=R'*Kg*R;
%
%SOLVE THE EIGENVALUE PROBLEM
%small problems usually use eig, and large problems use eigs.
%the eigs solver is not as stable as the full eig solver...
%old versions of strip did not have eigflag, if it is passed in without then
use "eig" solver
if ~exist('eigflag')
    eigflag=1;
end
if eigflag==1
    [modes,lf]=eig(Kff,Kgff);
else
    options.disp=0;
    options.issym=1;
    [modes,lf]=eigs(inv(Kgff)*Kff,6,'SM',options);
end
%CLEAN UP THE EIGEN SOLUTION
%eigenvalues are along the diagonal of matrix lf
    lf=diag(lf);
%find all the positive eigenvalues and corresponding vectors, squeeze out the
rest
    index=find(lf>0 & imag(abs(lf))<0.00001);
    lf=lf(index);
    modes=modes(:,index);
%sort from small to large
    [lf,index]=sort(lf);
    modes=modes(:,index);
%only the real part is of interest (eigensolver may give some small nonzero
imaginary parts)
    lf=real(lf);
    modes=real(modes);
%first time through, find the number of modes to be kept
if l==1
    num_pos_modes=length(lf);
if eigflag==1
%keep 10 modes or 1/2 of num_pos_modes whichever is less
if num_pos_modes<=4
    nummodes=round(min([10;num_pos_modes]));
else
    nummodes=round(min([10;1/2*num_pos_modes]));
end
elseif eigflag==2
    nummodes=3;
end
end
%
%truncate down to reasonable number of modes to be kept
%note when the GBT constraints are used the number of modes may fluctuate
with length
    num_pos_modes=length(lf);
    lf=lf(1:min([nummodes,num_pos_modes]));
    modes=modes(:,1:min([nummodes,num_pos_modes]));
%FORM THE FULL MODE SHAPE BY BRINGING BACK ELIMINATED DOF
    mode=R*modes;
%NORMALIZE MODE SHAPE (WE CHOOSE a strain energy normalization)
%Normalize the mode shape so that phi'*Kg*phi = 1/2

```

```

%this means SE=lambda=phi'*Ke*phi
alpha=diag(mode'*Kg*mode);
mode=mode*diag(sqrt(2./alpha));
%GENERATE OUTPUT VALUES
%curve = buckling curve with 3rd dimension = mode number
%shapes = mode shapes with 3rd dimension = mode shapes for higher modes
curve(1,1,1:min([nummodes,num_pos_modes]))=lengths(1);
curve(1,2,1:min([nummodes,num_pos_modes]))=lf;
shapes(:,1,1:min([nummodes,num_pos_modes]))=mode;
%WAITBAR MESSAGE
info=['Length ',num2str(lengths(1)), ' done.'];
waitbar(1/nlengths);
%
end
%close waitbar
if ishandle(wait_message)
    delete(wait_message);
end

```

mainspec_compression ():

```

function
[A,Pcre,Py,Ae,Fn,Pn,Pnd,Pcrl,Pcrd,Pcrd_dboost,loc_halfwave,dist_halfwave,answ]
]=
mainspec_compression(node,elem,kx,ky,kphi,E,nu,Fy,holetype,L,dims,CorZ,n,dh,L
hole,S,Send,curve,lengths)

%This function calculates the cold-formed steel column compressive strength
%using the AISI-S100-07 specification. Circular and noncircular web holes
%can be accounted for in the calculation.
%Fall 2008
%Cris Moen, Virginia Tech
%cmoen@vt.edu

%INPUTS

%kx          column effective length factor (strong axis)
%ky          column effective length factor (weak axis)
%kphi        column effective length factor (torsion)
%E           modulus of elasticity
%nu          Poisson's ratio
%Fy          steel yield stress
%holetype   1 for circular, 2 for noncircular
%L           column length
%dims        column cross section dimension (see below for nomenclature)
%dims=[H     B1      B2      D1      D2      F1      F2      S1      S2      RB1
       RB2     RT1      RT2      t      tbare]

%CorZ        switch for channel-zee template, 1 is channel, 2 is zee
%n           array of element spacing around the cross-section
%n=number of strips in each element [D1      RT1      B1      RB1      H      RB2      B2      RT2      D2]
%dh         web hole depth

```

```

%Lhole      web hole length
%S         web hole spacing
%Send      web hole clear spacing to end of column
%Pcrd      critical elastic distortional buckling load of column

%OUTPUTS

%Ae        effective area
%Pn        nominal column strength (local-global buckling interaction)
%Pnd       nominal column strength (distortional buckling limit state)

%define dimensions
t=dims(15)
H=dims(1)
B1=dims(2)
B2=dims(3)
D1=dims(4)
D2=dims(5)
F1=dims(6)*pi/180
F2=dims(7)*pi/180
S1=dims(8)*pi/180
S2=dims(9)*pi/180
RB1=dims(10)
RB2=dims(11)
RT1=dims(12)
RT2=dims(13)

%calculate node and element matrices
% [node,elem]=cztemplate(CorZ,dims,n)

%calculate Fe
%CALCULATE SECTION PROPERTIES
[A,xcg,ycg,Ix,Iy,Ixy,theta,I1,I2,J,xsc,ysc,Cw,B1p,B2p,wn] =
cutwp_prop2(node(:,2:3),elem(:,2:4))

%CALCULATE three roots of classical cubic buckling equation
[Pcre]= ftb(theta,I1,I2,L, A, Ix, Iy, kx, ky, kphi, J, Cw, xcg, xsc, ycg,
ysc, E, nu);
Pcre=min(Pcre);
Fe=Pcre/A;

rx=sqrt(Ix/A);
ry=sqrt(Iy/A);

%determine Fn
lambda_c=sqrt(Fy/Fe);

if lambda_c<=1.5
    Fn=0.658^((lambda_c)^2)*Fy;
else
    Fn=0.877/lambda_c^2*Fy;
end

%calculate effective width of web

```

```

if holetype==0
k=4
[bweb]=stiffel(RB1,RB2,pi-F1,pi-F2,H,t,Fn,E,nu, k);
elseif holetype==1
[bweb errortype(1:4)]=stiffel_circhole(RB1,RB2,pi-F1,pi-
F2,H,t,Fn,E,nu,dh,S);
else
[bweb errortype(5:9)]=stiffel_noncirchole(RB1,RB2,pi-F1,pi-
F2,H,t,Fn,E,nu,dh,S, Send, Lhole);
end

%calculate effective width of flange and lip (top)
[b1t b2t dst]=stiffel_simplelip(RB1,RT1,pi-F1,pi/2-S1,B1,D1,t,Fn,E,nu);

%calculate effective width of flange and lip (bottom)
[b1b b2b dsb]=stiffel_simplelip(RB2,RT2,pi-F2,pi/2-S2,B2,D2,t,Fn,E,nu);

%calculate corners
srbl=(RB1-t/2)*(pi-F1);
srbb=(RB2-t/2)*(pi-F2);
srtl=(RT1-t/2)*(S1+pi/2);
srtb=(RT2-t/2)*(S2+pi/2);

%calculate effective width
effwidth=bweb+b1t+b2t+b1b+b2b+dsb+dst+srbl+srbb+srtl+srtb ;
Ae=effwidth*t ; %effective area
Pn=Ae*Fn ;%column capacity

[Pcrl,Pcrd,Pcrd_dboost,loc_halfwave,dist_halfwave] =
LocDisBuckling(curve,lengths,L,CorZ,dims,n);

[answ] = Buckling(Pcrl,Pcrd_dboost,Pcre(1),A,Fy);

%calculate distortional buckling strength
Py=Fy*A;
[Pnd,lambda_D]=distDSM(Py,Pcrd_dboost);

```

ftb ():

```

%This function calculates the three roots of the classical cubic column
%buckling equation.

%Nomenclature is based on Chajes, Principles of Structural Stability
%Theory, Figure 5-4 and Eq. 5.49

%Cris Moen
%cmoen@vt.edu
%Created 9/3/08

%Revised 9/14/08 by CDM - added kx, ky, and kphi effective length options
%Revised 8/3/09 by CDM - fixed xo, yo to make sure they are in principal
%coordinates

%INPUTS

%L      column length
%A      column area
%I1     moment of inertia about x-axis (principal axis)
%I2     moment of inertia about y-axis (principal axis)
%kx    effective length, x-axis (e.g., kx=1 for simply supported)
%ky    effective length, y-axis
%kphi   effective length, z-axis (i.e., torsion)
%J      St. Venant torsional constant
%Cw    warping torsion constant
%xcg   x-coordinate of cross-section centroid (centroidal axis)
%xsc   x-coordinate of cross-section shear center (centroidal axis)
%ycg   y-coordinate of cross-section centroid (centroidal axis)
%ysc   y-coordinate of cross-section shear center (centroidal axis)
%E      elastic modulus
%nu    Poisson's ratio
%L      member length
%theta angle between principal axes and centroidal axes

%OUTPUT
%Pe    three roots of classical cub column buckling equation

function [Pe]= ftb(theta,I1,I2,L, A, Ix, Iy, kx, ky, kphi, J, Cw, xcg, xsc,
ycg, ysc, E, nu)

%x and y distances between cross-section centroid and shear center in
%centroidal coordinate system
%refer to Chajes Fig. 5-4
xo=xcg-xsc;
yo=ycg-ysc;

%transfer distances to principal coordinate system
xymat= [cos(theta) sin(theta); -sin(theta) cos(theta)]*[xo; yo];
xo12=xymat(1);
yo12=xymat(2);

% transfer the shear center coordinates to the centroid principal coordinates
s12 = [cos(theta) sin(theta); -sin(theta) cos(theta)]*[xsc-xcg; ysc-ycg];

```

```

%shear modulus
G=E/(2*(1+nu));
%
% compute the polar radius of gyration of cross section about shear center
ro = sqrt((I1+I2)/A+s12(1)^2+s12(2)^2);

Px=pi^2*E*I1/(kx*L)^2 ; %Flexural Euler buckling about x-axis
Py=pi^2*E*I2/(ky*L)^2; %Flexural Euler buckling about y-axis
Pphi=(1/ro^2)*((G*J)+((E*Cw*pi^2)/(kphi*L)^2)) %Torsional Euler buckling

%provide guess range for root solver
%guessrange=0:1:2*max([Px Pphi]);
guessrange=0:1:2*max([Px Pphi]);
%employ solver to find three roots of cubic column buckling equation,
%Chajes Eq. 5.49
for i=1:length(guessrange);
    x(i) = fzero(@(P) (Py-P)*(Px-P)*(Pphi-P)-(Py-P)*P^2*xo12^2/ro^2-(Px-P)*P^2*yo12^2/ro^2,guessrange(i));
    x(i)=round(x(i)*1000)/1000;
end

%three roots of equation (i.e., critical elastic column buckling loads)

%stop
Pe=unique(x);

end

```

stiffel_simplelip ():

```
function [b1 b2 ds]=stiffel_simplelip(R1,R2,angle1,angle2,W,D,t,f,E,nu)
```

```

%Calculate the effective width of a stiffened element with a simple lip
stiffener (AISI S-100-07 B4)

%calculate flat width
%web-flange corner
T1=R1*sin(angle1/2);
wr1=T1/cos(angle1/2);
%flange-lip corner
T2=R2*sin(angle2/2);
wr2=T2/cos(angle2/2);
%flange flat width
w=W-wr1-wr2;
%lip flat width
d=D-wr2;

S=1.28*sqrt(E./f);

%need unstiffened element
[dsprime]=unstiffel(R2,angle2,D,t,f,E,nu);

if w./t<=0.328*S
    Ia=0;
    b=w;
    b1=w/2;
    b2=w/2;
    ds=dsprime;
else
    Ia=399*t^4*(w/t/S-0.328)^3;
    if Ia>t^4*(115*w/t/S+5)
        Ia=t^4*(115*w/t/S+5);
    end
end

Is=d^3*t*(sin(angle2)^2)/12;

RI=Is/Ia;

if RI>1
    RI=1;
end

n=(0.582-w/t/(4*S));
if n<1/3
    n=1/3;
end

if (angle2 >= 40*pi/180 && angle2 <=140*pi/180)
if D/w<=0.25
    k=3.57*(RI)^n+0.43;
if k>4
    k=4;
end
elseif (D/w>0.25 & D/w<=0.9)
    k=(4.82-5*D/w)*RI^n+0.43;
if k>4

```

```

        k=4;
end
else
    error('D/w out of range')
end
else
    error('angle out of range')
end

[b]=stiffel(R1,R2,angle1,angle2,W,t,f,E,nu,k);

b1=b/2*RI;
b2=b-b1;
ds=dsprime*RI;

end

```

LocDisBuckling ():

% Karthik Ganesan, Fall 2008

```

function [Pcrl,Pcrd,Pcrd_dboost,loc_halfwave,dist_halfwave] =
LocDisBuckling(curve,lengths,L,CorZ,dims,n,Pcre,Py)

% find the difference between successive points and multiply them so...
% ... that the local minima can be found
diffcurve = diff(curve(:,2,1));
for i = 2:length(diffcurve)
    prod(i-1) = diffcurve(i-1)*diffcurve(i);
end;
locmin = find(prod <0);

Pcrl = curve((locmin(1)+1),2,1);
loc_halfwave = curve((locmin(1)+1),1,1);

Pcrd = NaN;
dist_halfwave = NaN;
Pcrd_dboost = NaN;

% figure(1)
% plot(lengths,curve(:,2,1),'.-');

```

Buckling ():

% This function calculates the column capacity corresponding to Local, Global (Flexural) and Distortional Buckling

```

% Karthik Ganesan, Fall 2008.

function [ans] = Buckling(Pcrl,Pcrd,Pcre,Ag,Fy)

Py = Ag*Fy;

%Flexural Buckling
lamc = ((Py)/Pcre)^0.5;
if lamc <= 1.5
    Pne = (0.658^(lamc^2))*Py;
else
    Pne = (0.877/(lamc^2))*Py;
end;
Pne;

%Local Buckling
laml = ((Pne)/Pcrl)^0.5;
if laml <= 0.776
    Pnl = Pne;
else
    Pnl = [1-0.15*((Pcrl/Pne)^0.4)]*((Pcrl/Pne)^0.4)*Pne;
end;
Pnl;

%Distortional Buckling

if Pcrd == NaN
    Pnd = NaN;
else
    lamd = ((Py)/Pcrd)^0.5;
if lamd <= 0.561
    Pnd = Py;
else
    Pnd = [1-0.25*((Pcrd/Py)^0.6)]*((Pcrd/Py)^0.6)*Py;
end;
end;
Pnd;

ans = [Pne Pnl Pnd];

```

Appendix 3

The following is the derivation of the resistance factor in a general form without the use of numerical values. As seen earlier, Eqs. (31) to (34) presented the expressions for the mean and coefficient of variation of the resistance, R , and the load effect, Q . Eq. (36) that presented the relationship between the resistance factor, ϕ_c , the nominal resistance, R_n , the nominal values of the dead and live loads, D_n and L_n , and the load factors, α_D and α_L is as follows:

$$\phi_c R_n = C(\alpha_D D_n + \alpha_L L_n), \quad (62)$$

Rearranging Eq. (31), the expression for nominal resistance, R_n , is obtained as follows:

$$R_n = \frac{R_m}{(M_m F_m P_m)} \quad (62)$$

Using the expression for the mean resistance, R_n , in Eq. (62), Eq. (36) can be expressed as

$$\begin{aligned} \phi_c \frac{R_m}{(M_m F_m P_m)} &= CL_n \left(\alpha_D \frac{D_n}{L_n} + \alpha_L \right) \\ \Rightarrow CL_n &= \frac{\phi_c \frac{R_m}{(M_m F_m P_m)}}{\left(\alpha_D \frac{D_n}{L_n} + \alpha_L \right)} \end{aligned} \quad (63)$$

It is assumed that the mean dead load is related to the nominal dead load as follows:

$$D_m = A(D_n). \quad (64)$$

Similarly, the mean live load is related to the nominal live load as follows:

$$L_m = B(L_n). \quad (65)$$

Here, A and B are constants that relate the mean loads to the nominal loads. Using Eqs. (64) and (65) in Eq. (32), the mean of the load effect, Q_m , can be expressed as follows:

$$\begin{aligned} Q_m &= CL_n \left(A \frac{D_n}{L_n} + B \right) \\ \Rightarrow CL_n &= \frac{Q_m}{\left(A \frac{D_n}{L_n} + B \right)} . \end{aligned} \quad (66)$$

Equating Eqs. (63) and (66), the following expression is obtained:

$$\frac{Q_m}{\left(A \frac{D_n}{L_n} + B \right)} = \frac{\phi_c \frac{R_m}{(M_m F_m P_m)}}{\left(\alpha_D \frac{D_n}{L_n} + \alpha_L \right)} \quad (67)$$

From Eq. (67), the ratio of the means of the resistance (R_m) to the load effect (Q_m) can be expressed as

$$\frac{R_m}{Q_m} = \frac{(M_m F_m P_m) \left(\alpha_D \frac{D_n}{L_n} + \alpha_L \right)}{\phi_c \left(A \frac{D_n}{L_n} + B \right)} \quad (68)$$

The ratio of the mean resistance to the mean load effect (R_m/Q_m) from Eq. (68), the coefficient of variation of resistance, V_R , and the coefficient of variation of the load effect, V_Q , from Eq. (35) are substituted in Eq. (30) and the following expression is obtained:

$$\beta = \frac{\ln \left(\frac{\left(M_m F_m P_m \right) \left(\alpha_D \frac{D_n}{L_n} + \alpha_L \right)}{\phi_c \left(A \frac{D_n}{L_n} + B \right)} \right)}{\sqrt{\left(V_M^2 + V_F^2 + V_P^2 \right) + \left(\frac{\sqrt{\left(A \frac{D_n}{L_n} \right)^2 V_D^2 + B^2 V_L^2}}{A \frac{D_n}{L_n} + B} \right)^2}} \quad (69)$$

Thus, rearranging the terms in Eq. (69), the expression for the resistance factor, ϕ_c , is obtained as follows:

$$\phi_c = \frac{\left(M_m F_m P_m \right) \left(\alpha_D \frac{D_n}{L_n} + \alpha_L \right)}{\left(A \frac{D_n}{L_n} + B \right) \exp \left(\beta \sqrt{\left(V_M^2 + V_F^2 + V_P^2 \right) + \left(\frac{\sqrt{\left(A \frac{D_n}{L_n} \right)^2 V_D^2 + B^2 V_L^2}}{A \frac{D_n}{L_n} + B} \right)^2} \right)} \quad (70)$$



**American
Iron and Steel
Institute**

25 Massachusetts Avenue, NW
Suite 800
Washington, DC 20001
www.steel.org

